FLORIDA INTERNATIONAL UNIVERSITY

Miami, Florida

EFFECTS OF DISCHARGE ON WATER QUALITY AND SEDIMENTS IN SOUTH FLORIDA'S EVERGLADES CANALS, USA

A dissertation submitted in partial fulfillment of

the requirements for the degree of

DOCTOR OF PHILOSOPHY

in

EARTH SYSTEMS SCIENCE

by

Ikechukwu Samuel Onwuka

2023

To: Dean Michael R. Heithaus
College of Arts, Sciences and Education

This dissertation, written by Ikechukwu Samuel Onwuka and entitled Effects of Discharge on Water Quality and Sediments in South Florida's Everglades Canals, USA, having been approved with respect to style and intellectual content, is referred to you for judgment.

We have read this dissertation and recommend that it be approved.

René Price

David Fugate

Piero Gardinali

Leonard J. Scinto, Co-Major Professor

Assefa Melesse, Co-Major Professor

Date of Defense: March 24, 2023

The dissertation of Ikechukwu Samuel Onwuka is approved.

Dean Michael R. Heithaus
College of Arts, Sciences and Education

Andrés G. Gil
Vice President for Research and Economic Development
and Dean of the University Graduate School

Florida International University, 2023

COPYRIGHT

DECLARATION STATEMENT

I, Ikechukwu Samuel Onwuka declare that the dissertation entitled Effects of Discharge on Water Quality and Sediments in South Florida's Everglades Canals, USA is the result of my original research work, and it has been written by myself under the supervision of my advisors, Leonard Scinto and Assefa Melesse. Reference to the literature, and acknowledgement of collaborative research and discussions are made and appropriate credit has been given within this dissertation. I confirm that this work has not been submitted for any other degree qualification.

DEDICATION

I dedicate this dissertation to the Onwuka and Udo Emeaba families: my late father, Professor S.K Onwuka, whose brilliance and devotion to family is the reason I am here; my mother Dr. Chinyere Onwuka (nee Udo Emeaba), whose tenacity in getting her Ph.D., and prayers were comfort and hope; my siblings: Ngozi who reviewed my manuscripts and fellowships, Okechukwu and Nkechi, who made me feel home away from home, and Emmanuel, who took care of the house and my mother when dad passed. To all my nephews and niece, thank you for giving me joy and hope.

ACKNOWLEDGMENTS

I am grateful to my major professor Dr. Leonard J. Scinto for his patience and guidance throughout this herculean journey. Thank you for the countless hours you invested in me and for teaching me how to be resourceful. I am grateful to my co-major professor, Dr. Assefa Melesse, who believed in me, provided excellent reference letters, reviewed my work, and ensured that I kept to my timeline. I appreciate my committee: Dr. René Price for encouraging me to apply for fellowships, for providing excellent reference letters and detailed feedback on my manuscripts; Dr. David Fugate for his time and expertise in helping me with the technical aspects of my work: and Dr. Piero Gardinali for providing financial resources and materials that I needed for my research.

I am grateful to the Everglades Foundation, Society for Freshwater Science, FIU University Graduate School, Institute of Environment, and the FCE-LTER for providing me with fellowships, logistics, and camaraderie. I am also thankful to NSF CREST CAChE and the program manager, Brad Schonhoff, for providing resources and support that enabled me to quickly conduct my studies and publish my work. I am grateful to Gail, Cary, Jessie, Rafael, and Sergio for helping me with administrative tasks and logistics. I am also grateful to Seema and Panneer for showing me the way when I was a teaching assistant. I am thankful to my squad: Jazmin, Angelica, Sam, Luke, and Vanessa for being familiar faces and providing much-needed support. To Luke, Jordan, Joshua, and Jonathan, thank you immensely for helping me with fieldwork.

I acknowledge my Miami family: Eliada, Rodney, Vanessa, Natalia Camilla, and many more.

Most of all, I am grateful to God Almighty for strength and grace.

ABSTRACT OF THE DISSERTATION

EFFECTS OF DISCHARGE ON WATER QUALITY AND SEDIMENTS IN SOUTH FLORIDA'S EVERGLADES CANALS, USA

Ikechukwu Samuel Onwuka

Florida International University, 2023

Miami, Florida

Professor Leonard J. Scinto, Co-Major Professor

Professor Assefa Melesse, Co-Major Professor

Water in the Everglades of central and southern Florida originally flowed from north to south as sheetflow. However, a network of canals, levees, and structures was created to drain the Everglades for agriculture and urban development. These changes altered the natural flow regime, allowing canals to shunt large volumes of water with high phosphorus (P) loads downstream. To remediate this, the Everglades is undergoing a multibillion-dollar hydrologic restoration. One of the restoration goals is to obtain the right water quality and quantity, that is, to provide a more "natural" flow of clean water. This dissertation sought to address this goal by focusing on canals: discharge releases, water quality, and sediment characteristics. The first study characterized and compared the flow regimes of a canal, river, and wetland slough and quantified the effect of flow on water quality constituent behavior using concentration-discharge (C-Q) relationships. The next study developed high-resolution estimates for suspended sediments and P to better assess how rapid changes in canal discharges could impact exports. The final study delineated the dynamics between discharge, water quality, and sediments in canals across the Lower Everglades. The results showed that characteristics of the canal, such as high

flow variability and lack of a floodplain, led to an increase in water quality constituent concentrations, especially at high flows. The proximity and discharge volume from a canal inflow structure increased the concentrations of the high-resolution estimates by mobilization and resuspension processes. The suspended sediments closest to the inflow structure had low P contents that increased with increasing distance. Similarly, surficial bed sediments closest to the inflow structure had high bulk density and low P content, while those farther away had the opposite. This indicated that discharges from the structure transported organic P-rich sediments further downstream and left behind heavier P-poor sediments. Thus, canal transport processes are crucial for evaluating restoration goals. I propose that the discharge threshold from C-Q relationships, which segments water quality constituent behavior at low and high flow, be used as a management tool to determine the range of canal discharges that will maximize freshwater delivery and minimize P export.

TABLE OF CONTENTS

CHAPTER PAGE

LIST OF TABLES

TABLES PAGE

LIST OF FIGURES

FIGURES PAGE

ABBREVIATIONS AND ACRONYMS

ADCP	Acoustic Doppler Current Profiler
ADV	Acoustic Doppler Velocimeter
b	Slope of the C-Q relationship
BD	Bulk Density
BMP	Best Management Practices
BT	Bottom Trap
Cl	Chloride
COP	Combined Operations Plan
C-Q	Concentration-Discharge
CAChE	Center for Aquatic Chemistry and Environment
DS	Downstream Site
EAA	Everglades Agricultural Area
EA	Eastern Site
ENP	Everglades National Park
EPA	Everglades Protection Area
FCE-LTER	Florida Coastal Everglades-Long Term Ecological Research
HART	High Aspect Ratio Trap
HC6	Hillsboro Canal at the S6 structure
IHA	Indicators of Hydrologic Alteration
INT	Interior Site
LEC	Lower East Coast
MAR	Mass Accumulation Rate

mg kg^{-1}	Milligram per kilogram
MWD	Modified Water Deliveries
NN	Nitrate-Nitrite
OM	Organic Matter
PCA	Principal Component Analysis
P	Phosphorus
PRB	Peace River at Bartow
R-B Index	Richards–Baker Flashiness Index
S333	Inflow Structure on L-29 Canal
S333N	Secondary Inflow Structure North of S333
SC	Specific Conductance
SFWMD	South Florida Water Management District
SRS	Shark River Slough at Bottle Creek
STAs	Stormwater Treatment Areas
SWFWMD	Southwest Florida Water Management District
TP	Total Phosphorus
TPP	Total Particulate Phosphorus
TSS	Total Suspended Solids
µg mg^{-1}	Microgram per milligram
UP	Upstream site
USACE	U.S. Army Corps of Engineers
USGS	United States Geological Survey
WCA	Water Conservation Area

CHAPTER 1: INTRODUCTION

1.1. Background

The Everglades in central and southern Florida are the largest subtropical wetland ecosystems in the United States (Figure 1.1). Historically, the Everglades was a continuous system originating in the Kissimmee River-Lake Okeechobee basin and flowed in "sheets" southward into Florida Bay and the southeast coast. Then, in the early 20th century, an extensive water management system - a network of canals, levees, roads, and water control structures - was created to drain the Everglades wetlands for agriculture and urban development (Davis and Ogden, 1994; Reddy and DeLaune, 2008). These changes in hydrology and the resultant change in land cover led to the loss of approximately 50% of the original Everglades (which extended up to approximately 9000 km^2) as well as the disruption of the natural sheet flow, which resulted in uncharacteristic ponding in some areas and shorter hydroperiods and drier conditions in others (Sklar et al. 1999; Sklar et al. 2001; Reddy and DeLaune, 2008; McVoy et al. 2011). The post drainage Everglades are composed of multiple distinct hydrologic units that include the Everglades Agricultural Area (EAA), Everglades Protection Area (EPA), and Lower East Coast (LEC), which broadly represent agricultural, natural wetland, and urban land use, respectively. Water flow in these units is regulated by canals and their associated structures to meet the agricultural, urban, and ecosystem needs of the region (Reddy and Delaune, 2008).

Canals are a unique feature in the South Florida landscape and are quite different from natural water bodies such as rivers, lakes, and streams. Canal discharges can

fluctuate widely, ranging from no flow periods (where the canal acts like a reservoir) to high flow periods, depending on operational needs. Canal sides are usually very steep and do not possess shallow areas needed to support flora and fauna. Thus, unlike rivers, canals, by design, have reduced or non-existent ability for bankfull discharge that can reduce flow velocities, and do not have mature vegetation that can stabilize channel banks and provide shade that can regulate water physiochemical parameters (e.g. dissolved oxygen, temperature) These canal features prevent the development of stable littoral and shoreline zones (Carter et al. 2010).

In terms of usage, South Florida canals serve many purposes including transportation, conveyance of surface and groundwater (including irrigation and drainage), regulation of water level to enhance local storage, and prevention of flooding and saltwater intrusion, and providing support for ecological systems (Carter et al. 2010). Some canals were created in the aftermath of the construction of levees or roadways. These “borrow” canals comprise the depressions left behind from the excavation of rock and soil used to build levees or roadways and are used for water conveyance purposes (Carter et al. 2010).

Canals vary greatly across the region. The dimensions (width and depth) of a canal depend on factors including the water conveyance needs, topographic changes, size and type of water control structures, and local needs. Similarly, the design of the side slopes depends on the substrate, water velocities, and operational discharges, to prevent failure of the canal banks (Carter et al 2010).

Four major (primary) canals provide regionwide regulatory functions and can move water south and southeast from Lake Okeechobee to and through the EAA, EPA, and

LEC. These canals are the Miami Canal, West Palm Beach Canal, Hillsboro Canal, and North New River Canal (Carter et al. 2010). The EAA was channelized and drained for agricultural use (Bhadha et al. 2017; Carter et al. 2010). Originally, the canals in the EAA were constructed for drainage purposes and were also used to transport farm products to urban markets, but they were enlarged and had water control structures including pumps installed to increase water deliveries to the agricultural and urban areas during dry periods and to provide drainage and flood protection during wet periods (Carter et al. 2010). These canals also move water south into the EPA (Carter et al. 2010). The EPA is made up of a series of wetlands and includes water conservation areas (WCA-1, WCA-2, and WCA-3) and the Everglades National Park (ENP) (Reddy and DeLaune, 2008; Carter et al. 2010). The LEC includes the urban and coastal cities of West Palm Beach, Broward, and Miami-Dade counties. The canals and associated structures were constructed primarily to enable flood protection, prevent saltwater intrusion, and convey water for urban and agricultural needs (Carter et al. 2010).

The original Everglades evolved under oligotrophic and phosphorus-poor conditions (Reddy and DeLaune, 2008). However, the drainage of the Everglades ecosystem and the resultant agricultural and urban development allowed the shunting of large volumes of nutrient (especially phosphorus)-rich water via canals into the southern regions, which has resulted in eutrophication, vegetation composition changes, and toxic algal bloom increases in the estuaries (Davis and Ogden, 1994; Noe et al. 2001; Childers et al. 2003; McCormick et al. 1999).

Phosphorus can exist in particulate and soluble pools. The soluble pools include dissolved inorganic phosphorus (DIP), which is also called soluble reactive phosphorus,

and dissolved organic phosphorus (DOP). DIP is the most bioavailable/labile form of phosphorus (Reddy and Delaune, 2008). The DOP pool is diverse and ranges from simple organic phosphorus compounds such as sugar phosphates to macromolecules such as phospholipids. DOP constitutes labile organic P (microbial biomass P) that can be produced and mineralized by leaching from senescing plant tissue and noncatalyzed hydrolysis of phosphate ester photolysis (Reddy and Delaune, 2008). The particulate pools of P include particulate inorganic phosphorus (PIP) and particulate organic phosphorus (POP). PIP compounds are associated with amorphous and crystalline forms of iron, aluminum, calcium, and magnesium (Reddy and Delaune, 2008). Calcium and magnesium are important because the Everglades is underlain by calcium carbonate (limestone) bedrock, and these elements regulate the solubilities of phosphorus contained in them. For example, calcium-bound P has been identified as a major P pool in Everglades canal sediments (Diaz et al. 2006; Wang et al. 2011). POP represents the phosphorus stored in organic matter (OM), both living and dead. Organisms can store orthophosphates or polyphosphates as POPs in their cells or tissues. POP in sediments is the form of P associated with humic and fluvic acids (Diaz et al. 2006), and POP can also constitute recalcitrant P that is generally not bioavailable (Reddy and Delaune, 2008).

Unlike nitrogen and carbon, which have sizeable atmospheric components, P has no environmentally present gaseous phase and accumulates in dissolved and particulate forms within the landscape (Reddy et al. 1999; Withers and Jarvie, 2008; Jarvie et al. 2013; Sharpley et al. 2013). Particulate phosphorus can be further transported as part of suspended sediment loads in flowing freshwater systems (Meybeck, 1982)

In the Everglades, decades of continuous phosphorus (P) loading to canals have further led to the sequestration of P, often referred to as “legacy P” in canal sediments (Diaz et al. 2006). Canal sediment inventories have estimated the mass of P to be twice that found in the surrounding wetlands (Wang et al. 2011). Depending on the hydrologic operations in canals, legacy P, concomitant with the sediments themselves, has the potential during high discharges to be exported downstream into the remnant Everglades (Diaz et al. 2006; Wang et al. 2011; Das et al. 2012), as higher flows can transport more sediments than lower flows (Wang et al. 2011).

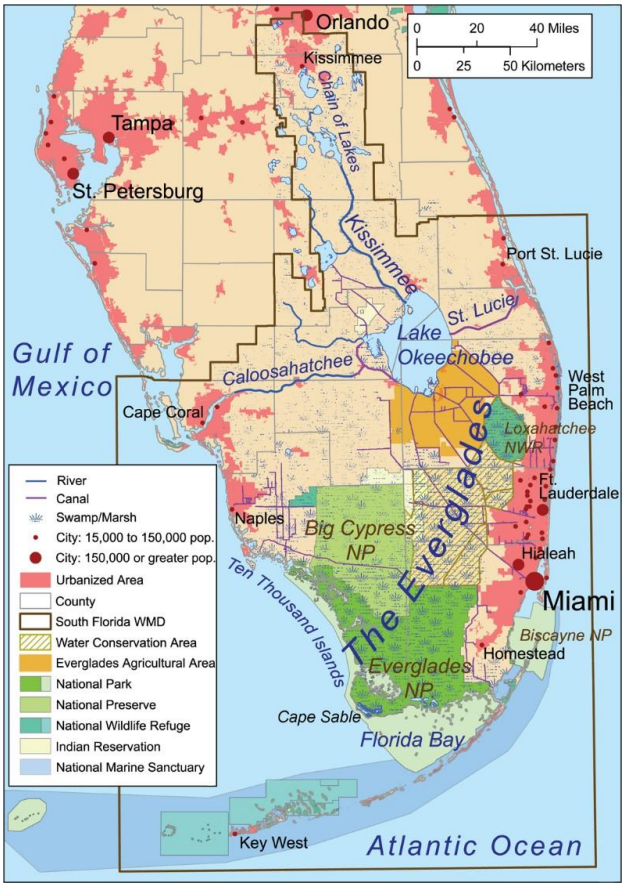

Figure 1.1 Map of the Everglades region in South and Central Florida. Source: Wikimedia Commons. (https://commons.wikimedia.org/wiki/File:Evergladesareamap.png)

1.2. Theory

Natural channels such as rivers and streams and their surrounding lands have been used by humans for millennia. They provide freshwater for drinking and farming, aquatic organisms for food and recreation, and services such as flood protection (Schmutz and Sendzimir, 2018). However, human changes to natural channels have resulted in channelization and divergence of flow regimes (Schoof, 1989; Brooker, 1985; Poff et al. 1997; Sklar et al. 1999). Channelization, or canalization, involves the straightening and shortening of existing natural channels to increase hydrologic transport capacity and the dredging of land surfaces to create new channels for navigation, water conveyance, and drainage purposes (Brooker, 1985; Carter et al. 2010). Furthermore, channelization can include the construction of levees and embankments along channel banks to restrict channel morphology and width, which, in some instances, can deepen the channel (Poff et al. 1997). Such changes in morphology disconnect channels from their riparian areas, reduce sediment exchange capacities, prevent overbank discharges, and change flow regimes (Poff et al. 1997; Schmutz and Sendzimir, 2018; Wohl, 2015). Flow or discharge regulation via water control structures can further change the flow regimes of channels (Carter et al. 2010). For example, pump stations, culverts, spillways, and weirs are used to regulate the flow of water within the canal networks of South Florida, USA (Carter et al. 2010; SWFMD, 2010). Overall, flow regime changes affect the natural variability and cyclical patterns of low and high flow conditions of channels, often changing the magnitude and frequency of low and high flows (Poff et al. 1997; Richter et al. 1998; Richter et al. 1996).

Changes in flow regimes can impact the export behavior of water quality constituents in channels. Depending on flow conditions, channels can act as both transformers and transporters of water quality constituents (O'Donnell and Hotchkins, 2019). Channels generally act as transformers when biogeochemical processes decrease the variability of the constituent concentrations and composition (homogenization), usually under low discharge flow conditions (Creed et al. 2015; O'Donnell and Hotchkiss, 2019). Under high flow, many canals act as transporters of materials/constituents (O'Donnell and Hotchkiss, 2019). Total phosphorus (TP) and total suspended solids (TSS) are water quality constituents that have been shown to increase in their concentrations at high discharges due to their associations with sediments (Rose et al. 2018; Diamond and Cohen, 2018).

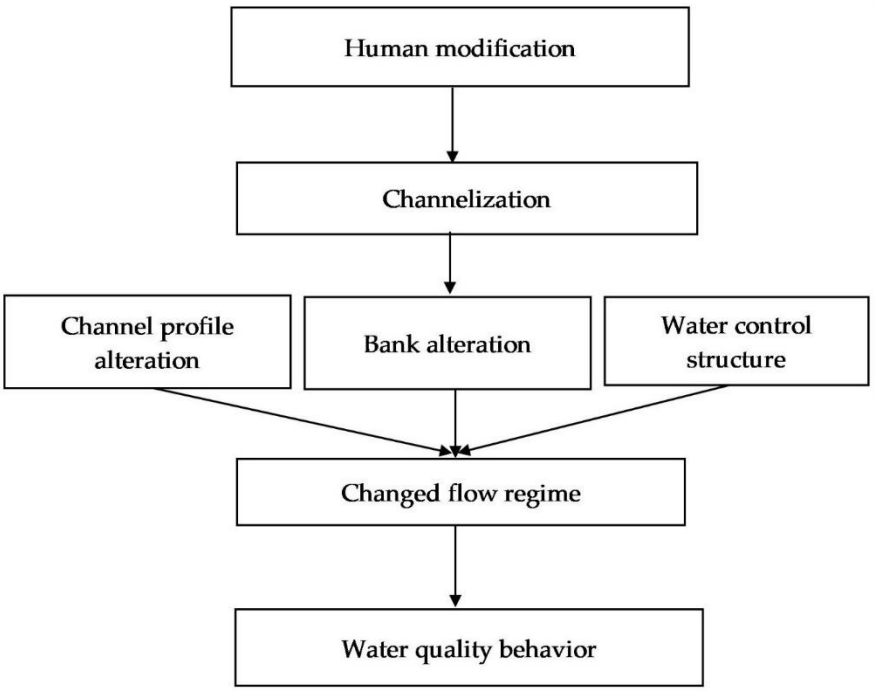

Figure 1.2 The effects of human modification of landscape via channelization on changes in flow regimes and the impacts on water quality (adapted from Brooker, 1985).

1.3. Objectives

To date, there has not been much work done to characterize how flow regimes impact the water quality in South Florida canals compared to more natural flowways. Canals are environmentally unnatural, human-made, and have manipulated discharges (Carter et al. 2010) compared to rivers and streams. Furthermore, studies in South Florida canals in the Everglades have quantified P release under conditions of zero or low flows through measurements of processes such as diffusion and sorption (Diaz et al. 2006; Wang and Li, 2010; Das et al. 2012). These processes, however, do not estimate the TP flux; hydrologic-driven P releases through sediment transport and resuspension are not accounted for. A holistic estimation of P release from canals requires the quantification of hydrologic drivers (e.g., discharge) and the measurements of their contributions to P exports. Although the water monitoring protocols in South Florida are quite robust and extensive, they are still temporally coarse (low resolution) and may not capture the necessary data needed to understand the impact of short-term changes in discharges that are common in a manipulated channel, so surrogate estimates are needed. Therefore, the objectives of this research were to:

- Characterize the flow regimes of South Florida canals and determine how changes in flow and morphology affect water quality constituent behavior.
- Develop high-resolution estimates of select crucial water quality constituents - suspended sediments and phosphorus - in South Florida canals to evaluate how short term canal discharges can impact their downstream export to the nutrient-sensitive southern Everglades.

- Delineate the processes by which canal discharges can affect particulates and P exports through measurements of discharges and sediment and P concentrations.

To answer these objectives the following research questions were asked:

- How does the flow regime in a human-made channel (canal) differ from that of a natural channel? Will theories and models created for rivers and streams, etc., to assess the effects of discharge on the behavior of water quality constituents apply to canals?
- Can high spatio-temporal resolution (e.g. hourly) estimates of suspended solids and phosphorus (water quality health indicators) be conducted? Could these estimates be used to evaluate how short term canal discharges impact their downstream export?
- How does discharge affect particulates and P dynamics (interactions and exports) in the water column and sediment layers of canals? How does proximity to canal inflow structures affect these dynamics?

1.4. Significance of this Research

Everglades restoration is a multibillion effort and the largest ecosystem and hydrologic restoration in the world (NRC, 2003b; Lemaire and Sisto, 2012) and involves many agencies and programs all working in tandem to meet certain goals. Estimating the impacts and long-term implications of nutrient loads, especially phosphorus (P), on the Everglades has been an important aspect of research in the restoration of the Everglades (Childers et al. 2003). One of the goals of the South Florida Everglades Restoration Task Force, an intergovernmental body created to

coordinate restoration efforts, is to “get the water right”. This is interpreted as restoring the Everglades region's water quality and quantity (SFERTF, 2010) and includes the adoption of the 10 μg L^{-1} total phosphorus water quality standard in the Everglades Protection Area (Everglades Forever Act of 1994). Historically, getting the water right encompassed timing, quantity, and quality; however, the hydrologic property of flow, encompassing discharge and velocity, which was previously overlooked, has been recognized as a key component even though evidence shows flow to be crucial as it impacts biological, physical and chemical processes, and it promotes mixing at the water- substrate (e.g., sediments) interface (NRC, 2003b).

1.5. Dissertation Organization

This dissertation is organized into five chapters, with three chapters arranged in manuscript format:

- Chapter 1. The introduction provides an overview of the research and its significance.
- Chapter 2: “Comparative Use of Hydrologic Indicators to Determine the Effects of Flow Regimes on Water Quality in Three Channels across Southern Florida, USA”, determined the relationship between water discharge and water quality in three channels in Southern Florida with varying degrees of channelization and/or changes in flow regimes.
- Chapter 3: “Estimation of High-Resolution Suspended Solids and Particulate Phosphorus using Acoustic Devices in a Hydrologically Managed Canal in South Florida, USA” used acoustic backscatter, the biproduct of velocimeters, to develop high spatial and temporal estimates of suspended solids and particulate phosphorus

in an important hydrologically managed canal in South Florida, USA. This study further evaluated how rapid changes in hydrology, typical of managed canals, impacted these water quality estimates.

- Chapter 4: “Particulate And Phosphorus Dynamics in the Water Column and Sediments of Canals in the Lower Everglades” analyzed water quality, discharge, suspended particulates, and bed sediment data to identify and characterize the processes that enable the export of particles and phosphorus in canals.
- Chapter 5: “Conclusion” is a summary of the main findings of this research and provides recommendations for future work.

1.6. References

Bhadha, J.H., Lang, T.A. and Daroub, S.H., 2017. Influence of suspended particulates on phosphorus loading exported from farm drainage during a storm event in the Everglades Agricultural Area. *Journal of Soils and Sediments*, *17*, pp.240-252.

Brooker, M.P., 1985. The ecological effects of channelization. *The Geographical Journal*, *151*(1), pp.63-69.

Carter, K., Redfield, G., Ansar, M., Glenn, L., Huebner, R., Maxted, J., Pettit, C. and VanArman, J., 2010. Canals in South Florida: A technical support document.

Childers, D.L., Doren, R.F., Jones, R., Noe, G.B., Rugge, M. and Scinto, L.J., 2003. Decadal change in vegetation and soil phosphorus pattern across the Everglades landscape. *Journal of Environmental Quality*, *32*(1), pp.344-362.

Creed, I.F., McKnight, D.M., Pellerin, B.A., Green, M.B., Bergamaschi, B.A., Aiken, G.R., Burns, D.A., Findlay, S.E., Shanley, J.B., Striegl, R.G. and Aulenbach, B.T., 2015. The river as a chemostat: fresh perspectives on dissolved organic matter flowing down the river continuum. *Canadian Journal of Fisheries and Aquatic Sciences*, *72*(8), pp.1272-1285.

Das, J., Daroub, S.H., Bhadha, J.H., Lang, T.A. and Josan, M., 2012. Phosphorus release and equilibrium dynamics of canal sediments within the Everglades Agricultural Area, Florida. *Water, Air, & Soil Pollution*, *223*, pp.2865-2879.

Davis, S. and Ogden, J.C., 1994. *Everglades: the ecosystem and its restoration*. CRC Press.

Diamond, J.S. and Cohen, M.J., 2018. Complex patterns of catchment solute–discharge relationships for coastal plain rivers. *Hydrological Processes*, *32*(3), pp.388-401.

Diaz, O.A., Daroub, S.H., Stuck, J.D., Clark, M.W., Lang, T.A. and Reddy, K.R., 2006. Sediment inventory and phosphorus fractions for water conservation area canals in the Everglades. *Soil Science Society of America Journal*, *70*(3), pp.863-871.

Everglades Forever Act, Section 373.4592(4)(f), F.S.

Lemaire, J. and Sisto, B., 2012. The Everglades Ecosystem: Under Protection or Under Threat?. *Miranda. Revue pluridisciplinaire du monde anglophone/Multidisciplinary peer-reviewed journal on the English-speaking world*, (6).

McCormick, P.V., Newman, S., Miao, S., Reddy, R., Gawlik, D., Fitz, C., Fontaine, T. and Marley, D., 1999. Ecological needs of the Everglades. *South Florida Water Management District, West Palm Beach, FL*.

McVoy, C., Said, W.P., Obeysekera, J., VanArman, J.A. and Dreschel, T.W., 2011. Landscapes and hydrology of the predrainage Everglades.

Meybeck, M. 1982. Carbon, nitrogen, and phosphorus transport by world rivers. *Am. J. Sci*, *282*(4), 401-450. https://doi.org/10.2475/ajs.282.4.401

National Research Council, 2003. *Does water flow influence Everglades landscape patterns?*. National Academies Press.

Noe, G.B., Childers, D.L. and Jones, R.D., 2001. Phosphorus biogeochemistry and the impact of phosphorus enrichment: why is the Everglades so unique?. *Ecosystems*, *4*, pp.603-624.

O'Donnell, B. and Hotchkiss, E.R., 2019. Coupling concentration-and process-discharge relationships integrates water chemistry and metabolism in streams. *Water Resources Research*, *55*(12), pp.10179-10190.

Poff, N.L., Allan, J.D., Bain, M.B., Karr, J.R., Prestegaard, K.L., Richter, B.D., Sparks, R.E. and Stromberg, J.C., 1997. The natural flow regime. *BioScience*, *47*(11), pp.769-784.

Reddy, K.R. and DeLaune, R.D., 2008. *Biogeochemistry of wetlands: science and applications*. CRC press.

Reddy, K.R., Kadlec, R.H., Flaig, E. and Gale, P.M., 1999. Phosphorus retention in streams and wetlands: a review. *Critical reviews in environmental science and technology*, *29*(1), pp.83-146.

Richter, B.D., Baumgartner, J.V., Braun, D.P. and Powell, J., 1998. A spatial assessment of hydrologic alteration within a river network. *Regulated Rivers: Research & Management: An International Journal Devoted to River Research and Management*, *14*(4), pp.329-340.

Ritcher, B.D., Baumgartner, J.V., Powell, J. and Braun, D.P., 1996. A method for assessing hydrologic alteration within ecosystem. *Conservation Biology*, *10*(4), pp.1163-1174.

Rose, L.A., Karwan, D.L. and Godsey, S.E., 2018. Concentration–discharge relationships describe solute and sediment mobilization, reaction, and transport at event and longer timescales. *Hydrological processes*, *32*(18), pp.2829-2844.

Schmutz, S. and Sendzimir, J., 2018. *Riverine ecosystem management: Science for governing towards a sustainable future*. Springer Nature.

Schoof, R., 1980. Environmental impact of channel modification 1. *JAWRA Journal of the American Water Resources Association*, *16*(4), pp.697-701.

SFERTF (South Florida Ecosystem Restoration Task Force). 2008-2010. Strategy and Biennial Report.

Sharpley, A., Jarvie, H.P., Buda, A., May, L., Spears, B. and Kleinman, P., 2013. Phosphorus legacy: Overcoming the effects of past management practices to mitigate future water quality impairment. *Journal of environmental quality*, *42*(5), pp.1308-1326.

Sklar, F., McVoy, C., Van Zee, R., Gawlik, D., Swift, D., Park, W., Fitz, C., Wu, Y., Rudnick, D., Fontaine, T. and Miao, S., 1999. Hydrologic needs: the effects of altered hydrology on the Everglades. *Everglades Interim Report, SFWMD, West Palm Beach, FL, USA*.

Sklar, F.H., Fitz, H.C., Wu, Y., Van Zee, R. and McVoy, C., 2001. South Florida: the reality of change and the prospects for sustainability: the design of ecological landscape models for Everglades restoration. *Ecological economics*, *37*(3), pp.379-401.

SWFMD. Canals in South Florida: A Technical Support Document. Appendix A. Basic Concepts, Hydrologic Terminology. Glossary of Terms and Abbreviations. 2010; pp. A1–A22. Available online: https://www.sfwmd.gov/sites/default/files/documents/canalssfl_appendixa-c.pdf (accessed on 8 May 2021).

Wang, Q. and Li, Y., 2010. Phosphorus adsorption and desorption behavior on sediments of different origins. *Journal of Soils and Sediments*, *10*, pp.1159-1173.

Wang, Q., Li, Y. and Ouyang, Y., 2011. Phosphorus fractionation and distribution in sediments from wetlands and canals of a water conservation area in the Florida Everglades. *Water Resources Research*, *47*(5).

Withers, P.J.A. and Jarvie, H.P., 2008. Delivery and cycling of phosphorus in rivers: a review. *Science of the total environment*, *400*(1-3), pp.379-395.

Wohl, E., 2015. Legacy effects on sediments in river corridors. *Earth-Science Reviews*, *147*, pp.30-53.

CHAPTER 2: COMPARATIVE USE OF HYDROLOGIC INDICATORS TO DETERMINE THE EFFECTS OF FLOW REGIMES ON WATER QUALITY IN THREE CHANNELS ACROSS SOUTHERN FLORIDA, USA

Onwuka, I. S., Scinto, L. J., & Mahdavi Mazdeh, A. (2021). Comparative Use of Hydrologic Indicators to Determine the Effects of Flow Regimes on Water Quality in Three Channels across Southern Florida, USA. *Water*, *13*(16), 2184. https://doi.org/10.3390/w13162184

Abstract

This study determines the relationships between water flow and water quality in three types of channels in southern Florida, USA: the Shark River Slough, Peace River, and Hillsboro Canal. The Peace River most resembles a natural channel with floodplain connectivity, sinuosity, and uninhibited flow. Shark River Slough has a natural, shallow channel with sheet flow, while the Hillsboro Canal is the most modified channel due to dredging, straightening, and regulated flow. Hydrologic indices for each channel were estimated to characterize flow regimes and flow variability, while concentration–discharge (*C*–*Q*) relationships were determined to quantify the impact of flow regime on water quality. The greatest variability in flow occurred at the Hillsboro Canal, followed by the Peace River and Shark River Slough. Connectivity to floodplains and long durations of low and high flow pulses at Peace River and Shark River Slough contributed to the dilution of water quality constituent concentrations at higher flows. Conversely, the channelized characteristics of the Hillsboro Canal resulted in an enrichment of constituents, especially during high flows. This study suggests that *C*-*Q* relationships can be used in canal discharge management to prevent water quality degradation of sensitive downstream wetland and aquatic ecosystems.

2.1. Introduction

Human modifications of natural channels (rivers and streams) have resulted in channelization and deviation from natural flow regimes (Schoof, 1989; Brooker, 1985; Poff et al. 1997; Sklar et al. 1999). Channelization, or canalization, involves the straightening and shortening of existing natural channels to increase hydrologic transport capacity and the dredging of land surfaces to create new channels for navigation, water conveyance, and drainage purposes (Brooker, 1985; Carter et al. 2010). Channelization includes the construction of levees and embankments along channel banks to restrict channel morphology and width, which, in some instances, results in the deepening of the channel (Poff et al. 1997). Such changes in morphology disconnect channels from their floodplains, reduce sediment exchange capacities, prevent overbank flows, and change flow regimes (Poff et al. 1997; Schmutz and Sendzimir, 2018; Wohl, 2015). Flow management via water control structures can further change the flow regimes of channels (Carter et al. 2010). For example, pump stations, culverts, spillways, and weirs are used to regulate the flow of water within the canal networks of South Florida, USA (Carter et al. 2010; SWFMD, 2010). Overall, flow regime changes affect the natural variability and cyclical patterns of low and high flow conditions of channels, often changing the magnitude and frequency of low and high flows (Poff et al. 1997; Richter et al. 1998; Richter et al. 1996).

A variety of hydrologic metrics have been developed to quantify deviations from natural flow regimes that are caused by human interventions. The indicators of hydrologic alteration (IHA) are widely used hydrologic indices that characterize the magnitudes, timings, frequencies, and rates of changes in water flow, all of which are

components of a flow regime (Richter et al. 1996). These components are important because they regulate bedload transport, which influences channel morphology and facilitates exchanges of water quality constituents (e.g., nutrients and organic matter) between a channel and its floodplain (Poff et al. 1997). Furthermore, flow regime changes in modified channels can cause water quality degradation by decreasing in-stream nutrient retention and increasing pollutant exports downstream to receiving ecosystems (O'Driscoll et al. 2010). Low flow conditions can increase the residence time of water quality constituents (Moatar et al. 2017), allowing biogeochemical processes such as biotic uptake, microbial reduction (e.g., denitrification), and sorption to regulate concentration variability (Moatar et al. 2017; Withers and Jarvie, 2008). Conversely, high flows can dilute the concentrations of point-sourced water quality constituents or mobilize concentrations of multisourced constituents, including particulates, which can then be transported downstream (Moatar et al. 2017; Nilsson and Renöfält, 2008; Underwood et al. 2017; Zhang, 2018).

Regression models have been developed to predict the behavior of the concentrations of constituents that affect water quality for specified flow regimes (Malan and Day, 2003). Specifically, several studies have used concentration–discharge (*C*–*Q*) relationship models to quantify the effect of flow on the behavior of water quality constituents within natural channel networks (Moatar et al. 2017; Underwood et al. 2017; Zhang, 2018; Godsey et al. 2009; Diamond and Cohen, 2018; Rose et al. 2018). A *C*–*Q* relationship is commonly expressed as a power-law function:

$$C = aQ^b \qquad (2.1)$$

where a and b are model coefficients that represent the intercept (same unit as concentration) and slope (unitless), respectively, on a logarithmic scale (Moatar et al. 2017). The slope (b) represents the pattern or behavior of the constituent (Godsey et al. 2009). A chemostatic or constant pattern, where $b = 0$ (Godsey et al. 2009), occurs when the concentration of a constituent is not influenced by discharge but by other factors such as biogeochemical cycling. For instance, chemostasis can result from the abundance of a constituent in the watershed (Thompson et al. 2011), stemming from nutrient legacies from agriculture (Basu et al. 2011), or active geogenic weathering (Godsey et al. 2009), which act as biogeochemical controls and regulate the concentration and loading of such constituents. Conversely, a chemodynamic pattern occurs when there is an effect of discharge on the concentration of a constituent, as denoted by a nonzero slope. A negative slope ($b < 0$) represents a dilution behavior in which concentration varies inversely with discharge, while a positive slope ($b > 0$) represents an enrichment or mobilization behavior where a constituent's concentration increases with increasing discharge (Moatar et al. 2017; Zhang, 2018). Oftentimes, there are changes in *C*–*Q* patterns, observable as inflections in slopes that further delineate the processes dominating the behavior of water quality constituents. These inflections in slopes, also known as discharge thresholds, reflect the interactions of hydrologic and biogeochemical forcing on the behavior of water quality constituents, whereby hydrology is more likely to dominate at high flow and biogeochemical processes at low flow (Moatar et al. 2017).

Furthermore, the presence of slope inflections in *C–Q* relationships can identify the ranges of discharges in a flow regime where hydrology increases the concentration and export of constituents (Moatar et al. 2017; Underwood et al. 2017; Rose et al. 2018). Theoretically, there are nine classifications (archetypes) of *C–Q* relationship patterns based on the presence of slope inflections (Figure 2.1) (Moatar et al. 2017).

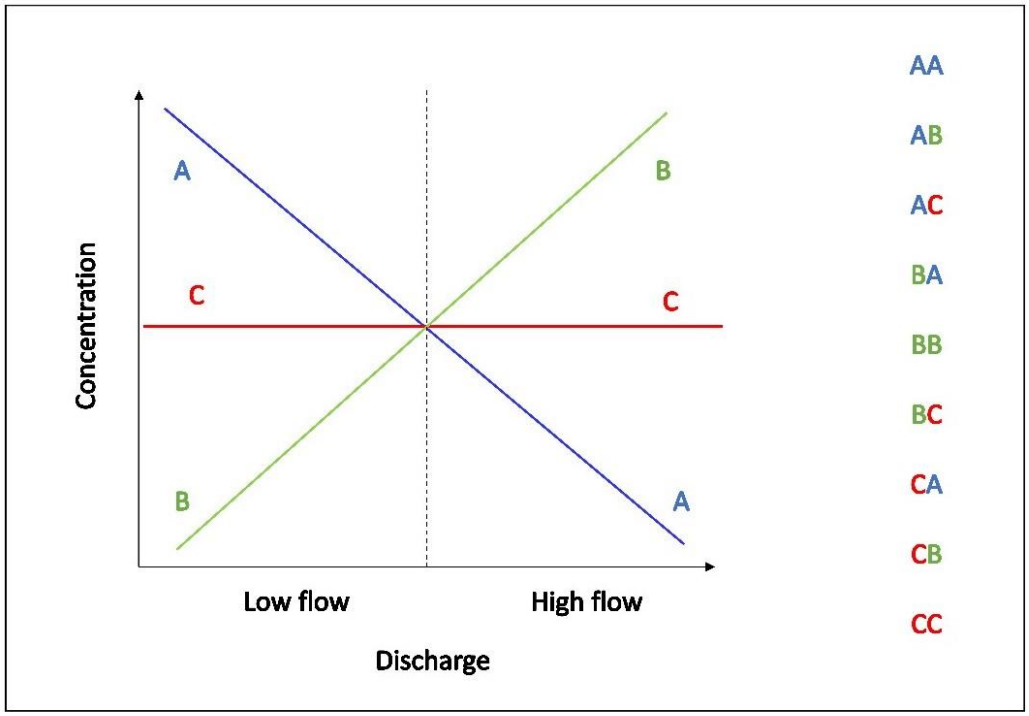

Figure 2.1 Nine possible archetypes for interpreting C–Q relationships with inflections in slopes (discharge thresholds) as adapted from Moatar et al. 2017. Blue, red, and green represent dilution, chemostatic, and enrichment, respectively.

Previous research has used the flow regime characteristics of channels to assess the impacts of flow changes caused by dams on river ecology (Richter et al. 1998; Richter et al. 1996; Hayes et al. 2018; Graf, 2006), while few studies have addressed the effects of channelization (Shields et al. 2010). This study expands on previous research by determining the impacts of flow regime changes on the behavior of water quality

constituents in three channels in southern Florida, USA, whose channel morphologies and/or flow characteristics deviate from the flow regimes of natural channels. The objectives of this study were to (1) characterize and compare the flow regimes of a wetland slough, a river, and a flow-regulated, human-made canal and (2) test the applicability of *C–Q* relationship models that have been traditionally used in channels with natural flow regimes to other channels that are different morphologically (channel) and hydrologically (flow regime). Predictions include the following: (1) the flow regime in the human-made canal will have the greatest variability compared to the slough and river; and (2) *C–Q* relationship models will be applicable in nonriverine channels to quantify the effect of flow on the behavior of water quality constituents.

2.2. Materials and Methods

2.2.1. Study Locations

Three channels were selected for this study: Shark River Slough, Peace River, and Hillsboro Canal, which are all located in southern Florida (Figure 2.2). This region broadly has a subtropical to tropical climate and relatively flat topography and is underlain by carbonate (karst) formations that hold groundwater (Lodge, 2010; Metz and Lewelling, 2009).

Shark River Slough is within Everglades National Park (ENP), a protected ecosystem comprising fresh-water wetlands, marshes, prairies, tidal flats, and mangroves (Sklar et al. 1999). The slough is a shallow, slow-moving, broad river with channel depths on the order of centimeters (Bolster et al. 2002) and is the primary pathway for surface-water flow through ENP mangroves (Sklar et al. 1999). Everglades National Park is underlain by porous marine limestone formations, including Miami Limestone

(Everglades National Park; Daroub et al. 2011). As part of a larger effort to drain the larger Everglades region for agriculture and urban development, discharges into Shark River Slough have been reduced by changes in the volume, timing, and distribution of water through regional canals, which diverted freshwater flows into the Atlantic Ocean (Sklar et al. 1999).

The Peace River starts in south-central Florida and flows southwest until it discharges into the Charlotte Harbor Estuary. The river drainage basin is 6086.47 sq km, with a length of approximately 168.98 km, and the basin geology consists of clastic sediments that overlie carbonate rocks (Table 2.1) (SWFWMD, 2002). The river, although a natural watercourse, has had its flow regime modified by land use activities such as phosphate mining, urbanization, and agricultural development (Kelly, 2001). This has resulted in the loss and channelization of some of the headwater tributaries and reduced surface inflows into the river (Kelly, 2001). However, much of the river corridor remains undeveloped; it has floodplains that support riparian vegetation, and the river flows unrestricted over its entire reach (Kelly, 2001). For example, the river reach at the town of Bartow, Florida, is within the upper river watershed (2139.33 sq km) and has abundant riparian vegetation and wetlands, including cypress and hardwood swamps (SWFWMD, 2002). Additionally, the channel reach is characterized by low bank heights and shallow bank slope angles (SWFWMD, 2002) and is sinuous. Given these channel and hydrologic characteristics, the Peace River most resembles a channel with a natural flow regime.

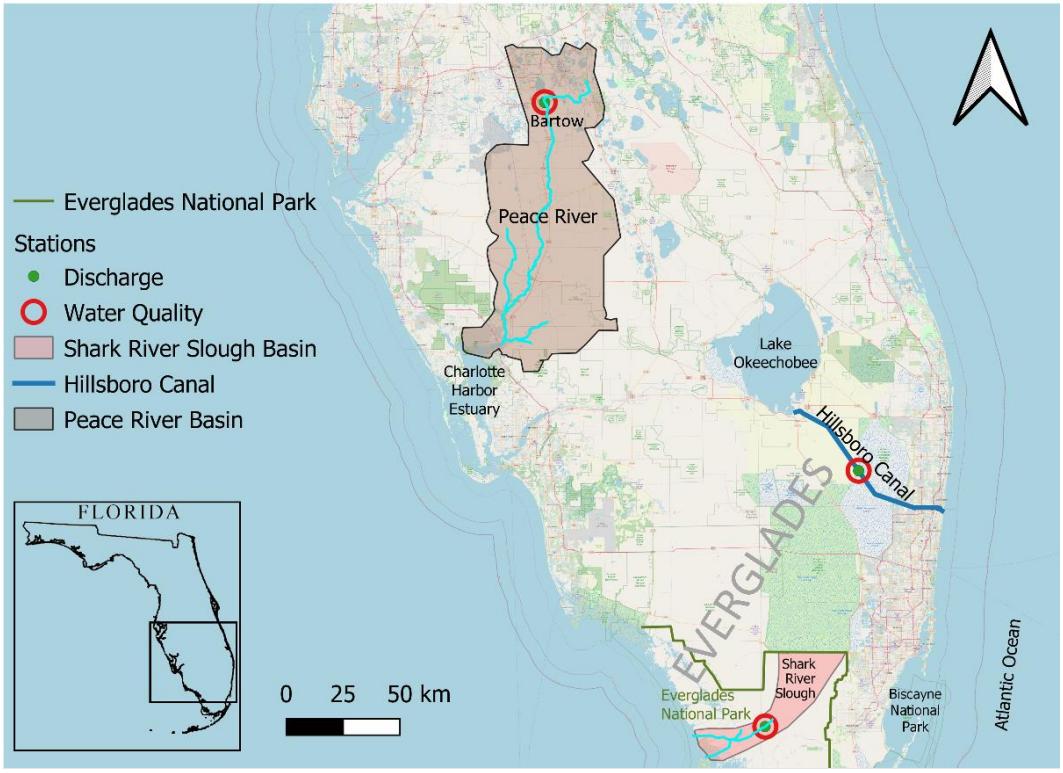

Figure 2.2 Locations of study sites: Shark River Slough, Peace River, and Hillsboro Canal.

The Hillsboro Canal is a major canal that originates from Lake Okeechobee and flows southeast, draining agricultural, wetland, and urban basins before discharging into the Atlantic Ocean (SWFMD, 2010). The geology of the canal basin is made up of the Fort Thompson formation, which consists of alternating layers of limestone, shell, sand, and marl punctured by solution holes, and the southern portion grades into the more porous Miami Limestone formation (Daroub et al. 2011). The Hillsboro Canal is one of the regional canals, constructed between 1910 and 1920, that was dredged to drain the Everglades and reroute freshwater, originally headed south, eastward into the ocean (Sklar et al. 1999).

Like all South Florida canals, the Hillsboro Canal lacks the natural channel features necessary to dissipate high-energy discharges, such as floodplains, but rather has levees and steep slopes to confine the flow to the channel and prevent overbank discharge (Carter, 2010; SWFMD, 2010). Discharge in the canal is managed via water control structures to prevent flooding, drain excess water from farmlands, convey watershed runoff, recharge the surficial aquifer, and prevent saltwater intrusion (Carter, 2010; SWFMD, 2010). The channelization and flow regulation in the Hillsboro Canal make it the most modified of the three channels in this study.

Table 2.1 General basin characteristics of the channels.

Channel	**Basin Size (sq. km)**	**Geology**	**Dominant Land Use**
Shark River Slough	1034	Miami Limestone	Wetland (100%)
Peace River	6086	Undifferentiated sand, shell and clay, underlain by carbonates, e.g., Suwannee Limestone and Hawthorn Group	Agriculture (40%)
Hillsboro Canal	479	Fort Thompson Formation	Agriculture (62%)

2.2.2 Data Collection

Discharge and water quality concentration data for fifteen years (2004–2018) were used in this study. The sites selected on the channels were Shark River Slough at Bottle Creek (SRS), Peace River at Bartow (PRB), and Hillsboro Canal at the S6 structure (HC6). Mean daily discharge data at SRS (25°28′04.8″ N, 80°51′16.2″ W) and HC6 (26°28′19.3″ N, 80°26′45.3″ W) were downloaded from the South Florida Water Management District's online data repository—DBHYDRO (https://www.sfwmd.gov/science-data/dbhydro, accessed on 12 January 2021). Mean daily discharge measurements for PRB (27°54′07.0″ N, 81°49′03.0″ W) were obtained from the United States Geological Survey-National Water Information System (https://waterdata.usgs.gov/nwis, accessed on 26 February 2020).

Water quality constituents, including total phosphorus (TP), nitrate-nitrite (NN), chloride (Cl), specific conductance (SC), total suspended solids (TSS), and turbidity, which varied over a range of temporal sampling resolutions, from daily to monthly, were considered for this study. At SRS, only SC, TP, and NN were available. Specific conductance was downloaded from DBHYDRO (25°28′04.8″ N, 80°51′16.2″ W), while TP and NN were obtained from the online repository of the Florida Coastal Everglades-Long Term Ecological Research [33] (https://fce-lter.fiu.edu/data/core/, accessed on 12 December 2019) at a site 130 m upstream from the discharge station (25°28′05.5″ N, 80°51′11.8″ W). At PRB, water quality constituent concentrations were retrieved from the Water Management Information System of the Southwest Florida Water Management District (https://www18.swfwmd.state.fl.us/ResData/Search/ExtDefault.aspx, accessed on 12 February 2020) (27°54′08.6″ N, 81°49′03.4″ W) at a station 50 m upstream from the

discharge station (27°54′08.6″ N, 81°49′03.4″ W), and at HC6, the water quality data were adjacent to the discharge station and were also retrieved from DBHYDRO.

2.2.3. Data Analysis

2.2.3.1. Flow Regime Characterization

The discharge data in each channel were analyzed using the IHA program developed by the Nature Conservancy (Richter et al. 1996; Nature Conservancy Manual, 2009). This program is free and user-friendly. The selected groups of hydrologic indices were the magnitude of annual flow conditions, frequency and duration of high and low pulses, and rate of change in water flow (see Table 2.2 for definitions). The Richards–Baker Flashiness Index (R-B Index), developed to determine the fluctuations in discharge relative to the total discharge (Baker et al. 2004), was calculated as an additional index of flow variability (Oueslati et al. 2015). Because hydrologic data are usually not normally distributed, nonparametric statistics were used in the IHA program to calculate the values of the hydrologic indices, and the median values were reported, except for the magnitudes, which were computed as the means (Nature Conservancy Manual, 2009).

Principal component analysis (PCA) was used to identify the dominant hydrological indices that best described the flow regimes of the three channels. Principal component analysis is a multivariate analysis tool that is primarily used to reduce the dimensionality of large data by transforming the original variables in a dataset into new uncorrelated variables known as principal components, and the new variables or axes are linear combinations of the starting variables (Sârbu et al. 2005). However, PCA can also be used to determine the relationships between variables and highlight the similarities and differences between categories (PCA Basics).

2.2.3.2. Concentration–Discharge (*C*–*Q*) relationships

The linear expression of the concentration–discharge (*C*–*Q*) relationship is written as follows:

$$\log_{10} C = \log_{10} a + b \log_{10} Q \qquad (2.2)$$

For each channel, discharge and constituent concentration data were paired by date. Since flow is regulated at HC6, the discharge data used were restricted to pumping events when the canal was flowing. The data pairs were then log-transformed and regressed to yield slopes (*b*) (Moatar et al. 2017), which were then used to understand the influence of flow on the concentrations of the water quality constituents. Student's t test was conducted to ascertain the statistical significance of *b* being different from zero, with a level of significance at $p < 0.05$ (O'Donnell and Hotchkiss, 2019; Botter et al. 2019) . *P* values lower than 0.05 indicated a significant log (*C*)-log (*Q*) slope; otherwise, *b* was not different from zero, which meant that the concentration was not discharge-dependent (Botter et al. 2019). Next, piecewise (segmented) linear regressions were conducted on *C*–*Q* relationships to detect the presence of inflections in the slopes, which would signify changes in the behavior of the water quality constituents with discharge (Rose et al. 2018). To do this, Davies' test from the 'segmented' package in the R programming language (R Core Team, 2019) was used to iteratively search across 10 quantiles of the explanatory variable (*Q*) for breakpoints in the slope (*b*) of the log (*C)*-log (*Q*) regression for each constituent, with $p < 0.05$ selected as the level of significance (Diamond and Cohen, 2018; O'Donnell and Hotchkiss, 2019). When the significance level was met, breakpoint analysis from the package was conducted to estimate two new regression

models, separated by an inflection in *b*. This indicated a change in the linear relationship between concentration and discharge (Muggeo, 2016; 2017). An ANOVA test of independence was then conducted on the slopes above and below the inflection points to determine if they were significantly different from zero (O'Donnell and Hotchkiss, 2019). Flow duration curves, which are one of the outputs of the IHA program, were used to calculate the probabilities of exceeding the discharge thresholds for the constituents that had slope inflections. All statistical analyses were conducted in the R programming language (R Core Team, 2019).

2.3. Results

2.3.1. Flow Regime Characterization

Flow regime characteristics differed between the three sites (Table 2.2). The 1-day minimum discharge was highest at PRB (river), while the 90-day minimum and 1- and 90-day maximum discharges were highest at HC6 (canal). The channels SRS (slough) and PRB had low frequencies of high pulse counts, while HC6 had the highest frequency of high pulse counts. SRS had the longest low-pulse duration (31 days), while PRB had the longest high-pulse duration (12 days), which was approximately twice (6.25 days) and four times (3 days) that of SRS and HC6, respectively. Conversely, HC6 had the highest hydrograph rise rate, fall rate, and highest flashiness (R-B Index) of the three channels. With consistently lower differences between low-flow and high-flow indices, the flow regime of SRS had the least variability, while HC6 had the greatest flow variability between the low- and high-flow indices and had the highest values across most hydrologic indices.

In the PCA, SRS and PRB were noticeably distinguished from HC6 (Figure 2.3). For instance, SRS and PRB were differentiated from HC6 by low pulse duration and low pulse count. Additionally, PRB was differentiated by the fall rate, high pulse duration, 1-day minimum discharge, and 90-day minimum and maximum discharges, while HC6 was differentiated by R-B Index, high pulse count, 1-day maximum discharge and rise rate (rise rate is highly correlated with R-B Index and is thus omitted for clearer illustration) (Figure 2.3).

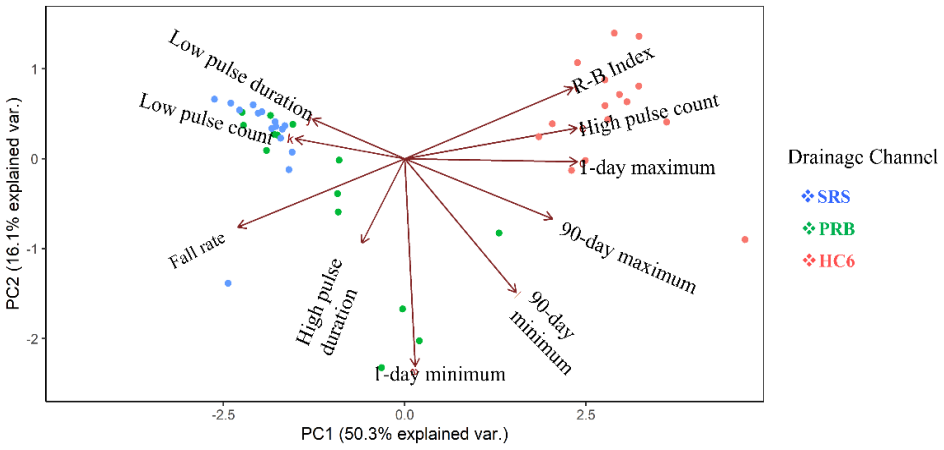

Figure 2.3 Principal component analysis plot of the hydrologic indices used to characterize the flow regimes of the SRS, PRB, and HC6.

Table 2.2 Calculated indicators of hydrologic alteration (IHA) (Richter et al. 1996, Nature Conservancy Manual) and Richards–Baker Flashiness Index (R-B Index) (Baker et al. 2004) for SRS (slough), PRB (river), and HC6 (canal) for the years 2004 to 2018.

Flow Regime Characteristics	**Description**	**Hydrologic Indices**	**Unit**	**SRS**	**PRB**	**HC6**
Magnitude	The mean (moving average) magnitude of minimum and maximum yearly flow conditions of various durations (daily to seasonal)	1-day minimum	m^3s^{-1}	0.002	0.052	0.000
		90-day minimum	m^3s^{-1}	0.111	0.580	1.538
		1-day maximum	m^3s^{-1}	0.878	27.160	76.780
		90-day maximum	m^3s^{-1}	0.782	7.147	22.980
Frequency	Number of yearly occurrences during which the magnitude of the water conditions exceeds an upper threshold (75%) or remains below a lower threshold (25%) of the long-term daily mean flows	Low pulse count	Count	2	6	0
		High pulse count	Count	4	4	20
Duration	Yearly duration of low and high flow pulses	Low pulse duration	Days	31.00	6.00	
		High pulse duration	Days	6.25	12.00	3.00
Rate of change	The rate of both positive (rise) and negative (fall) changes in the daily hydrographs during a year	Rise rate	m^3s^{-1} day^{-1}	0.03	0.12	6.31
		Fall rate	m^3s^{-1} day^{-1}	−0.03	−0.10	−6.95
Flashiness	Measurement of oscillations in discharge (day to day changes) relative to total discharge during a year	R-B Index	Unitless	0.04	0.09	0.47

2.3.2. Concentration–Discharge (C–Q) Relationships across the Channels

The flows in the channels had quantifiable impacts on the concentrations of water quality constituents (Table 2.3). At SRS and PRB, dilution patterns tended to dominate with higher flows (negative *b*), particularly for TP, NN, SC, and Cl (PRB only). Conversely, turbidity and TSS were enriched with higher flows in the PRB. At HC6, enrichment patterns were observed with higher flows (positive *b*) for TP, NN, and turbidity, and chemostatic patterns (*b*~0) were observed for TSS, SC, and Cl.

Piecewise regression analysis further revealed the presence of statistically significant slope inflections in the linear log (*C*)-log (*Q*) regressions for some water quality constituents across the channels (Table 2.4). Five of the nine possible (*C*–*Q*) archetypes were found across SRS, PRB, and HC6 combined. At SRS, NN exhibited the CA archetype, that is, chemostasis at low flow and dilution at high flow, while SC exhibited the AA archetype, signifying continual dilution with discharge (Figure 2.4).

Table 2.3 Log (C)-log (Q) regression slopes (*b*) for water quality constituents at SRS, PRB, and HC6 for the period 2004 to 2018.

Constituent	Channel	Data pairs (n)	Slope (*b*)
TP	SRS	155	−0.23 *
	PRB	173	−0.06 *
	HC6	382	0.22 *
NN	SRS	157	−0.38 *
	PRB	166	−0.24 *
	HC6	302	0.20 *
Turbidity	PRB	177	0.08 *
	HC6	64	0.30 *
TSS	PRB	151	0.21 *
	HC6	42	0.06
SC	SRS	4666	−0.28 *
	PRB	177	−0.15 *
	HC6	380	0.01
Cl	PRB	179	−0.26 *
	HC6	302	−0.02

* Significant *p* values ($p < 0.05$) indicate that the slope is significantly different from zero.

At PRB, four of the five water quality constituents with statistically significant slope inflections (NN, turbidity, TSS, and SC) exhibited the BA archetype, which is enriched at low flow and diluted at high flow (Figure 2.5). The fourth constituent, Cl, exhibited the AA archetype.

At HC6, TP exhibited the BB archetype—enrichment at both high and low flow—while NN and turbidity exhibited the CB archetype, which is chemostasis at low flow and enrichment at high flow (Table 2.4, Figure 2.6). The levels of significance for a change in slope according to Davies' test were marginal for turbidity (0.05) (Table 2.4). For SC, the archetype was CA, and although the *p* value for Davies' test was marginally significant at 0.04, ANOVA revealed that the slopes were not significantly different from zero. Furthermore, visual inspection of the *C–Q* plot shows that there is not truly a definite pattern (Figure 2.6).

Table 2.4 Piecewise (segmented) linear regression slopes (*b*) for water quality constituents that have statistically significant inflections in b (discharge thresholds) according to Davies' test for the different channels.

Channel	**Constituent**	**Davies' Test**	**Discharge Threshold (m^3s^{-1})**	**Exceedance Probability of Discharge Threshold**	**Piecewise Regression Slopes *(b)***		**Archetype**
					Low	High	
SRS	NN	$p = 0.0008$	0.46	0.56	−0.01	−1.81 *	CA
	SpC	$p < 0.0001$	0.74	0.22	−0.28 *	−0.20 *	AA
PRB	NN	$p < 0.0001$	1.05	0.58	0.51 *	−0.60 *	BA
	Turbidity	$p = 0.0004$	7.24	0.20	0.2 *	−0.32 *	BA
	TSS	$p = 0.0004$	8.91	0.17	0.36 *	−0.38 *	BA
	SpC	$p < 0.0001$	0.35	0.84	0.25 *	−0.19 *	BA
	Cl	$p < 0.0001$	1.74	0.43	−0.36 *	−0.19 *	AA
HC6	TP	$p < 0.0001$	23.82	0.15	0.12 *	0.87 *	BB
	NN	$p < 0.0001$	21.72	0.17	0.08	0.97 *	CB
	Turbidity	$p = 0.05$	4.39	0.40	0.12	0.59 *	CB
	SpC	$p = 0.04$	70.96	0.015	0.02	−4.73	CA

Significant *p* values at 0.05 (*) according to ANOVA test of independence indicating slopes are significantly different from zero.

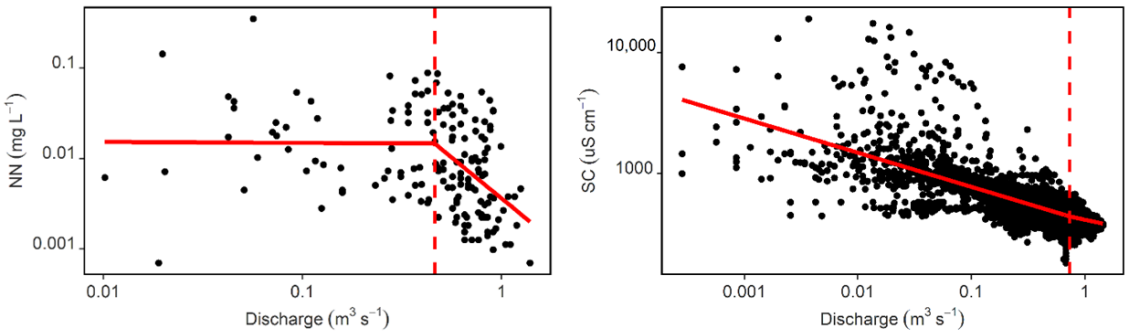

Figure 2.4 Concentration–discharge (C–Q) relationship plots for nitrate-nitrite (NN) and (b) specific conductance (SC) with discharge thresholds at SRS.

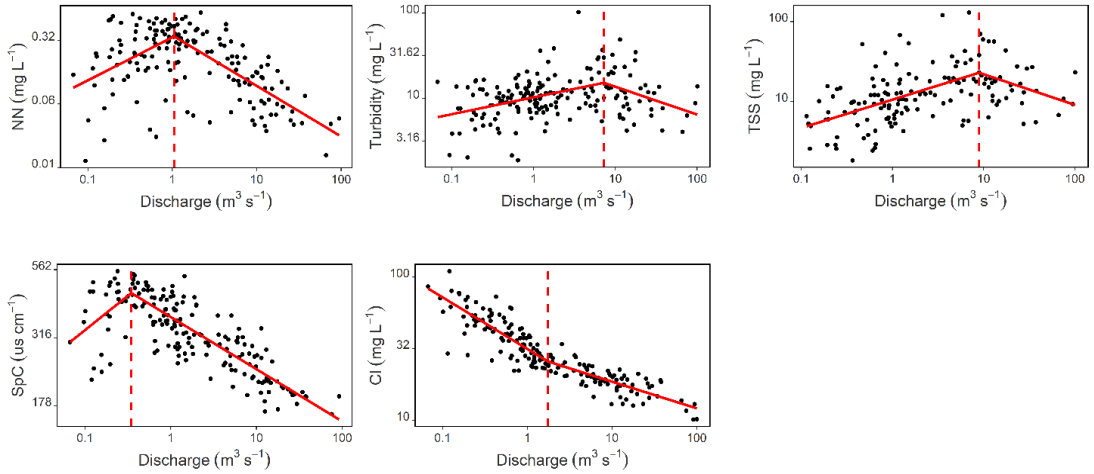

Figure 2.5 Concentration–discharge (C–Q) relationship plots for water quality constituents with discharge thresholds at PRB.

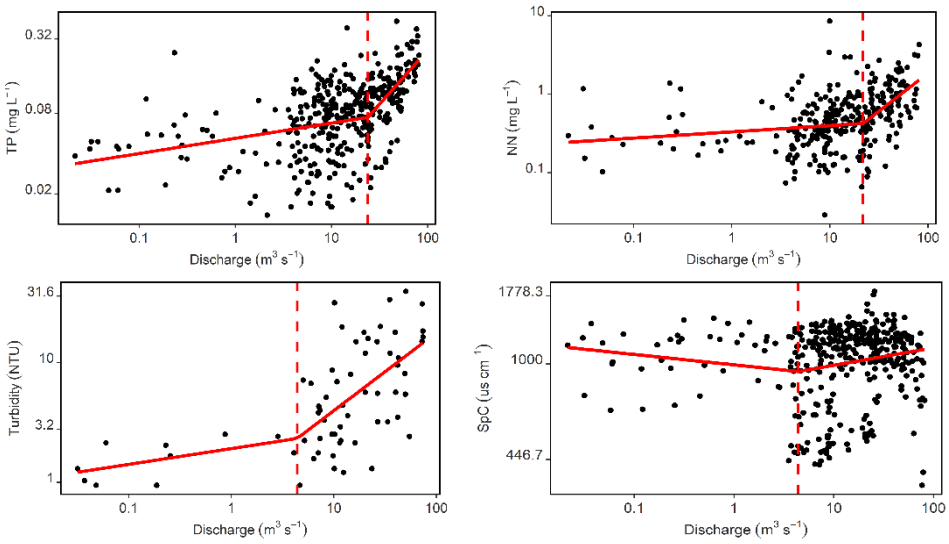

Figure 2.6 Concentration–discharge (C–Q) relationship plots for water quality constituents with discharge thresholds at HC6.

2.4. Discussion

2.4.1. Impacts of Flow Regime Characteristics on Water Quality in the Channels

The longer low pulse duration at SRS translates into a longer residence time of low flow conditions where biogeochemical transformation can dominate water quality constituent behavior (Moatar et al. 2017). Furthermore, the low magnitude and flow variability at SRS, combined with the low pulses, resulted in chemostatic and dilution behavior and the absence of enrichment behavior.

At PRB, a recurring behavior of the water quality constituents was an initial enrichment in concentrations at low flow followed by dilution at high flow (BA in Table 2.4, Figure 2.5). The flow regime characteristic most responsible for this is the high pulse duration. Previous studies suggest that low flow concentration enrichment can result from the abundance and proximity of widespread constituent pools that are easily exported and mobilized to (or from) the channels (Diamond and Cohen, 2018; Zhang, 2018; O'Donnell and Hotchkiss, 2019), while the switch to dilution at high flows is indicative of constituent exhaustion (source limitation)

(Moatar et al. 2017; Diamond and Cohen, 2018; Zhang, 2018). Key reasons for the exhaustion of constituents in the PRB are the extensive high flow duration, the presence of riparian vegetation, and gentle channel slopes. As a result, there is ample opportunity for the extended deposition of water quality constituents from the channels into the floodplains (Richter et al. 1998; O'Donnell and Hotchkiss, 2019). Additionally, the high frequency of low pulses at the PRB indicates more in-channel sediment deposition (Graf, 2006: Hayes et al. 2018).

Channel HC6 had the greatest flow variability, which resulted in strong enrichment behavior at high flow. The unnatural and regulated discharges at HC6 resulted in higher flashiness and steeper hydrographs that contributed to the increases in the concentrations of water quality constituents. Flashier hydrologic responses have been linked to higher concentrations of nutrients, turbidity, and TSS from channel erosion and sediment mobilization (Shields et al. 2010). The results from a comparative study between a rural incised (channelized) stream and an urban unchanneled stream revealed a flashier hydrologic response and higher concentrations of water quality constituents in the rural stream for all measured components except nitrate (Shields et al. 2010). Just as storm events are periods of high sediment mobilization (Rose et al. 2018), so are canal discharge events, which explain the predominant enrichment behavior at HC6. The higher frequency of high pulse flows at HC6 translates into a greater export of sediment loads and the constituents they contain, such as TP. Furthermore, the absence of floodplains at HC6 means that a greater volume of water quality constituents and pollutant loads can be transported downstream into ecologically sensitive ecosystems. The clear differentiation of HC6 from the PRB and SRS, as shown by the PCA, alludes to the fundamental differences between natural and human-made channels. The high discharge maximums, pulse count, rise rate, and flashiness reflect the regulated flow management in the canal as well as the

channel homogeneity. This contrasts with the slough and the river that have more natural heterogeneous features and generally lower values for their flow regime characteristics.

2.4.2. Behavior of Water Quality Constituents at Low and High Flow Conditions across the Channels

All three channels had discharge thresholds for NN. The low flow chemostasis for NN at SRS and HC6 can be attributed to greater biogeochemical control on NN availability. Nitrogen species are biogeochemically active and can have high turnover rates (Musolff et al. 2015). This rapid cycling of NN between biotic and abiotic pools can regulate availability and can lead to a chemostatic response at low flow. For most of the water quality constituents in the PRB, NN exhibited a shift from low flow enrichment to high flow dilution. In Florida, NN-rich groundwater discharge that dominates at low flow conditions may be diluted with NN-poor temporary pools (rainfall and soil water) that are activated during high flow conditions, resulting in a shift from enrichment to dilution (Diamond and Cohen, 2018; Rose et al. 2018).

Although the Upper Peace River watershed mainly recharges the groundwater, high flow periods can raise the groundwater head higher than the river stage, which then discharges into the channel and is facilitated by the porous kart formations (sinkholes and sand-filled depressions) (Metz and Lewelling, 2009). At HC6, the low flow chemostasis of NN reflects the biogeochemical influence from the buildup of nutrient legacy stores that is typical of managed agricultural systems (Rose et al. 2018; Basu et al. 2011). Conversely, the high flow enrichment indicates that higher discharges are responsible for the internal release and subsequent transport of NN in the canal.

For Cl at PRB, the greater dilution at low flow and the lesser dilution at high flow can be attributed to a point source contribution from the watershed. Dilution is common for Cl because

it is not significantly altered by biogeochemical processes, making it a good conservative tracer (Jarvie et al. 2012). Specific conductance followed the dominant PRB pattern of dilution, but the discharge threshold occurred at a lower value compared to the other constituents, suggesting a relatively scarce pool of the constituent that is quickly diluted. Although the Shark River Slough is tidal, SRS is within the upstream freshwater zone, which accounts for the dilution of SC with increasing discharge. At HC6, the high variability of SC with discharge could result from the multiple natural sources of ions in the Everglades region, including trapped seawater in groundwater intersected by canals (Chen et al. 2006). In addition, the complexities associated with canal discharge operations may have contributed to its high concentration variability.

Of the three channels, HC6 had a discharge threshold for TP, with moderate enrichment occurring at low flow and high enrichment at high flow. Under low flow conditions, more phosphorus (P) can be retained in the channel and cycled physiochemically through sorption–desorption reactions and mineral precipitation–dissolution processes and biologically through biotic uptake and decomposition of organic matter (Withers and Jarvie, 2008). However, as flow increases, P can be transported through advection, which can cause entrainment of sediment-bound particulate P and desorption of P from suspended particles (Withers and Jarvie, 2008; Diamond and Cohen, 2018). Decades of continuous nutrient loading from agriculture to South Florida canals, including the Hillsboro Canal, have led to the sequestration of P, often referred to as “legacy P” in canal sediments (Diaz et al. 2006). These sediments are highly organic and have low bulk density that makes them easily entrained and susceptible to downstream transport (Daroub et al. 2002a; Das, 2010).

At PRB, turbidity and TSS had identical behavior and discharge thresholds, indicating the similarity between the two sediment-associated constituents. The low flow enrichment of TSS results from outer bank erosion and entrainment of particles from the channel bed (Rose et al. 2018), while the change to dilution at high flow indicates an exhaustion of the eroded sediments and their deposition in the floodplains (Zhang et al. 2018). At HC6, the strong enrichment behavior at high flow for turbidity results from transport limitation, whereby higher flows allow more connectivity between the watershed and the channel and lead to greater mobilization and transport of sediments (Moatar et al. 2017).

2.4.3. Limitations on the Use of C–Q Relationship Models of Human-made and Regulated Channels

Unlike natural channels that may be free flowing, the human-made canals of South Florida do not flow freely; rather, their discharges are managed to meet the water needs of the region. As a result, canals exhibit extended periods of zero flow with stagnant conditions punctuated by short durations of high flows. Therefore, the *C–Q* relationship models could only explain the behavior of water quality constituents for periods where there was flow. This resulted in the flow exceedance probabilities of the water quality constituents with discharge thresholds at HC6 being consistently lower than the median discharge (0.5 flow exceedance probability). Median discharge is commonly used in natural channels, especially when analyzing riverine networks, as opposed to individual channels (Moatar et al. 2017; Diamond and Cohen, 2018; Botter et al. 2019). Consequently, median discharge may not always be the appropriate metric to use as the discharge threshold in *C–Q* slopes for singular channels or nonriverine channels. Furthermore, at HC6, a direct interpretation for the low discharge threshold probabilities (especially for TP and NN) is that the potential of canal flows mobilizing higher concentrations

of these constituents is low. This means that the flows at HC6 that can export nutrients occur infrequently; however, the discharge thresholds and their associated probabilities will vary at other locations along the Hillsboro Canal and other South Florida canals depending on discharge operations. Therefore, *C–Q* relationships in such canals are useful in the determination of discharge that can limit the transport of nutrients to sensitive ecosystems, which can be a potential benefit to water resource managers.

2.5. Conclusions

This study described the relationships between water quality and flow in three morphologically and hydrologically different channels in southern Florida: the Shark River Slough, Peace River, and Hillsboro Canal. The unchanneled and shallow Shark River Slough exhibited the least flow variability, which when combined with its naturally nutrient-poor conditions, resulted in predominantly dilution behavior of its water quality constituents at higher flows. The meandering Peace River, whose characteristics most resemble a natural flow regime, exhibited intermediate flow variability. Furthermore, the Peace River had the highest pulse duration that afforded an extended temporal connectivity to its floodplains and resulted in dilution behavior of all the water quality constituents at higher flows. The heavily channelized Hillsboro Canal, whose flow regime is regulated by water control structures, had the greatest flow variability and was dominated by the enrichment behavior of its water quality constituents with higher flows. This study found that *C–Q* relationships can be applied to canals and should be considered by water managers in discharge operations to reduce the transport of nutrient and pollutant loads downstream to ecologically delicate ecosystems.

2.6. References

Baker, D.B., Richards, R.P., Loftus, T.T. and Kramer, J.W., 2004. A new flashiness index: Characteristics and applications to midwestern rivers and streams 1. *JAWRA Journal of the American Water Resources Association*, *40*(2), pp.503-522.

Basu, N.B., Thompson, S.E. and Rao, P.S.C., 2011. Hydrologic and biogeochemical functioning of intensively managed catchments: A synthesis of top-down analyses. *Water Resources Research*, *47*(10).

Bolster, C.H. and Saiers, J.E., 2002. Development and evaluation of a mathematical model for surface-water flow within the Shark River Slough of the Florida Everglades. *Journal of Hydrology*, *259*(1-4), pp.221-235.

Botter, M., Burlando, P. and Fatichi, S., 2019. Anthropogenic and catchment characteristic signatures in the water quality of Swiss rivers: a quantitative assessment. *Hydrology and Earth System Sciences*, *23*(4), pp.1885-1904.

Brooker, M.P., 1985. The ecological effects of channelization. *The Geographical Journal*, *151*(1), pp.63-69.

Carter, K., Redfield, G., Ansar, M., Glenn, L., Huebner, R., Maxted, J., Pettit, C. and VanArman, J., 2010. Canals in South Florida: A technical support document.

Chen, M., Daroub, S.H., Lang, T.A. and Diaz, O.A., 2006. Specific conductance and ionic characteristics of farm canals in the Everglades Agricultural Area. *Journal of environmental quality*, *35*(1), pp.141-150.

Conservancy, N., 2009. Indicators of Hydrologic Alteration (IHA) Software Version 7.1 User's Manual. *The Nature Conservancy: Charlottesville, VA, USA*.

Daroub, S.H., Stuck, J.D., Lang, T.A. and Diaz, O.A., 2002. Particulate phosphorus in the everglades agricultural area: I–Introduction and sources. *Soil Water Department of University of Florida IFAS Extension Publication SL*, *197*.

Daroub, S.H., Van Horn, S., Lang, T.A. and Diaz, O.A., 2011. Best management practices and long-term water quality trends in the Everglades Agricultural Area. *Critical Reviews in Environmental Science and Technology*, *41*(S1), pp.608-632.

Das, J., 2010. *Characterization of physicochemical properties, phosphorus (P) fractions and P release of the Everglades Agricultural Area (EAA) canal sediments*. University of Florida.

Das, J., Daroub, S.H., Bhadha, J.H., Lang, T.A. and Josan, M., 2012. Phosphorus release and equilibrium dynamics of canal sediments within the Everglades Agricultural Area, Florida. *Water, Air, & Soil Pollution*, *223*, pp.2865-2879.

Diamond, J.S. and Cohen, M.J., 2018. Complex patterns of catchment solute–discharge relationships for coastal plain rivers. *Hydrological Processes*, *32*(3), pp.388-401.

Diaz, O.A., Daroub, S.H., Stuck, J.D., Clark, M.W., Lang, T.A. and Reddy, K.R., 2006. Sediment inventory and phosphorus fractions for water conservation area canals in the Everglades. *Soil Science Society of America Journal*, *70*(3), pp.863-871.

Everglades National Park (U.S. National Park Service). Available online: https://www.nps.gov/ever/learn/nature/evergeology.htm (accessed on 31 July 2021).

Gaiser, E.; Childers, D. Water Quality Data (Grab Samples) from the Shark River Slough, Everglades National Park (FCE), from May 2001 to Present. Environmental Data Initiative. 2019. Available online: https://agris.fao.org/agris-search/search.do?recordID=QN2019001307404 (accessed on 12 December 2019).

Godsey, S.E., Kirchner, J.W. and Clow, D.W., 2009. Concentration–discharge relationships reflect chemostatic characteristics of US catchments. *Hydrological Processes: An International Journal*, *23*(13), pp.1844-1864.

Graf, W.L., 2006. Downstream hydrologic and geomorphic effects of large dams on American rivers. *Geomorphology*, *79*(3-4), pp.336-360.

Hayes, D.S.; Brändle, J.M.; Seliger, C.; Zeiringer, B.; Ferreira, T.; and Schmutz, S.,2018. Advancing towards functional environmental flows for temperate floodplain rivers. Sci. Total Environ. 633, 1089–1104, doi:10.1016/j.scitotenv.2018.03.221.

Jarvie, H.P., Sharpley, A.N., Scott, J.T., Haggard, B.E., Bowes, M.J. and Massey, L.B., 2012. Within-river phosphorus retention: accounting for a missing piece in the watershed phosphorus puzzle. *Environmental Science & Technology*, *46*(24), pp.13284-13292.

Kelly, M., 2001. Peace River Comprehensive Watershed Management Plan Draft. I. *Brooksville, FL: Np Print*.

Lodge, T.E., 2010. *The Everglades handbook: understanding the ecosystem*. 3rd ed.; CRC Press: Cleveland, OH, USA, 2010; 424p.

Malan, H.L. and Day, J.A., 2003. Linking flow, water quality and potential effects on aquatic biota within the Reserve determination process. *Water SA*, *29*(3), pp.297-304.

Metz, P.A. and Lewelling, B.R., 2009. *Hydrologic conditions that influence streamflow losses in a karst region of the upper Peace River, Polk County, Florida*. US Department of the Interior, US Geological Survey.

Moatar, F., Abbott, B.W., Minaudo, C., Curie, F. and Pinay, G., 2017. Elemental properties, hydrology, and biology interact to shape concentration-discharge curves for carbon, nutrients, sediment, and major ions. *Water Resources Research*, *53*(2), pp.1270-1287.

Muggeo, V.M. and Muggeo, M.V.M., 2017. Package 'segmented'. *Biometrika*, *58*(525-534), p.516.

Muggeo, V.M.R., 2016. Testing with a nuisance parameter present only under the alternative: A score-based approach with application to segmented modelling. J. Stat. Comput. Simul. 86, 3059–3067, doi:10.1080/00949655.2016.1149855.

Musolff, A., Schmidt, C., Selle, B. and Fleckenstein, J.H., 2015. Catchment controls on solute export. *Advances in Water Resources*, *86*, pp.133-146.

National Academies of Sciences, Engineering, and Medicine. 2022. Progress Toward Restoring the Everglades: The Ninth Biennial Review-2022.

Nilsson, C. and Renöfält, B.M., 2008. Linking flow regime and water quality in rivers: a challenge to adaptive catchment management. *Ecology and Society*, *13*(2).

O'Driscoll, M., Clinton, S., Jefferson, A., Manda, A. and McMillan, S., 2010. Urbanization effects on watershed hydrology and in-stream processes in the southern United States. *Water*, *2*(3), pp.605-648.

O'Donnell, B. and Hotchkiss, E.R., 2019. Coupling concentration-and process-discharge relationships integrates water chemistry and metabolism in streams. *Water Resources Research*, *55*(12), pp.10179-10190.

Oueslati, O., De Girolamo, A.M., Abouabdillah, A., Kjeldsen, T.R. and Lo Porto, A., 2015. Classifying the flow regimes of Mediterranean streams using multivariate analysis. *Hydrological Processes*, *29*(22), pp.4666-4682.

PCA basics in #Rstats. Available online: https://swampthingecology.org/blog/pca-basics-in-rstats/ (accessed on 8 May 2021).

Poff, N.L., Allan, J.D., Bain, M.B., Karr, J.R., Prestegaard, K.L., Richter, B.D., Sparks, R.E. and Stromberg, J.C., 1997. The natural flow regime. *BioScience*, *47*(11), pp.769-784.

R Core Team. 2019. R: A language and environment for statistical computing. R Foundation for Statistical Computing, Vienna, Austria. Available online: https://www.R-project.org/ (accessed on 8 May 2021).

Reddy, K.R., Diaz, O.A., Scinto, L.J. and Agami, M., 1995. Phosphorus dynamics in selected wetlands and streams of the Lake Okeechobee Basin. *Ecological Engineering*, *5*(2-3), pp.183-207.

Reddy, K.R., Newman, S., Osborne, T.Z., White, J.R. and Fitz, H.C., 2011. Phosphorous cycling in the greater Everglades ecosystem: legacy phosphorous implications for management and restoration. *Critical Reviews in Environmental Science and Technology*, *41*(S1), pp.149-186.

Richter, B.D., Baumgartner, J.V., Braun, D.P. and Powell, J., 1998. A spatial assessment of hydrologic alteration within a river network. *Regulated Rivers: Research & Management: An International Journal Devoted to River Research and Management*, *14*(4), pp.329-340.

Ritcher, B.D., Baumgartner, J.V., Powell, J. and Braun, D.P., 1996. A method for assessing hydrologic alteration within ecosystem. *Conservation Biology*, *10*(4), pp.1163-1174.

Rose, L.A., Karwan, D.L. and Godsey, S.E., 2018. Concentration–discharge relationships describe solute and sediment mobilization, reaction, and transport at event and longer timescales. *Hydrological processes*, *32*(18), pp.2829-2844.

Sârbu, C. and Pop, H.F., 2005. Principal component analysis versus fuzzy principal component analysis: a case study: the quality of Danube water (1985–1996). *Talanta*, *65*(5), pp.1215-1220.

Schmutz, S. and Sendzimir, J., 2018. *Riverine ecosystem management: Science for governing towards a sustainable future*. Springer Nature.

Schoof, R., 1980. Environmental impact of channel modification 1. *JAWRA Journal of the American Water Resources Association*, *16*(4), pp.697-701.

Shields Jr, F.D., Lizotte Jr, R.E., Knight, S.S., Cooper, C.M. and Wilcox, D., 2010. The stream channel incision syndrome and water quality. *Ecological engineering*, *36*(1), pp.78-90.

Sklar, F., McVoy, C., Van Zee, R., Gawlik, D., Swift, D., Park, W., Fitz, C., Wu, Y., Rudnick, D., Fontaine, T. and Miao, S., 1999. Hydrologic needs: the effects of altered hydrology on the Everglades. *Everglades Interim Report, SFWMD, West Palm Beach, FL, USA*.

SWFMD. Canals in South Florida: A Technical Support Document. Appendix A. Basic Concepts, Hydrologic Terminology. Glossary of Terms and Abbreviations. 2010, A1–22. Available online: https://www.sfwmd.gov/sites/default/files/documents/canalssfl_appendixa-c.pdf (accessed on 8 May 2021).

SWFWMD. Upper Peace River: An Analysis of Minimum Flows and Levels. Volume 2: Technical Appendices. 2002, pp. 1–294. Available online: https://www.researchgate.net/profile/CliffordDahm/publication/267260603_A_Review_of_Upper_Peace_River_An_Analysis_of_Minimum_Flows_and_Levels_Prepared_by/links/549b39730cf2b803713719ea/A-Review-of-Upper-Peace-River-An-Analysis-of-Minimum-Flows-and-Levels-Prepared-by.pdf (accessed 8 May 2021)

Thompson, S.E., Basu, N.B., Lascurain Jr, J., Aubeneau, A. and Rao, P.S.C., 2011. Relative dominance of hydrologic versus biogeochemical factors on solute export across impact gradients. *Water resources research*, *47*(10).

Underwood, K.L., Rizzo, D.M., Schroth, A.W. and Dewoolkar, M.M., 2017. Evaluating spatial variability in sediment and phosphorus concentration-discharge relationships using Bayesian inference and self-organizing maps. *Water Resources Research*, *53*(12), pp.10293-10316.

Withers, P.J.A. and Jarvie, H.P., 2008. Delivery and cycling of phosphorus in rivers: a review. *Science of the total environment*, *400*(1-3), pp.379-395.

Wohl, E., 2015. Legacy effects on sediments in river corridors. *Earth-Science Reviews*, *147*, pp.30-53.

Zhang, Q., 2018. Synthesis of nutrient and sediment export patterns in the Chesapeake Bay watershed: Complex and non-stationary concentration-discharge relationships. *Science of the Total Environment*, *618*, pp.1268-1283.

CHAPTER 3: HIGH-RESOLUTION ESTIMATION OF SUSPENDED SOLIDS AND PARTICULATE PHOSPHORUS USING ACOUSTIC DEVICES IN A HYDROLOGICALLY MANAGED CANAL IN SOUTH FLOd5RIDA, USA

Onwuka, I.S.; Scinto, L.J.; Fugate, D.C. (2023). High-Resolution Estimation of Suspended Solids and Particulate Phosphorus Using Acoustic Devices in a Hydrologically Managed Canal in South Florida, USA. *Sensors*, 23, 2281. https://doi.org/10.3390/s23042281

Abstract

Conventional methods of measuring total suspended sediments (TSS) and total particulate phosphorus (TPP) are typically low-resolution and miss critical processes that impact their exports in aquatic environments. To create high-resolution TSS and TPP estimates, echo intensity (EI), a biproduct of velocity measurements from acoustic devices, was utilized. An acoustic Doppler velocimeter (ADV) and an acoustic Doppler current profiler (ADCP) were deployed in three locations in the L-29 Canal in South Florida, USA, to obtain estimates near the canal bed and in the water column, respectively. Corrections for transmission losses from the ADCP proved unnecessary due to the low vertical variability in the measured EI. EI calibrations were performed using artificially created TSS obtained from bed sediments (ADV) and gravimetrically measured TSS from water samples that matched the depths and times of the ADCP deployments. The measured TSS values were then analyzed for total phosphorus and converted to TPP estimates. The results showed that high TSS and TPP were caused by the rapid discharge releases typical of managed canals. This work demonstrates that high-resolution estimates are imperative for assessing the effects of such swift hydrologic changes on the potential export of sediments and nutrients to delicate ecosystems downstream.

3.1. Introduction

The movement of suspended sediments impacts the quality of aquatic systems, including freshwater environments, because they transport particulate nutrients (Kronvang et al. 1997; Wood, 1997; Gartner, 2002; Latosinski et al. 2014). Phosphorus (P) is one such nutrient (Noe et al. 2007; 2010; Zhao et al. 2015), and excess P is responsible for adverse water quality effects, such as eutrophication and harmful algal blooms (Dorioz et al. 1998; Jordan-Meille et al. 2004). Because of hydrologic and biogeochemical processes, suspended sediments and their associated nutrients are dynamic in space and time. Therefore, high-resolution measurements are necessary to fully evaluate the conditions that can increase sediment and nutrient loadings to enable the restoration and preservation of impaired aquatic systems (Gartner, 2002; 2004: Rai and Kumar, 2015, Harrison et al. 2021).

Total suspended sediment (TSS) concentrations are generally determined in two ways, namely, through direct and surrogate methods. Direct methods involve the conventional collection of water samples via bottles and pumps, which are then analyzed gravimetrically in the laboratory (Gartner, 2004; Dwinovantyo et al. 2017; Öztürk, 2017). This method is usually expensive and labor intensive, often requiring costly field sampling techniques and laboratory protocols; intrusive, as delicate flocculated aggregates can easily be broken down during sample retrieval or handling; and, in some instances, sampling is physically impossible or dangerous for field personnel (Gray and Gartner, 2009; Cristiano, 2010; Dominguez Ruben et al. 2020). Furthermore, the collected samples may not be representative of the range of conditions in aquatic systems due to the low temporal and spatial resolutions of the sampling regimes employed (Gartner, 2002; Gray and Gartner, 2009; Öztürk, 2017).

Surrogate methods are indirect ways of estimating TSS concentrations without a reliance on water sample collection and can thus be implemented autonomously (Öztürk, 2017). Examples of surrogate methods include optical backscatter sensors, transmissometers, laser diffraction, and acoustic devices, which all make nonintrusive high-temporal-resolution estimates of TSS (Fugate et al. 2003; Gartner, 2004; Öztürk, 2017). Acoustic devices are resistant to biofouling, unlike optical backscatter sensors (Schoellhamer and Wright, 2003; Hamilton et al. 1998), and can also make high-resolution spatial measurements (Öztürk, 2017; Dominguez Ruben et al. 2020).

Commonly used acoustic devices include acoustic Doppler velocimeters (ADVs) and acoustic Doppler current profilers (ADCPs). These devices are primarily velocity instruments that measure the frequency shift (Doppler shift) of transmitted sound waves (back) scattered by suspended materials in the water and convert the sound waves or echoes to three-dimensional (north/south, east/west, and vertical) flow velocities (Gartner, 2004; Kostaschuk et al. 2005; Öztürk, 2017). Acoustic Doppler velocimeters (ADVs) make single-point velocity measurements for a small water volume (measurement volume) at a point approximately 5–10 cm away from the device (Öztürk, 2017). Acoustic Doppler current profilers (ADCPs) can further provide velocity by splitting reflected sound signals into segments (range gating) so that velocities of water current can be determined at preset or user-predetermined intervals along the acoustic path (called cells or bins) (Gartner, 2004). ADCPs have the added advantage of providing data that reflect conditions across large areas in the water column (Öztürk, 2017).

Backscattered sound waves (acoustic backscatter) from ADV and ADCP velocity measurements have been used to estimate TSS in aquatic systems (Thevenot, et al. 1992; Fugate et al. 2003; Gartner, 2004; Wall et al. 2006; Chanson et al. 2008; Landers et al. 2016;

Dwinovantyo et al. 2017). The fundamental theory is that acoustic waves moving through water containing sediments scatter and attenuate depending on the characteristics of the fluid, sediment (concentration, shape size), and acoustic device (Landers et al. 2016). Furthermore, adjustments (corrections) are usually introduced to account for the influence of the fluid and device characteristics (Landers et al. 2016; Öztürk, 2017). Estimates of TSS are obtained by calibrating the acoustic backscatter with actual measured TSS from the deployment site using regressions (Fugate et al. 2002; Gartner, 2004). This calibration can then be used to provide a time series of TSS estimates during the deployment of the acoustic sensor at the site.

Although high-resolution estimates of TSS now exist, there is still a need to develop similar estimates for sediment-associated constituents such as particulate phosphorus to monitor and prevent excessive nutrient loading into delicate ecosystems. Studies have found higher concentrations of TSS and phosphorus during high discharge events in rivers and canals, with sediment resuspension and desorption of sediment P highlighted as potential reasons for such high concentrations (Diamond and Cohen, 2018; Onwuka et al. 2021).

The human-made canals of South Florida (home of the Everglades) were constructed to meet the agricultural, urban, and environmental needs of the region (Carter et al. 2010; Harvey et al. 2011). Discharges in these canals are highly managed through inflow structures (Carter et al. 2010), and it is not uncommon to have large masses of water discharged into canals over relatively short periods. Therefore, there is a need to understand how rapid discharge releases can impact the export of sediments and phosphorus into the receiving oligotrophic Everglades wetlands. The objectives of this study were to (1) use acoustic backscatter to develop high-resolution TSS and TPP estimates in a major South Florida canal and (2) evaluate how canal discharges can impact the downstream export of TSS and TPP.

3.2. Materials and Methods

3.2.1. Instrumentation

3.2.1.1. Characteristics and Limitations of Acoustic Devices

Acoustic devices collect many types of data, including velocity, signal amplitude/signal-to-noise ratio (SNR), correlation coefficient, temperature, and pressure (Table 1). Velocity is typically the primary parameter of interest, while the signal amplitude and correlation are used to provide data quality information (Velasco and Huhta, 2010). The main purpose of the signal amplitude is to determine if there are enough particles in the water, making it an excellent illustration of sediment dynamics and fluctuations (Sontek, 2001). This signal amplitude constitutes the acoustic backscatter parameter used as a surrogate for total suspended solids. The signal amplitude data are usually accessed from the device as either signal amplitude (units of counts) or the SNR. For SONTEK instruments, the SNR is obtained from the signal amplitude by subtracting the ambient, background electronic noise level and converting it to decibel units (dB) (multiplying by 0.43) (Sontek, 2001). To obtain accurate velocity measurements, SNR values must be at least 5 dB (ADV) and 3 dB (ADCP) (Table 3.1). An SNR value of 0 dB indicates that the water is too clear and that there is no distinction between the signal (acoustic energy) and the ambient noise level (Sontek, 2001; Velasco, and Huhta, 2010). The ADV uses the correlation coefficient as a second data quality parameter, and it is expressed as a percentage. A correlation score of 100% means reliable low-noise velocity measurements, which occur at an SNR level of approximately 15 dB, while a 0% correlation reflects velocity measurements dominated by noise (Sontek, 2001; Velasco, and Huhta, 2010). Interferences that can lead to low correlation values include high velocities, turbulence, and aerated water. A score of 70% or higher indicates accurate velocity data (Sontek, 2001).

Table 3.1 Characteristics of acoustic devices manufactured by SONTEK—a Xylem brand.

Parameters	Acoustic Doppler Velocimeters (ADVs)	Argonaut Acoustic Doppler Current Profilers (ADCPs)	References
Sampling volume distance/Max profiling range	5–18 cm	40 m	(Sontek, 2001; Current profiling solutions brochure)
Max depth range	60–400 m	10–200 m	Current profiling solutions brochure, Acoustic Doppler Velocimeters-Xylem)
Min blanking distance	-	0.07 m	(Sontek, 2009)
Bin size	-	0.2–30 m	(Sontek, 2009)
Max number of bins	-	10 + 1	Current profiling solutions brochure; Sontek, 2009)
Pressure sensor	0.1% accuracy	0.1% accuracy	(Acoustic Doppler Velocimeters-Xylem; Argonaut-XR)
Temperature Resolution, Accuracy	0.01 °C ± 0.1 °C	0.01 °C ± 0.1 °C	(Acoustic Doppler Velocimeters-Xylem; Argonaut-XR)
Velocity accuracy, resolution	1% of measured velocity, 0.01 cm s^{-1}	±1% of measured velocity, 0.1 cm s^{-1}	(Acoustic Doppler Velocimeters-Xylem; Argonaut-XR)
Min and max velocity	0.1 cm s^{-1}–5 m s^{-1}	<0.01 m s^{-1}–6.0 m s^{-1}	(Sontek, 2001; Acoustic Doppler Velocimeters-Xylem; Sontek, 2009)
Min Signal to Noise Ratio (SNR) for reliable velocity measurements	5 dB	3 dB	(Sontek, 2001; Sontek, 2009)
Min correlation coefficient for reliable velocity measurements	>=70%	-	(Sontek, 2001)

3.2.1.2. Acoustic Method

The conversion of the acoustic backscatter to TSS estimates (TSS) requires a series of steps that are summarized in this equation:

$$\mathrm{TSS} = 10^{[\mathrm{A}+\mathrm{B}*\mathrm{RB}]} \quad (3.1)$$

where A—intercept, B—slope, and RB—relative acoustic backscatter.

The exponent of Equation (1) contains a term for the relative acoustic backscatter, RB, measured by the acoustic device, and the terms for the equation coefficients—intercept, A, and slope, B. These coefficients are determined by regressions of backscatter with artificially created TSS concentrations or gravimetrically (differences in weights) measured TSS from water samples (Gartner, 2004). This equation can also be expressed as:

$$\mathrm{Log\ TSS} = \mathrm{A} + \mathrm{B} * \mathrm{RB} \quad (3.1)$$

RB is composed of the measured acoustic backscatter and a correction for transmission losses (Thevenot et al. 1992) in units of counts or decibels (dB), as shown below:

$$\mathrm{RB} = \mathrm{RL} + 2\mathrm{TL} \quad (3.2)$$

where RL is the reverberation level (the measured backscatter) and 2TL is the two-way transmission loss, assumed to be the same in each direction. The RL can be used directly as the actual reported values from the device (or the reported values minus the noise level) if the noise level is relatively constant (Öztürk, 2017). This RL is multiplied by a

manufacturer-supplied scale factor to convert it from count to decibels (dB). After the conversion, the RL can be referred to as the echo intensity (EI).

The two-way transmission loss, 2TL, is introduced to compensate for losses due to the spherical spreading of the acoustic beam from the acoustic device and losses due to absorption in the water, as shown below:

$$2TL = 20 \log_{10} [R \Psi] + 2\alpha R \quad (3.3)$$

where R—Range, Ψ—near-field correction, and α—absorption correction.

The first part of the equation is the correction for beam spreading, and the second part is the absorption correction. R is the slant range from the transducer head (ADCP) to the measured bin (m) given as:

$$R = r + \frac{D}{4} \quad (3.4)$$

where r is the slant distance from the transducer head to the center of the bin in meters and D is the bin size in meters (Wall et al. 2006). The next term, Ψ, is the transducer near-field correction (Downing et al. 1995) that accounts for the nonspherical spreading of acoustic energy close to the transducer and is defined as:

$$\Psi = [1 + 1.35z + (2.5z)^{3.2}]/[1.35z + (2.5z)^{3.2}] \quad (3.5)$$

and

$$z = \frac{R * \lambda}{\pi * a_t^2} \quad (3.6)$$

where a_t is the transducer radius in meters and λ is the acoustic wavelength in meters. However, Ψ is empirically derived and generally not as reliable as the other parts of the transmission loss equation and could thus introduce some level of uncertainty (Landers et al. 2016).

The next term in the 2TL equation is the α coefficient, which describes the absorption of energy by water (α_w) and attenuation due to suspended sediments (α_s)—that is, $\alpha = \alpha_w + \alpha_s$ (all in dB m^{-1}). The coefficient α_w describes the absorption of energy by water and depends on the salinity, temperature, and pressure of the water and the sound frequency of the acoustic device (Öztürk, 2017; Landers et al. 2016). Pressure does not have a significant effect for shallow water environments (depth $\leq$ 20 m), and salinity is not applicable in freshwater systems (Öztürk, 2017; Wall et al. 2006), leaving temperature and frequency as the determining variables in canals, rivers, and lakes. Next, the coefficient α_s, the sediment attenuation coefficient, is controlled by the sediment characteristics for a given acoustic frequency and is negligible in water with a TSS concentration less than 300 mg L^{-1} (Gartner and Cheng, 2001).

The correction for transmission losses is more significant for ADCPs, where the range, R, can extend many meters, while ADVs have much shorter ranges (e.g., 10 cm), and any losses are comparatively negligible (Öztürk, 2017).

3.2.2. Study Area

The Tamiami (L-29) Canal in the Everglades region in South Florida was created by means of the excavation of limestone used to construct the Tamiami Trail roadway (Figure 3.1). The roadway acted as a barrier to natural overland flow and restricted

freshwater inflows to the Northeast Shark River Slough (NESRS) within Everglades National Park (ENP). To remediate the limitations on freshwater inflows, the Modified Deliveries Project was created to develop the necessary infrastructure to allow more freshwater delivery into the ENP and restore a "more natural" hydrologic condition McLean, 2015; COP, 2020). The infrastructure includes the construction of approximately 5.8 km of bridges on the Tamiami Trail to enable more flow into the NESRS through the S333 water control (inflow) structure (spillway) along L-29 (Sarker et al. 2020). A section of the L-29 Canal east of the spillway was used in this study.

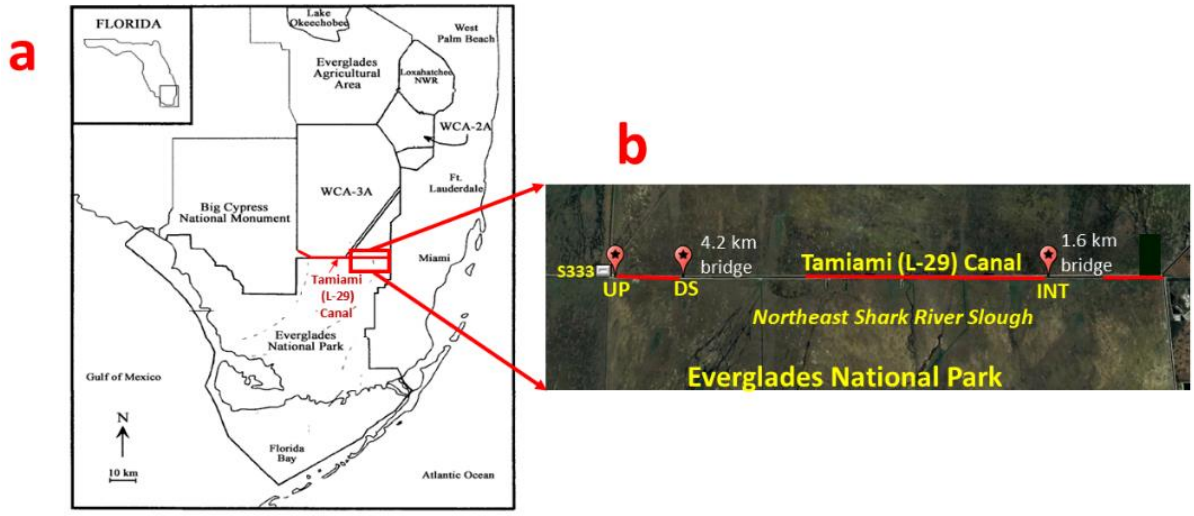

Figure 3.1 (a) Map of the Everglades region showing the Tamiami (L-29) Canal (in red) and (b) study sites in the Tamiami (L-29) Canal, where the acoustic devices were deployed. The sites were upstream (UP), downstream (DS), and interior (INT) (Google Earth, 2023).

3.2.3 Deployment in the Tamiami (L-29) Canal and Backscatter Processing

Two acoustic devices, a 10 MHz side-looking ADV and a 1500 kHz Argonaut ADCP, both manufactured by SonTek (SonTek—a Xylem Brand, San Diego, CA, USA), were deployed at three sites in the Tamiami (L-29) Canal, namely, upstream (UP—

25°45′40.8″ N, 80°40′18.8″ W), downstream (DS—25°45′40.6″ N, 80°39′06.3″ W), and interior (INT—25°45′39.1″ N, 80°32′03.5″ W), at different periods between June and December 2021. The ADV and ADCP were deployed during the same period at DS (June) and INT (August), while at UP, the ADV was deployed in November, and the ADCP was deployed in September. UP was closest to inflow structure S333, while DS and INT were located before the 4.2 km and 1.6 km bridges, respectively. These sites were strategically chosen to determine how discharge releases into the L-29 Canal can transport suspended sediments and particulate phosphorus into the ENP via bridges.

3.2.3.1 Acoustic Doppler Velocimeter (ADV)

The ADV was deployed near the canal bed (0.14 m–0.5 m above the bed) to measure the velocity and backscatter every 2 h. The ADV had three receivers and made measurements 10 cm away from the probe (sampling volume). The backscatter from the three receivers was averaged and converted from signal amplitude (counts) into echo intensity (decibels) by multiplying by a 0.43 scaling factor (Sontek, 2001) before being used for calibration.

3.2.3.2 Acoustic Doppler Current Profiler (ADCP)

The three-beamed Argonaut ADCP was deployed at the bottom of the canal in an upward facing direction and was configured to make temporal and vertical velocity and backscatter measurements with a vertical resolution (bin size) that was either set at 0.5 m or 1 m (Figure 3.2). During deployments, the water depths in the canal ranged from 3.6 to 5.0 m and provided between 4 and 7 measurement bins. During longer deployments (1–3 weeks), the ADCP was programmed to make either 120- or 300-s measurements (averaging interval) every 1200 or 3000 s, respectively (sampling interval). For shorter

deployments, the ADCP was programmed to make 10-s measurements every 100 s. Additionally, the blanking distance—the region directly above the ADCP where no measurements can be made—ranged from 0.5 m to 1 m.

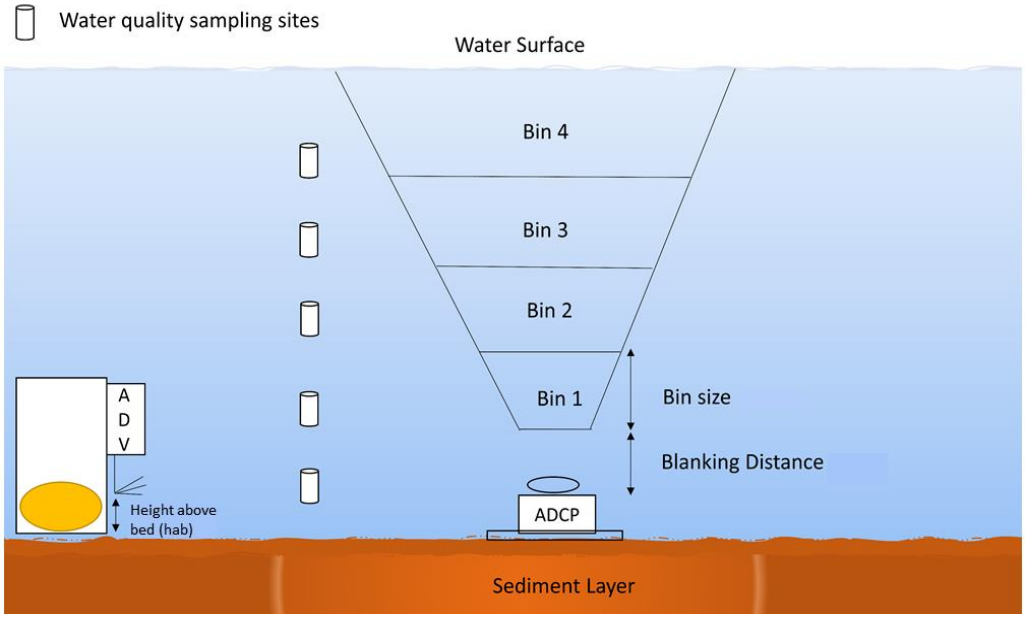

Figure 3.2 An illustration of a typical deployment of the acoustic devices: acoustic Doppler velocimeter (ADV) and acoustic Doppler current profiler (ADCP). Across deployment events, the user-determined blanking distance and bin sizes of the ADCP ranged from 0.5 to 1 m, and the number of bins varied from 4 to 7. The height above the bed (hab) for the ADV deployments ranged from 0.14 to 0.5 m.

3.2.4 Acoustic Backscatter Conversion and Correction

For the ADV, laboratory experiments were conducted to develop calibration curves between TSS and echo intensity (EI). Sediment cores from the surface of the canal bed were first taken from each site. Then, portions of the cores were weighed (wet weight), dried to a constant weight and reweighed to determine the water content of the sediments. Next, more fresh wet surface sediments were weighed, and the water content was accounted for so that the true (dry) weights of the sediments could be calculated. These true weights were then diluted in measured volumes of tap water in a bucket to

artificially create TSS between 5 mg L^{-1} and 150 mg L^{-1} in a large bucket. Next, a pump was inserted into the bucket to create velocity and keep the sediments in suspension (Chanson et al. 2008). During agitation, the ADV was introduced into the bucket and programmed to make 15-s velocity and backscatter measurements for approximately 2 minutes. The agitation and measurements were repeated for all the created TSS (between 5 mg L^{-1} and 150 mg L^{-1}), and the corresponding acoustic backscatter from the ADV was recorded, converted to echo intensity (EI) by multiplying by 0.43, and used to generate a calibration curve for each site.

To develop time series profiles of suspended sediments from ADCP backscatter, a series of steps were followed. First, the backscatter was downloaded from the ADCP and averaged (the three beams of the ADCP produced three backscatter values per measurement). In cases when the backscatter from one beam was much higher than the other or when the difference in SNR values was greater than 10 dB (Jenner, 2021), the averages of the other two beams were used. Next, the backscatter was converted to EI in dB at each bin. Since the noise level was relatively constant during deployment, it was not subtracted from the backscatter before conversion to EI. Then, the EI was corrected for transmission loss from beam spreading and attenuation due to water to give the final RB (Equation (3)). The αw values were based on the instrument frequency and water temperature since the study site was a freshwater canal with a water depth much less than 20 m. Published αw values provided by Landers et al. (2016) were used. Attenuation due to sediment was ignored because of the low TSS measured in the water column. Data and graphical analyses were conducted using R (R, 2023), Microsoft Excel and PowerPoint,

and MATLAB (Mathworks, 2023). An alpha (p) value to define statistical significance was set at 0.05 for calibration regressions.

3.2.5 Water Sampling for TSS and TPP for Calibrations and Estimations

To provide TSS measurements for the calibration of the ADCP backscatter, water samples were collected simultaneously during the ADCP deployments (at UP, a calibration performed in November was applied to the September deployment). To perform the calibrations, water samples were collected from different depths in the water column that matched the bins of the ADCP (Figure 3.2). A peristaltic pump was used to collect the water samples in prerinsed 1 L sampling bottles, which were kept on ice and transported to the lab where they were analyzed gravimetrically for TSS. In the laboratory, predried (105 °C for 1 h) and preweighed 47 mm GFF Whatman filters were used to filter 1 L (volume) of the collected water samples (Wpre). After filtration, the filter and particles (residue) were dried again (105 °C for 1 h), cooled in a desiccator, and weighed (Wpost) (Dwinovantyo et al. 2017; Standard Operating Procedure, 2007). TSS was then calculated according to the following equation:

$$\mathrm{TSS\ (mg\ L^{-1})} = \frac{\mathrm{Wpost(g)} - \mathrm{Wpre\ (g)} * 1000}{\mathrm{V(L)}} \tag{3.7}$$

where W—weight and V—volume.

During the November calibration, filtering was performed in the field using predried and preweighed filters in a container. After filtering, the filters were kept, sealed, and labeled in 47 mm Petri dishes.

After analysis for TSS, the filters together with the residues were digested and analyzed to obtain the concentration of total phosphorus on the particles—total particulate phosphorus (TPP)—using the ascorbic acid method (USEPA, 1983). This TPP (termed TPP in TSS, μg mg^{-1}) was multiplied by the TSS estimates (mg L^{-1}) that were derived from applying the calibration curve to obtain the total particulate phosphorus (TPP in μg L^{-1}) at each depth in the water column for every deployment. The equation is shown below:

$$\text{TPP estimate in water } (\mu g\ L^{-1}) = \text{TSS estimate } (mg\ L^{-1}) * \text{TPP in TSS } (\mu g\ mg^{-1}) \quad (3.8)$$

3.2.6 Discharge Data

Instantaneous discharges at UP (25°45′40.8″ N, 80°40′18.8″ W) were downloaded from the S333 inflow structure available at South Florida Water Management District's online data repository—DBHYDRO (https://www.sfwmd.gov/science-data/dbhydro, accessed on 12 November 2022). Instantaneous discharges at DS (25°45′41″ N, 80°39′17″ W) and INT (25°45′41.0″ N, 80°32′12.0″ W) were downloaded from the United States Geological Survey-National Water Information System (https://waterdata.usgs.gov/nwis, accessed on 26 October 2022). The discharges at INT had both positive and negative values. The negative discharges were taken as flows in the reverse direction (east to west) caused by factors including gate operations at a pump at the eastern end of the canal and wind (Lopez Roque, 2022). Such negative values were converted to positive values for analyses.

3.3. Results

3.3.1. Acoustic Backscatter Processing for the Acoustic Doppler Current Profiler (ADCP)

After converting the RL in counts to EI in decibels (dB) and correcting for beam spreading and water absorption, the relative acoustic backscatter (RB, Equation (3)) from the ADCP was obtained. The RB was not clearly distinguishable between depths in the water column (Figure 3a, b). Using the RB values to develop calibration curves resulted in a very narrow range of backscatter values, for instance, 75.5–77.5 dB at UP (not shown). Applying the equation coefficients (slope and intercept) of the calibration curves to obtain the TSS estimates resulted in values that ranged from 0 to over 1000 mg L^{-1} at UP, which was unrealistic in this relatively low-particulate-level canal (Table 3.2). Similarly, converting the estimated TSS into TPP resulted in higher concentrations in the surface layer of the water compared to the deeper layer, which conflicted with the measured results that were used for the calibrations. Plots using only the EI yielded better results, with the values being more distinguishable between depths (Figure 3c, d).

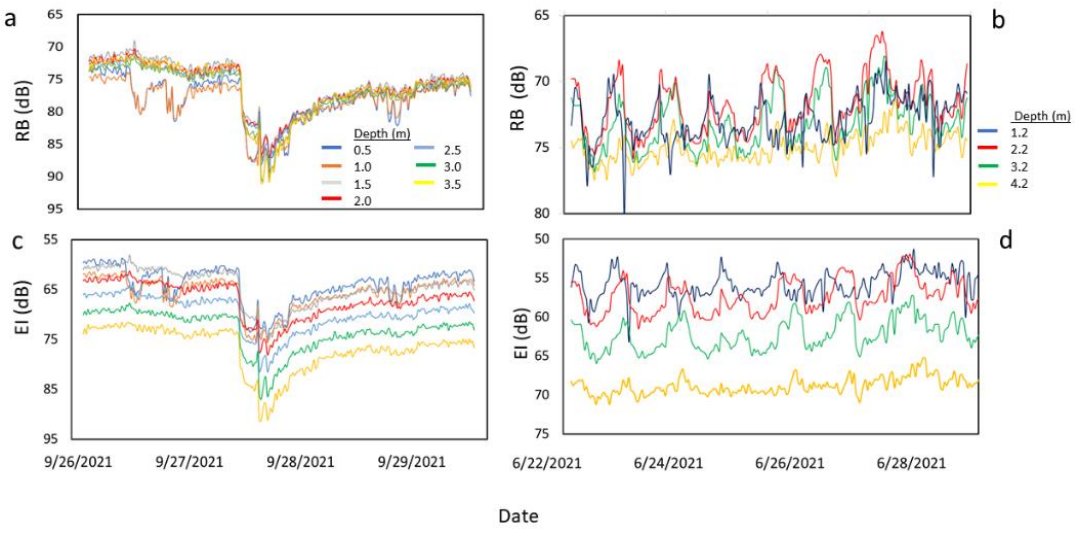

Figure 3.3 Water column time series of the vertical distribution of the relative acoustic backscatter (RB) (using the average of the beams of each preset bin), corrected for transmission losses, from the acoustic Doppler current profiler (ADCP) at the (a) upstream (UP) and (b) downstream (DS) sites. Time series of echo intensity (EI) at the UP (c) and DS (d) show greater differentiation between depths.

Table 3.2 Total suspended solids (TSS, gravimetrically determined) and total particulate phosphorus (TPP) content of the TSS (TPP in TSS μg mg^{-1}) and in the water column (μg L^{-1}), with increasing depth from the water surface of the L-29 Canal. The TSS values were used to calibrate the echo intensity (EI) from the acoustic Doppler velocimeter (ADV) and the acoustic Doppler current profiler (ADCP).

Site	Date	Depth (m) [1]	TSS (mg L^{-1}) *	TPP	
				(μg mg^{-1})	(μg L^{-1})
Upstream (UP)	24 November 2021	0.25	2.10	1.19	2.50
		0.75	1.75	1.27	2.23
		1.25	3.35	0.79	2.66
		1.75	2.50	0.92	2.31
		2.25	3.15	0.91	2.85
		2.75	3.35	0.89	2.97
		3.25	3.25	0.88	2.87
		4.25	2.75	0.95	2.62
Downstream (DS)	22 June 2021	1.2	4.50 *	2.50	11.25
		2.2	5.40	2.23	12.02
		3.2	5.10	2.09	10.64
		4.2	8.20	1.78	14.60
		5.0	26.0	1.15	29.87
Interior (INT)	19 August 2021	0.5	1.20	3.33	3.99
		1.0	1.10	3.66	4.03
		1.5	1.20	3.50	4.20
		2.0	1.30	3.57	4.64
		2.5	1.70	3.26	5.54
		3.0	1.60	3.25	5.19
		3.5	1.80	2.82	5.07

[1] The lowest depth corresponded to the depth of the ADV and was used to convert the estimated TSS (from calibration) to TPP estimates near the canal bed. * The calibration curve generated using the TSS sampled in June at DS was applied to a second deployment in December.

3.3.2 Calibration Curves

There were statistically significant positive correlations between echo intensity and log TSS for ADV and ADCP across all three sites, as shown in the calibration curves (Figure 3.4a, b). Additionally, the uncorrected EI produced better regression for calibration because there was more spread in the EI: 60–70 dB at UP, 50–70 dB at DS, and 55–65 dB at INT (Figure 3.4b).

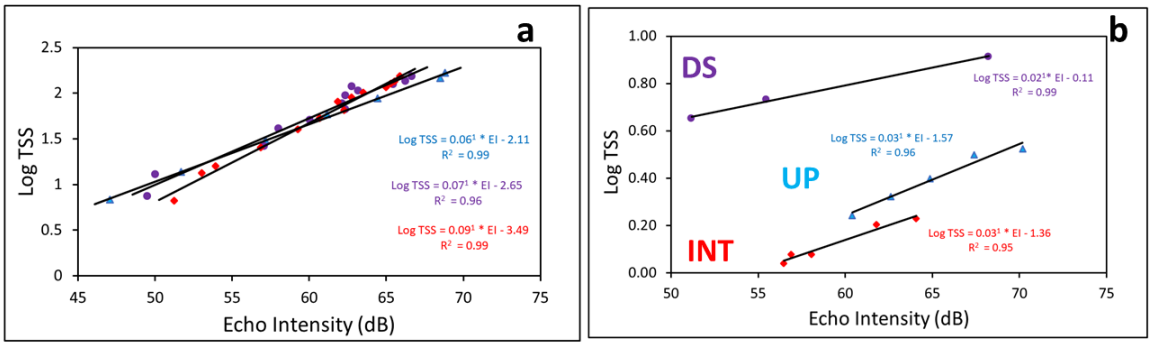

Figure 3.4 Calibration curves developed using the echo intensity (EI) from the (a) ADV and (b) ADCP at the upstream (UP), downstream (DS), and interior (INT) sites in the L−29 Canal (for the ADCP, two data pairs were removed at UP, while a pair each was removed at DS and IN to improve the fit of the regressions).

3.3.3 Measured Total Suspended Solids (TSS) and Total Particulate Phosphorus (TPP) Used in Calibrations

The gravimetrically analyzed TSS (mg L^{-1}) and the resulting calculated TPP in the water column (µg L^{-1}) revealed that the top layers of the water column generally had lower concentrations than the deeper layers across the three sites (Table 3.2). Conversely, the phosphorus fraction of the analyzed sediments (TPP in TSS, µg mg^{-1}) generally decreased from the top to the deeper layers. Although the sample collections and analyses were performed at different times of the year across sites, the TPP in TSS was lowest at UP, which was closest to the inflow structure, and highest at INT, which was the most downstream site (Table 3.2).

During the deployment of the acoustic devices, the discharges at UP had values up to 60 m^3 s^{-1} (ADV, November) and 40 m^3 s^{-1} (ADCP, September) (Figures 3.5a and 3.6b). During the combined ADV and ADCP deployments at DS in June (DS-Jun), the maximum discharge was approximately 22 m^3 s^{-1} (Figure 3.5b), while the discharges during the second ADCP deployment in December (DS-Dec) reached 40 m^3 s^{-1} (Figure

3.6f). The DS-Dec deployment had higher discharges because the main inflow structure, S333, and a newer secondary structure, S333N (located north of S333), were both operational (released discharge into the canal) at that time, while during the DS-Jun deployment, only S333N was operational. At INT, the maximum discharge during the combined deployments did not exceed 14 $m^3 s^{-1}$ (Figure 3.5c).

In terms of water quality estimates, at UP, the TSS and TPP estimates (concentrations) did not exceed 18 mg L^{-1} and 17 μg L^{-1}, respectively, near the canal bed (ADV, Figure 5a) and 15 mg L^{-1} and 13 μg L^{-1}, respectively, in the water column (ADCP, Figures 6a and 7a). At DS-Jun, concentrations were less than 14 mg L^{-1} for TSS and 16 μg L^{-1} for TPP near the canal bed (Figure 3.5b), while in the water column, the concentrations were less than 9 mg L^{-1} for TSS and 17 μg L^{-1} for TPP (Figures 3.6c and 3.7b). At DS-Dec, the TSS concentration in the water column peaked at 11 mg L^{-1} (Figure 3.6e), and the higher concentrations compared to DS-Jun can be attributed to the higher discharges in December. No estimation for TPP in Dec-DS was performed because the number and sizes of measurement depths (ADCP bins) were different between the two deployments. DS-Jun had four 1-m bins, while DS-Dec had five 0.5-m bins, so they were not compatible beyond the calibration curve. Last, at the INT, the near-bed concentrations did not exceed 5 mg L^{-1} for TSS and 12 μg L^{-1} for TPP (Figure 3.5c), while in the water column, the concentrations did not exceed 2.5 mg L^{-1} for TSS and 8 μg L^{-1} for TPP (Figures 3.6 g and 3.7c). These results generally showed higher TSS and TPP concentrations near the canal bed than in the water column.

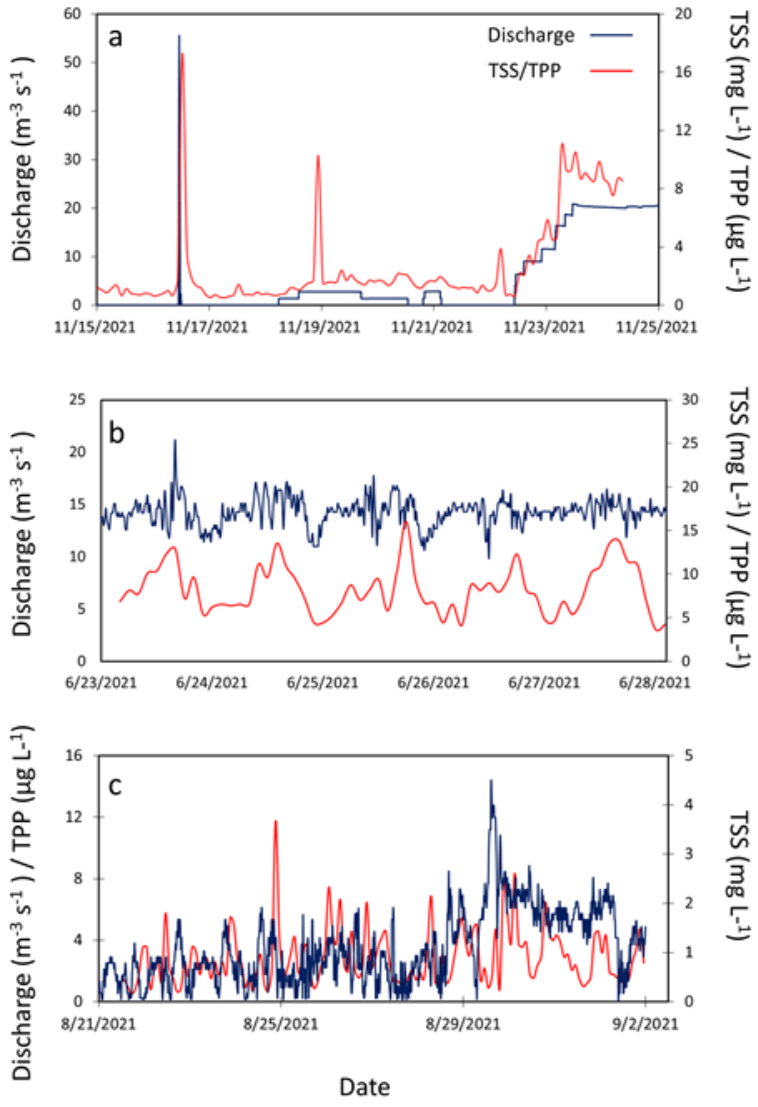

Figure 3.5 Time series of discharge and estimates of TSS and TPP from the ADV deployments at (a) upstream (UP), (b) downstream (DS), and (c) interior (INT) sites. The TSS and TPP estimates are those near the canal bed. During the field deployments at UP and INT, the measured backscatter obtained from the ADV was lower than the measured backscatter obtained during the lab calibrations because of the inability to artificially create very low TSS concentrations in the lab (<5 mg L^{-1}).

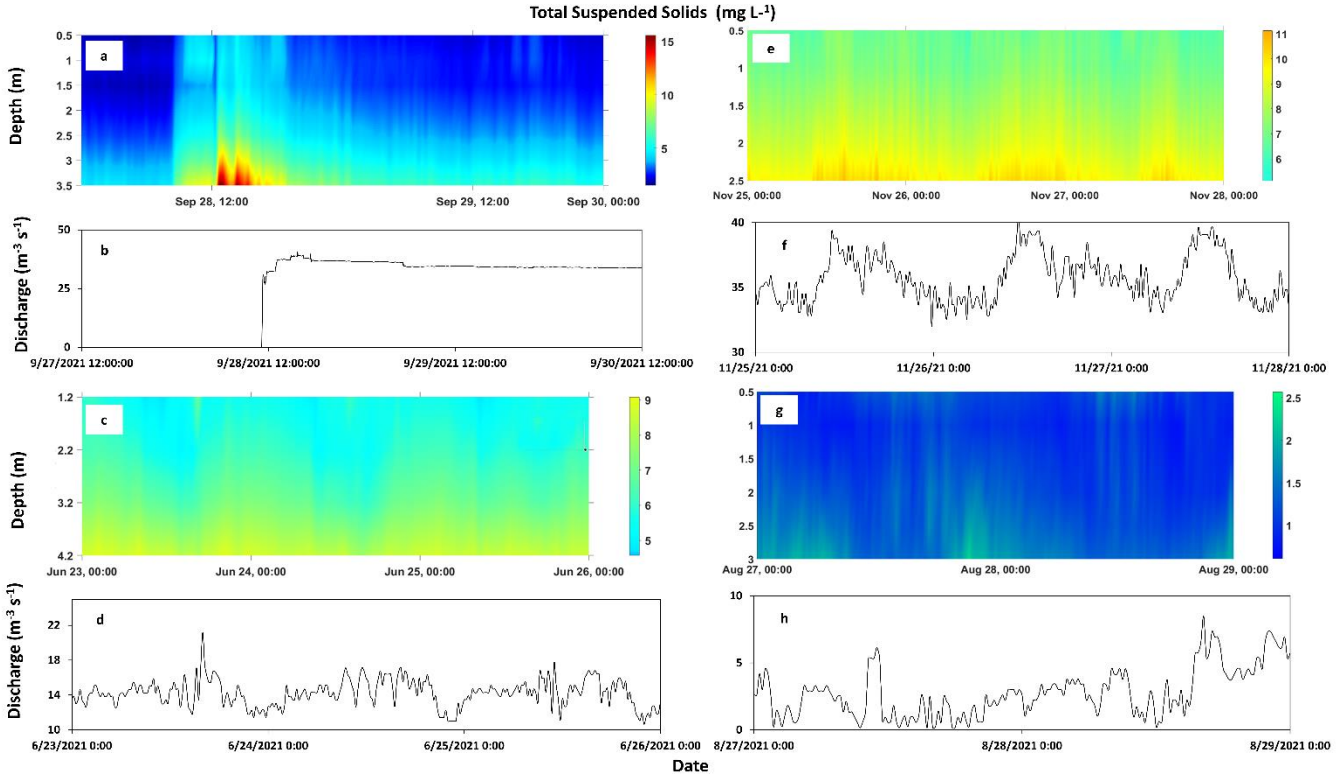

Figure 3.6 Vertical distribution of estimates of total suspended sediments (TSS) in the water column and the corresponding discharges at the upstream, UP (a, b), downstream in June, DS−Jun (c, d), downstream in December, DS−Dec (e, f), and interior, INT (g, h), sites in the L−29 Canal in 2021. The depths are the sizes of the user-determined bins of the ADCP. The uncorrected echo intensity (EI) from the acoustic Doppler current profiler (ADCP) was used to generate the TSS estimates via calibration curves. The calibration curve developed for DS−Jun was also used to estimate TSS for DS−Dec. For clarity, these plots are portions of the deployment time series.

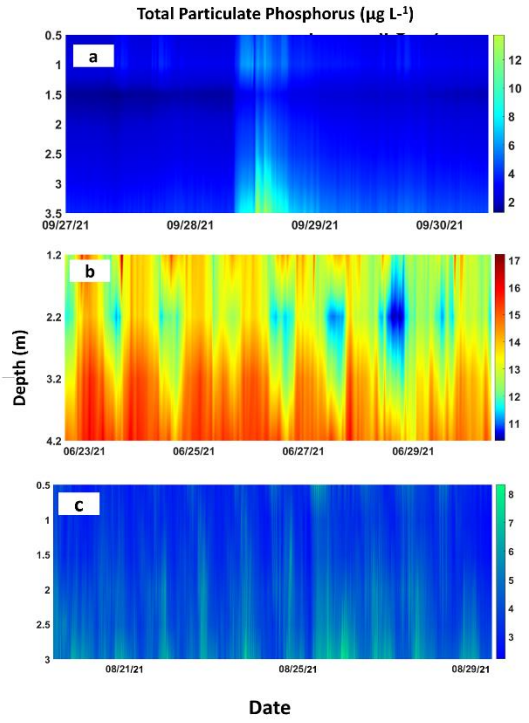

Figure 3.7 Vertical distribution of total particulate phosphorus estimates (TPP µg L^{-1}) in the water column at the (a) upstream (UP), (b) downstream in June (DS−Jun), and (c) interior (INT) sites in the L−29 Canal. The TPP from the lab-analyzed TSS (TPP in TSS) that was used to create the calibration curves (unit of mg g^{-1}) was multiplied by the TSS estimated from applying the calibration curves (units of mg L^{-1}) to obtain the TPP (unit of µg L^{-1}) in the water column.

An observation of the relationship between discharge and the estimates showed clear associations between higher discharges and higher concentrations of TSS and TPP at UP (Figures 3.5a and 3.6a,b). The instantaneous and subsequent sustained discharge releases from the S333 structure caused a noticeable increase in TSS and TPP concentrations. Similarly, higher discharges matched higher TSS and TPP concentrations, while lower discharges matched lower TSS and TPP concentrations near the canal bed at DS-Jun (Figure 3.5b) and for TSS in the water column at DS-Dec (Figure 3.6e,f). This synchronization was not as strong in the water column at DS-Jun, probably due to fewer

particles in the water column compared to the bed (Table 3.2), while at INT, there was no discernable relationship between discharge and TSS/TPP concentrations due to the relatively lower values of all three parameters.

3.4. Discussion

3.4.1. Justification for Not Correcting Transmission Losses for ADCP Backscatter Processing

Studies that used ADCPs for TSS estimations and corrected for transmission losses had a wide range of concentrations, relatively high TSS concentrations, and/or greater water depths when compared to this study. For example, in a study performed in the Lembeh Strait in Indonesia, the measured water depth was between 15 and 30 m, and the measured TSS ranged from 55 to 74 mg L^{-1} (Dwinovantyo et al. 2017). Similarly, in another study performed in the Tidung Island seawater of Indonesia, the water depth was greater than 40 m, and the TSS ranged from <45 to 80 mg L^{-1} (Manik et al. 2021). A study performed in the Hudson River in New York, USA, was conducted at a water depth of 18 m that had TSS concentrations that ranged from <10 to 100 mg L^{-1} (Wall et al. 2006; 2008). Another study performed in San Francisco Bay, USA, had water depths between 7.3 and 16.1 m and TSS concentrations that were greater than 100 mg L^{-1} (Gartner, 2004). Comparatively, the concentrations in our study were quite low (generally <10 mg L^{-1}) and did not vary much between depths, and the water depth in the canal was approximately 5 m. Thus, the poor suitability of the relative backscatter (RB) for developing a useable calibration curve for TSS estimations in this study could be due to

the relatively narrow range of acoustic backscatter and TSS in the water column in the L-29 Canal compared to other studies.

The correction introduced for transmission losses increases with increasing distance from the ADCP because the range (distance) from the device is considered. This means that more corrections are applied with increasing distance from the ADCP. Even though, in our study, the bin closest to the ADCP (Bin 1) had the highest RB values that corresponded with the generally higher TSS concentrations at the deeper water column (Table 3.2), the difference in RB between this bin and the farthest bin was not enough; when the corrections were introduced, the RB values became very similar among all the bins. This resulted in the lack of clear distinction between the RB values with depth, as shown in the results, while the backscatter, uncorrected for transmission losses, produced clearer distinctions with depth. Therefore, the application of such correction "overcorrected" the farthest bins. The use of the Downing near-field factor (Ψ) can overcorrect and bias the relative backscatter, and thus, it may be preferable to use uncorrected data (Landers et al. 2016), although in some cases, this overcorrection may be marginal (Venditti et al. 2016). Therefore, it was prudent to remove the two-way correction losses from the relative backscatter processing.

3.4.2. Vertical Profiles of Total Suspended Solids and Total Particulate Phosphorus in the Water Column of the L-29 Canal

The low values of TSS and TPP estimates from this study are not uncommon in the region of Central and South Florida [51,52]. For example, studies conducted in Lake Worth Lagoon (South Florida) and in the tributaries of the Indian River Lagoon (East

Central Florida) generally had TSS concentration averages less than 12 mg L^{-1} (Trefry et al. 2009; 2021) and an average TPP concentration in the water column of less than 70 μg L^{-1} (Trefry et al. 2021). Similarly, in a study performed along the L-40 Canal, north of the L-29 Canal (our study), the average TSS concentration did not exceed 18 mg L^{-1}, and the average TPP concentration was 71 μg L^{-1} (Daroub et al. 2007). Such low TSS concentrations have been found in <5% of rivers globally (Trefry et al. 2021). However, the average TPP in TSS from our L-29 study, which was 2.05 μg mg^{-1}, is higher than the range of global averages for rivers (1–2.01 μg mg^{-1}) (Savenko, 2007; Viers et al. 2009). Therefore, despite the relatively low TSS in the L-29 Canal, the relatively higher TPP in TSS can threaten the ecological integrity of downstream waters.

The general increase in TSS and TPP estimates from the water surface to the canal bed was expected. We surmise that this is due to resuspension from the bed that caused higher concentrations of TSS (Dwinovantyo et al. 2017; Li et al. 2017) and the tendency for more suspended sediments to settle out in deeper waters (Wang et al. 2011). Therefore, higher suspended sediment levels in deeper waters will result in higher TPP (μg L^{-1}) in deeper waters as well. The opposite (decreasing) trend with depth observed for TPP in TSS (μg mg^{-1}) has been reported in other studies (e.g., Li et al. 2017). A possible explanation for this trend is that the composition of suspended sediments varied from the water surface to the canal bed. The higher TPP in TSS suggests that the water surface had light, organic, and P-rich particles, while the deeper water had denser, more mineral, and P-poor particles. Light and flocculent P-rich organic material (aquatic plant

detritus) has been found suspended on the water surface of farm canals (Daroub et al. 2002a;b).

3.4.3 Impact of Canal Discharges and Hydrology on Total Suspended Solids and Total Particulate Phosphorus

In southern Florida, canal discharge releases via inflow structures have been shown to increase the concentration and export of suspended sediments and particulate phosphorus in two steps. The first step, referred to as the first flush, marks the start of canal discharge release from the inflow structure after a greater than 24-h quiescent period. This first flush mobilizes and entrains materials deposited from the previous event as well as new material that may have accumulated or grown during the quiescent period. After the first flush is the second step, termed the cumulative flush, where sustained high discharges can mobilize more sediments and their associated P contents (Daroub et al. 2002b). In this study, the effects of first flush and cumulative flush were also observed at the upstream site, closest to the S333 inflow structure, where the increases in TSS and TPP closely followed the discharges from the structure. Instantaneous discharges have been compared to storm events in their capacity to mobilize sediments and increase their concentrations and export (Onwuka et al. 2021). In rivers, the first flush occurs at the start of a rain or storm event, where higher TSS can be recorded during the onset of very high flows that decrease over the duration of the event (Trefry et al. 2021).

Even though the deployments and water quality estimates at the sites were performed at different times during the year, inferences can be made as to the origins and

types of suspended sediments in the three canal sites by considering their proximities to the S333 inflow structure. The lower TPP in TSS at UP possibly occurred because high discharges from S333 exported all the fresh, low-density, and P-rich organic particles that accumulated or grew during the quiescent period and left behind the older and denser P-poor particles. Studies have shown that organic particles have a high phosphorus content and are easily transportable, while older particles are more mineral, P-poor, and heavier, which makes them harder to transport (Daroub et al. 2002b). The higher TPP concentrations in the water column at DS suggest that discharges from the secondary inflow structure, S333N, as well as earlier discharges from the main S333 structure, transported P-rich organic particles from upstream, which accumulated at the downstream site. Another reason is that the transporting power of the canal discharges was attenuated with increasing distance from the S333 inflow structure; therefore, only the lightest particles made it the farthest downstream. This decrease in transport power downstream also implies the dominant effect of biogeochemical processes on the kind of particles present and the P availability of such particles. Biogeochemical processes such as adsorption–desorption, biologic uptake, and the decomposition of organic matter have been shown to dominate P availability during low-flow periods (Withers and Jarvie, 2008; Moatar et al. 2017), and in this case, the downstream reaches of the canal can display these low flow conditions. Similarly, the highest TPP in TSS found in the canal interior, at the most downstream site from the S333 inflow structure, indicates that the particles therein may be of biological origin. A high phosphorus mass content has been associated with fresh biological organic matter (Daroub et al. 2002b). These inferences are noteworthy because DS and INT are located close to the bridges that open into the

Everglades National Park, and the potential export of P-rich particles into the park will be detrimental to Everglades restoration efforts.

3.5. Conclusions

This study used acoustic backscatter (echo intensity), a biproduct of velocity measurement from two acoustic devices, an acoustic Doppler velocimeter (ADV) and an acoustic Doppler current profiler (ADCP), to estimate total suspended solids (TSS) and total particulate phosphorus (TPP) in the L-29 Canal in South Florida, USA. The echo intensity from the ADCP, uncorrected for beam spreading and attenuation due to water and sediments, proved sufficient to develop suitable calibration curves to estimate realistic TSS in canal locations that varied by distance from a managed inflow structure, S333. The suspended sediments used in the calibrations were then analyzed for total particulate phosphorus concentrations to obtain the TPP estimates in the water column (ADCP) and near the canal bed (ADV). Time series plots of discharges, TPP and TSS revealed that the site closest to S333, the upstream site, had the highest concentrations, driven by instantaneous and rapid discharge releases. Analyses of the TSS particles further revealed differences between the upstream and downstream sites. Suspended sediments further downstream had a higher phosphorus (P) content per suspended sediment (TPP in TSS $\mu g\ mg^{-1}$) because they likely had higher organic matter (biological origin). Conversely, the particles upstream had a lower P content because of their proximity to the high discharges from S333, which transported the lighter P-rich organic particles downstream and left behind denser, P-poor mineral particles. Such important observations and inferences in this study were made possible using high-resolution data

from acoustic devices. Therefore, the ability to evaluate how rapid changes in hydrology affect the potential export of sediments and phosphorus is critical for canal discharge management to enable the preservation of the integrity of downstream aquatic systems, such as the Florida Everglades.

This work is novel because it extends the use of backscatter from acoustic devices, which has been traditionally used as a surrogate for TSS, to also use it as a surrogate for TPP. This is crucial for effective water quality and nutrient (phosphorus) monitoring because it reduces the human and material risks and costs of routine manual samplings and provides high spatiotemporal data. Additionally, this work practically tests the lower limits of using acoustic backscatter as a surrogate for TSS because the concentrations were at the low end of detection (generally less than 10 mg L^{-1} of TSS), while other studies have focused on much higher concentrations. A general limitation of using acoustic devices as surrogates for TSS and TPP in low-particulate-level water is the possibility of weak signal amplitudes and low echo intensities, which may be indistinguishable from background noise. Another limitation is the potential difficulty in creating low TSS in the laboratory for the calibration of the low echo intensities that may occur under certain field conditions and in certain locations. In many locations, specifically in the highly managed systems of South Florida, where flow conditions rapidly respond to pumping operations and other water management manipulations, short-term response measurements are needed, as they provide information not obtained by longer-term, less temporally robust data. Future studies should be conducted in several additional canal systems to better determine the range of applicability of these methods.

3.6. References

Acoustic Doppler Velocimeters (ADVs®)—Xylem. Available online: https://www.xylem.com/siteassets/brand/sontek/resources/brochure/sontek-acoustic-doppler-velocimeters-2017.pdf. (accessed on 8 February 2023).

Argonaut-XR MULTI-CELL DOPPLER CURRENT PROFILER. Available online: https://www.ysi.com/File%20Library/Documents/Brochures%20and%20Catalogs/argonaut-xr-brochure.pdf. (accessed on 8 February 2023).

Carter, K., Redfield, G., Ansar, M., Glenn, L., Huebner, R., Maxted, J., Pettit, C. and VanArman, J., 2010. Canals in South Florida: A technical support document.

Chanson, H., Takeuchi, M. and Trevethan, M., 2008. Using turbidity and acoustic backscatter intensity as surrogate measures of suspended sediment concentration in a small subtropical estuary. *Journal of environmental management*, *88*(4), pp.1406-1416.

Christian D Lopez Roque (Person)—Science Base-Directory (Internet). Available online: https://www.sciencebase.gov/directory/person/6250 (accessed on 6 April, 2022).

Current Profiling Solutions Brochure Available online: https://www.ysi.com/File%20Library/Documents/Brochures%20and%20Catalogs/current-profiling-solutions.pdf. (accessed on 8 February 2023).

Daroub, S.H., Josan, M.S., Lang, T.A. and Waldon, M.G., 2009. L40 Canal Water Quality Survey Study Progress Report for 2007.

Daroub, S.H., Stuck, J.D., Lang, T.A. and Diaz, O.A., 2002. Particulate phosphorus in the everglades agricultural area: I–Introduction and sources. *Soil Water Department of University of Florida IFAS Extension Publication SL*, *197*.

Daroub, S.H., Stuck, J.D., Lang, T.A. and Diaz, O.A., 2002. Particulate phosphorus in the Everglades Agricultural Area: II–Transport mechanisms. *Inst. of Food and Agric. Sci., Ext. Office. Univ. of Florida, Gainesville*.

Diamond, J.S. and Cohen, M.J., 2018. Complex patterns of catchment solute–discharge relationships for coastal plain rivers. *Hydrological Processes*, *32*(3), pp.388-401.

Dorioz, J.M.; Cassell, E.A.; Orand, A.; Eisenman, K.G. Phosphorus storage, transport and export dynamics in the Foron River watershed. *Hydrol. Process.* 1998, *12*, 285–309.

Downing, A., Thorne, P.D. and Vincent, C.E., 1995. Backscattering from a suspension in the near field of a piston transducer. *The Journal of the Acoustical Society of America*, *97*(3), pp.1614-1620.

Dwinovantyo, A., Manik, H.M., Prartono, T. and Susilohadi, S., 2017. Quantification and analysis of suspended sediments concentration using mobile and static acoustic Doppler current profiler instruments. *Advances in Acoustics and Vibration, 2017*.

Fugate, D.C. and Friedrichs, C.T., 2002. Determining concentration and fall velocity of estuarine particle populations using ADV, OBS and LISST. *Continental Shelf Research*, *22*(11-13), pp.1867-1886.

Fugate, D.C. and Friedrichs, C.T., 2003. Versatility of the Sontek ADV: measurements of sediment fall velocity, sediment concentration, and TKE production from wave contaminated velocity data. In *Proceedings of Coastal Sediments 2003*.

Gartner, J.W. and Cheng, R.T., 2001. The promises and pitfalls of estimating total suspended solids based on backscatter intensity from acoustic Doppler current profilers. In *Proceedings of the Seventh Federal Interagency Sedimentation Conference, March* (Vol. 25).

Gartner, J.W., 2002, April. Estimation of suspended solids concentrations based on acoustic backscatter intensity: Theoretical background. In *Turbidity and other sediment surrogates workshop* (Vol. 30).

Gartner, J.W., 2004. Estimating suspended solids concentrations from backscatter intensity measured by acoustic Doppler current profiler in San Francisco Bay, California. *Marine geology*, *211*(3-4), pp.169-187.

Gray, J.R. and Gartner, J.W., 2009. Technological advances in suspended-sediment surrogate monitoring. *Water resources research*, *45*(4).

Hamilton, L.J., Shi, Z. and Zhang, S.Y., 1998. Acoustic backscatter measurements of estuarine suspended cohesive sediment concentration profiles. *Journal of Coastal Research*, pp.1213-1224.

Harrison, J.W., Lucius, M.A., Farrell, J.L., Eichler, L.W. and Relyea, R.A., 2021. Prediction of stream nitrogen and phosphorus concentrations from high-frequency sensors using Random Forests Regression. *Science of the Total Environment*, *763*, p.143005.

Harvey, R.G., Loftus, W.F., Rehage, J.S. and Mazzotti, F.J., 2011. Effects of Canals and Levees in Everglades Ecosystems: WEC304/UW349, 12/2010. *EDIS*, *2011*(1).

Jacksonville District > Missions > Environmental > Ecosystem Restoration > Combined Operational Plan (Internet). Available online: https://www.saj.usace.army.mil/Missions/Environmental/Ecosystem-Restoration/G-3273-and-S-356-Pump-Station-Field-Test/(accessed on 7 January 2023).

Jenner, B. Beam Separation in ADPs and ADCPs. Available online: https://www.ysi.com/File%20Library/Documents/Technical%20Notes/beam-separation-in-adps-and-adcps.pdf. (accessed on 5 July 2021).

Jordan-Meille, L. and Dorioz, J.M., 2004. Soluble phosphorus dynamics in an agricultural watershed. *Agronomie*, *24*(5), pp.237-248.

Kostaschuk, R., Best, J., Villard, P., Peakall, J. and Franklin, M., 2005. Measuring flow velocity and sediment transport with an acoustic Doppler current profiler. *Geomorphology*, *68*(1-2), pp.25-37.

Kronvang, B., Laubel, A. and Grant, R., 1997. Suspended sediment and particulate phosphorus transport and delivery pathways in an arable catchment, Gelbaek stream, Denmark. *Hydrological Processes*, *11*(6), pp.627-642.

Landers, M.N., Straub, T.D., Wood, M.S. and Domanski, M.M., 2016. *Sediment acoustic index method for computing continuous suspended-sediment concentrations* (No. 3-C5). US Geological Survey.

Latosinski, F.G., Szupiany, R.N., García, C.M., Guerrero, M. and Amsler, M.L., 2014. Estimation of concentration and load of suspended bed sediment in a large river by means of acoustic Doppler technology. *Journal of Hydraulic Engineering*, *140*(7), p.04014023.

Li, J., Reardon, P., McKinley, J.P., Joshi, S.R., Bai, Y., Bear, K. and Jaisi, D.P., 2017. Water column particulate matter: A key contributor to phosphorus regeneration in a

coastal eutrophic environment, the Chesapeake Bay. *Journal of Geophysical Research: Biogeosciences*, *122*(4), pp.737-752.

Manik, H.M. and Firdaus, R., 2021. Quantifying Suspended Sediment using Acoustic Doppler Current Profiler in Tidung Island Seawaters. *Pertanika Journal of Science & Technology*, *29*(1).

MathWorks—Makers of MATLAB and Simulink (Internet). Available online: https://www.mathworks.com/(accessed on 7 January 2023).

McLean, A. Modified Water Deliveries: Improving Hydrologic Condition in Northeast Shark River Slough. 2015. Available online: https://www.nps.gov/ever/learn/nature/modwater.htm (accessed on 10 May 2020).

Moatar, F., Abbott, B.W., Minaudo, C., Curie, F. and Pinay, G., 2017. Elemental properties, hydrology, and biology interact to shape concentration-discharge curves for carbon, nutrients, sediment, and major ions. *Water Resources Research*, *53*(2), pp.1270-1287.

Noe, G.B., Harvey, J.W. and Saiers, J.E., 2007. Characterization of suspended particles in Everglades wetlands. *Limnology and Oceanography*, *52*(3), pp.1166-1178.

Noe, G.B., Harvey, J.W., Schaffranek, R.W. and Larsen, L.G., 2010. Controls of suspended sediment concentration, nutrient content, and transport in a subtropical wetland. *Wetlands*, *30*(1), pp.39-54.

Onwuka, I.S., Scinto, L.J. and Mahdavi Mazdeh, A., 2021. Comparative Use of Hydrologic Indicators to Determine the Effects of Flow Regimes on Water Quality in Three Channels across Southern Florida, USA. *Water*, *13*(16), p.2184.

Öztürk, M., 2017. Sediment size effects in acoustic Doppler velocimeter-derived estimates of suspended sediment concentration. *Water*, *9*(7), p.529.

Poleto, C. and Charlesworth, S.M. eds., 2010. *Sedimentology of aqueous systems*. John Wiley & Sons.

R: The R Project for Statistical Computing (Internet). Available online: https://www.r-project.org/(accessed on 7 January 2023).

Rai, A.K. and Kumar, A., 2015. Continuous measurement of suspended sediment concentration: Technological advancement and future outlook. *Measurement*, *76*, pp.209-227.

Ruben, L.D., Szupiany, R.N., Latosinski, F.G., Weibel, C.L., Wood, M. and Boldt, J., 2020. Acoustic Sediment Estimation Toolbox (ASET): A software package for calibrating and processing TRDI ADCP data to compute suspended-sediment transport in sandy rivers. *Computers & Geosciences*, *140*, p.104499.

Sarker, S.K., Kominoski, J.S., Gaiser, E.E., Scinto, L.J. and Rudnick, D.T., 2020. Quantifying effects of increased hydroperiod on wetland nutrient concentrations during early phases of freshwater restoration of the Florida Everglades. *Restoration Ecology*, *28*(6), pp.1561-1573.

Savenko, V.S., 2007. Chemical composition of sediment load carried by rivers. *Geochemistry International*, *45*, pp.816-824.

Schoellhamer, D.H. and Wright, S.A., 2003. Continuous measurement of suspended-sediment. *Erosion and sediment transport measurement in rivers: technological and methodological advances*, p.28.

SonTek. *ADVField Technical Manual*; SonTek Technical Documentation; Sontek: San Diego, CA, USA, 2001.

SonTek. *Argonaut™-SL System Manual Firmware*, Version 12.0; SonTek™/YSI Corporation: San Diego, CA, USA, 2009; p. 316.

Standard Operating Procedure for: Total Suspended Solids. 2007. Available online: https://betastatic.fishersci.com/content/dam/fishersci/en_US/documents/programs/scientific/technical-documents/white-papers/apha-total-suspended-solids-procedure-white-paper.pdf (accessed on 2 March 2021).

Thevenot, M.M., Prickett, T.L. and Kraus, N.C., 1992. *Tylers Beach, Virginia, Dredged Material Plume Monitoring Project, September 27 to October 4, 1991*. COASTAL ENGINEERING RESEARCH CENTER VICKSBURG MS.

Trefry, J.H. and Fox, A.L., 2021. Extreme runoff of chemical species of nitrogen and phosphorus threatens a Florida barrier island lagoon. *Frontiers in Marine Science*, *8*, p.752945.

Trefry, J.H., Trocine, R.P. and Bennett, H., 2009. Sediment Sourcing Study of Lake Worth Lagoon and C-51 Basin, Palm Beach County. *Final Report to Palm Beach County and the South Florida Water Management District for Contract R2008-0985*.

United States Environmental Protection Agency, 1983. *Methods for Chemical Analysis of Water and Wastes*; Environmental Monitoring and Support Laboratory: Cincinnati, OH, USA. pp. 475–490.

Velasco, D.W. and Huhta, C.A., 2010. Experimental verification of acoustic Doppler velocimeter (ADV) performance in fine-grained, high sediment concentration fluids. *App Note SonTek/YSI*, pp.1-19.

Venditti, J.G., Church, M., Attard, M.E. and Haught, D., 2016. Use of ADCPs for suspended sediment transport monitoring: An empirical approach. *Water Resources Research*, *52*(4), pp.2715-2736.

Viers, J., Dupré, B. and Gaillardet, J., 2009. Chemical composition of suspended sediments in World Rivers: New insights from a new database. *Science of the total Environment*, *407*(2), pp.853-868.

Wall, G.R., Nystrom, E.A. and Litten, S., 2006. *Use of an ADCP to compute suspended-sediment discharge in the tidal Hudson River, New York* (No. 2006-5055).

Wall, G.R., Nystrom, E.A. and Litten, S., 2008. Suspended sediment transport in the freshwater reach of the Hudson River estuary in eastern New York. *Estuaries and Coasts*, *31*, pp.542-553.

Wang, Q., Li, Y. and Ouyang, Y., 2011. Phosphorus fractionation and distribution in sediments from wetlands and canals of a water conservation area in the Florida Everglades. *Water Resources Research*, *47*(5).

Withers, P.J.A. and Jarvie, H.P., 2008. Delivery and cycling of phosphorus in rivers: a review. *Science of the total environment*, *400*(1-3), pp.379-395.

Wood, P.J. and Armitage, P.D., 1997. Biological effects of fine sediment in the lotic environment. *Environmental management*, *21*(2), pp.203-217.

Zhao, H.; Piccone, T. and Diaz, O., 2015. *Supporting Information for Canal Evaluations*; Technical Publication WR-2015-003; South Florida Water Management District: West Palm Beach, FL, USA.

CHAPTER 4: PARTICULATE AND PHOSPHORUS DYNAMICS IN THE WATER COLUMN AND SEDIMENTS OF CANALS OF THE LOWER EVERGLADES

Abstract

Phosphorus (P) in flowing systems, depending on discharge conditions, can be transported with suspended particulates or be deposited as part of sediments in the channel bed. However, the accurate assessment of the long- and short-term effects of discharge on the export dynamics of particulates and P requires the availability of temporally robust concentrations. In this study lower temporal resolution (mean daily to weekly) and higher temporal resolution (minutes) discharge and P data across South Florida's Everglades canals were subjected to concentration-discharge (C-Q) relationships to determine the discharges that increased P transport. Additionally, in-depth studies were conducted in the L-29 Canal, a major Southern Everglades canal, to characterize suspended particulates and bed sediments, and evaluate their ease of transport and settling in relation to canal discharges. The results showed that higher discharges generally increased P concentrations in the water column. Piecewise regression analysis on C-Q regression further revealed inflections in C-Q regression slopes that denoted discharge thresholds, where P export dynamics changed from low to high discharges. Discharge thresholds ranged from 0.57-7.67 $m^3 s^{-1}$ for total P and from 16.12-52.54 $m^3 s^{-1}$ for total particulate P. In the L-29 Canal, higher discharges transported suspended particulates farther downstream from the inflow structure (S333). There were also strong relationships between the discharge and: a) mass accumulation rates (r^2= 0.50, $p<0.01$) and b) bulk density (r^2= 0.90, $p<0.0001$) for sediment particulates collected in the water column. Furthermore, the top sediment layer of site closest to S333 had the lowest organic matter (0.71 %) and P content (71.58 mg kg^{-1}) and

the highest bulk density (1.30 g cm^{-3}), indicating that canal discharges transported lighter, organic P-rich material downstream. Therefore, identifying the discharges that can mobilize P, transport P-rich suspended particulates, and resuspended bed sediments is crucial to achieving the Everglades restoration goal of increasing freshwater delivery and reducing P export.

4.1. Introduction

Globally, the dominant form (up to 95%) of phosphorus (P), an essential limiting nutrient, transported by flowing freshwater systems is associated with suspended particulates (Meybeck, 1982; Dorioz et al. 1998; Beusen et al. 2005). Particulate phosphorus (PP) and dissolved phosphorus comprise total phosphorus (TP). Particulate phosphorus (PP) includes P minerals that contain calcium, or iron, and P adsorbed to particles (inorganic) and P in living and detrital matter (organic) (Trefry et al. 2021; Labry et al. 2013; Yoshimura et al. 2007).

Phosphorus loading to flowing systems (rivers, streams, canals) can stay in the water column either in the dissolved form or attached to suspended particulates, or can accrue in the channel bed sediments. During high discharges, PP may be resuspended by the shearing force of moving water (Reddy et al.1999), as higher stream velocities transport more sediments than lower velocities (Wang et al. 2011). Furthermore, higher concentrations of suspended sediments (Dwinovantyo et al. 2017; Rahul et al. 2020) and P (Wang et al. 2011) have been observed in deeper water layers compared to the surface layers, possibly due to discharge-driven turbulence near the channel bed which resuspends sediments and releases P (Daroub et al. 2002b). During quiescent and low discharge events,

PP can settle out of the water column into the bed sediments (Reddy et al. 1999; Svendsen and Kronvang, 1993).

The mass of P stored in settled bed sediments is higher than in the water column (Diaz et al. 2006, Wang et al. 2011) and the accumulation of bed sediments can be long-term storages of phosphorus (Reddy et al. 1999; Diaz et al. 2006). This storage could also result from long-term continuous P loading to channels referred to as "legacy P" in sediments (Diaz et al. 2006). Channel sediment inventories have estimated the mass of P to be twice that found in surrounding wetlands (Wang et al. 2011).

A widely-used approach in flowing systems to assess and predict the effects of discharge on the concentrations of suspended particulates and particulate-bound nutrients including phosphorus is via the development of concentration–discharge (C-Q) relationships (Godsey et al. 2009; Diamond and Cohen, 2018; Rose et al. 2018; Moatar et al. 2017; Onwuka et al. 2021). Particulate export patterns or behaviors are determined by assessing the relationship between changes in concentration and changes in discharge. Generally, decreasing concentrations with increased discharges (flows) indicate dilution while increasing concentrations with increased discharges denote mobilization and enrichment (Zhang, 2018). Particulate export behaviors that are driven by discharge are termed chemodynamic (hydrologic dominance) and include processes such as resuspension and transport. Conversely, when the concentrations of particulates are insensitive to changes in discharges, biogeochemical processes can be said to control their behavior, and this is termed chemostatic (biogeochemical dominance). A critical discharge can exist where the behavior of a constituent changes with increasing discharge. This critical discharge, also called discharge threshold, is identifiable as an inflection in the

slope of the C-Q plot and can be used to predict the behavior of a system at low (below critical) discharge and high discharge (Moatar et al. 2017; Underwood et al. 2017). The slope (*b*) of the log-transformed C-Q is the metric used to quantify the export behavior of constituents. The threshold can be used to distinguish between hydrologic dominance and biogeochemical dominance on the behavior of constituents. A common C-Q relationship export behavior for particulates is chemostasis at low discharges and chemodynamic enrichment or mobilization at high discharges. The mobilization of sediment and dislodging of sorbed nutrients at higher discharges (e.g., P) increases their concentrations (Diamond and Cohen, 2018).

In South Florida canals, studies have quantified P release and export under conditions of zero or low flows, through measurements of processes such as diffusion and sorption (Diaz et al. 2006; Wang and Li, 2010; Das et al. 2012). These processes, however, do not estimate the total phosphorus (TP) flux; hydrologic-driven P releases through sediment transport and resuspension are unaccounted for. A more complete estimation of P release from canals requires the quantification of hydrologic drivers such as discharge and the measurement of their contributions to P export. The overarching objective of this study was to quantify the effects of managed canal discharges on suspended particulates and P export in South Florida's Everglades. This is critical because improvements in freshwater delivery to the Everglades without ensuring the water is clean may partially defeat the purpose of restoration and may incur additional costs to remediate. The specific objective was to determine how canal discharge rates affect particulates and P transport within the lower Everglades canals. Predictions include: 1) increased P concentrations will be observed during higher discharges, 2) at some critical discharge, there will be a change

from chemostatic to chemodynamic behavior of P, and 3) physicochemical characteristics of sediments (suspended and bed) will vary according to the magnitude of discharge and proximity to canal inflow structures.

4.2. Materials and Methods

4.2.1 Study site

The portion of the Everglades south of Lake Okeechobee, which we are terming the lower Everglades, encompasses areas including the Everglades Agricultural Area (EAA), the Lower East Coast (LEC), and the Everglades Protection Area (EPA) which generally correlate to agricultural, urban, and wetland regions respectively (Figure 4.1). These areas are connected by complex drainage features of human-made canals that are regulated by inflow structures including pumps, spillways, and culverts. These canals are managed for drainage, flood control, navigation, and water supply to meet the agricultural, urban, and ecosystem needs of the region (Carter et al. 2010). The EAA underwent channelization and drainage for agricultural development (Carter et al. 2010; Bhadha et al. 2017). As a result, phosphorus-rich drainage from the EAA was shunted through canals and sent south and southeast to the EPA and portions of the LEC (Bhadha et al. 2017; Abtew and Obeyeskera, 1996; Chimney and Goforth, 2001). The LEC includes the urban and coastal areas of Palm Beach, Broward, and Miami-Dade counties (Carter et al. 2010; Abtew et al. 2019). In the LEC, the canals and associated structures were designed to provide flood control, deliver water for urban and agricultural use, stop saltwater intrusion, and convey water into the EPA (Carter et al. 2010; Abtew et al. 2019). The EPA is a major freshwater and historical phosphorus-poor (oligotrophic) wetland ecosystem (Faridmarandi, and Naja, 2018) that has suffered from high phosphorus and suspended

sediment loads from EAA drainage that led to poor water quality and impacted the native flora and fauna and the food chain (Whalen et al. 1992). The EPA consists of a series of wetlands and includes three Water Conservation Areas (WCA 1, 2 and 3) and Everglades National Park (ENP) (Carter et al. 2010). Once part of the contiguous Everglades, the WCAs became large-scale water impoundments of wetland habitats, and serve as flood and saltwater intrusion control and enhancement of fish and wildlife and recreation (Abtew et al. 2019; Carter et al. 2010). ENP is located south of the WCAs and is the only area that still has some natural flow (Childers et al. 2003).

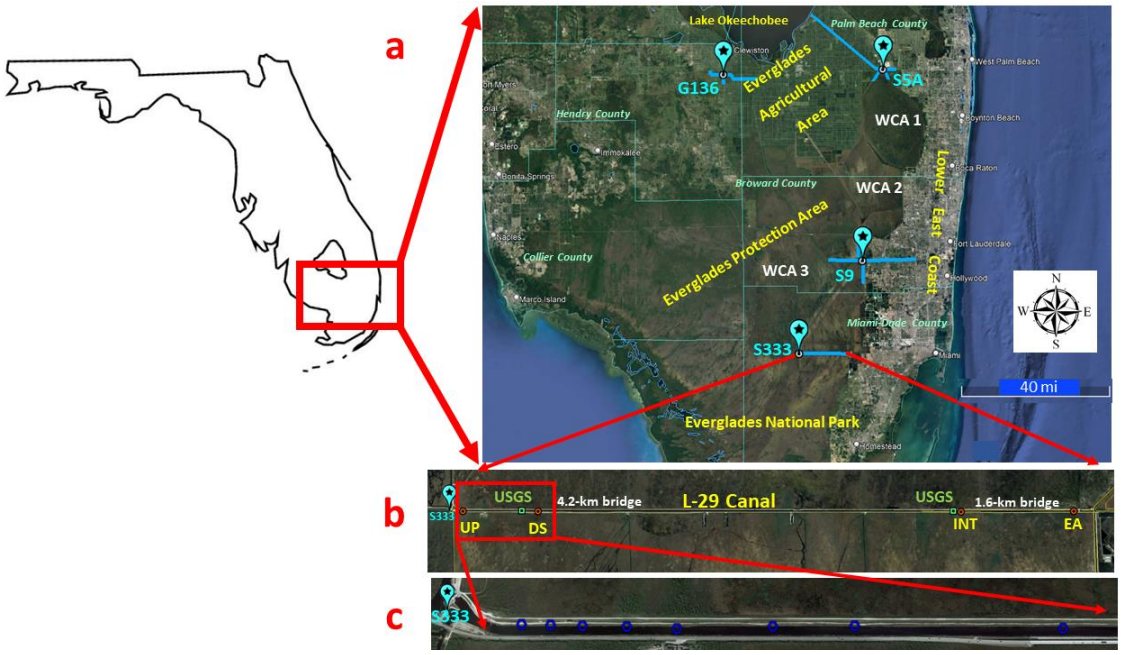

Figure 4.1 a): Satellite image of lower Everglades in South Florida showing canal locations in the Everglades Agricultural Area (G136, S5A), Lower East Coast (S9), and Everglades Protection Area (S333). The South Florida Water Management District (SFWMD) monitors these sites with the data stored in their online repository - DBHYDRO. b) L-29 portion of the Tamiami Canal showing four sites where samples were collected: The sites are: Upstream (UP), Downstream (DS), Interior (INT), and Eastern (EA). Water, velocity, suspended particulates, and bed sediments were collected at all sites, except at EA (only bed sediments). c) Sites 1-8 are the sites of single bottom traps (settling particulates collection) between UP and DS. DS is at the western bridge opening that allows flow into

Everglades National Park (ENP). Maps are created from Google Earth (2022). The USGS discharge sites in the L-29 Canal are shown as well.

Canals that drain and interact with the EAA, LEC, and EPA, including the Tamiami Canal (L-29) were selected for this study. The L-29 Canal is a major EPA canal that delivers water to ENP. The L-29 Canal was created by limestone excavation subsequently used to build the Tamiami roadway that connected Miami to Tampa. As part of the Modified Waters Deliveries project, about 5.8 km of bridges have been created along the roadway to enable more freshwater input to ENP (Mclean, 2015, USACE, 2020). Additional details on the L-29 Canal are found in Onwuka et al 2023.

4.2.2 Data collection and analysis

4.2.2.1 Discharge and phosphorus data

Discharge and P data for twenty-five years (1995–2019) were used in this study. The sites selected on the canals were the L-1 Canal (G136), located in Hendry country at the G136 structure (26°40'03.5"N 80°56'57.3" W), West Palm Beach Canal (S5a) at the S5a structure (26°41'02.7"N 80°22'03.9" W), South New River Canal at the S9 structure (26°03'41.5"N 80°26'36.8"W), and the L-29 Canal (S333) at the S333 structure (25°45'43.2"N 80°40'26.2"W) (Figure 4.1a). These sites' mean daily discharge and weekly grab TP concentration data were downloaded from the South Florida Water Management District's online data repository—DBHYDRO (https://www.sfwmd.gov/science-data/dbhydro, accessed on 12 October 2022).

In the L-29 Canal, velocity and echo intensity (a biproduct of velocity measurements) from an upward-looking acoustic Doppler current profiler (ADCP) (SonTEK-a Xylem Brand, San Diego, CA, USA) (Figure 4.2), was used to determine high

temporal resolution (every 20 to 50 minutes) discharge and total particulate phosphorus (TPP) concentrations respectively at two sites. The sites were upstream (UP - 25°45'40.8"N, 80°40'18.8"W) located in-stream of the S333 structure (data collected in November 2021) and downstream (DS - 25°45'40.6"N 80°39'06.3"W) located before the start of the 4.2 km bridge (data collected in June 2021) (Figure 4.1b). To convert the velocity to discharge, the velocity from the ADCP was multiplied by the cross-sectional area (CSA) of the site on the canal. The CSA was estimated using the average water depth in the canal and the width of the canal (from Google maps). Additionally, mean daily discharges in the L-29 Canal at DS (25°45'41"N, 80°39'17"W) and INT (25°45'41.0"N 80°32'12.0"W) were also downloaded from the United States Geological Survey-National Water Information System (https://waterdata.usgs.gov/nwis, accessed on 26 October 2022). The discharges at INT had both positive and negative values. The negative discharges were taken as flows in the reverse direction (east to west) caused by factors including gate operations at a pump at the eastern end of the canal, and wind (Christian Lopez -Roque, USGS, 2022). Such negative values were converted to positive values for analyses.

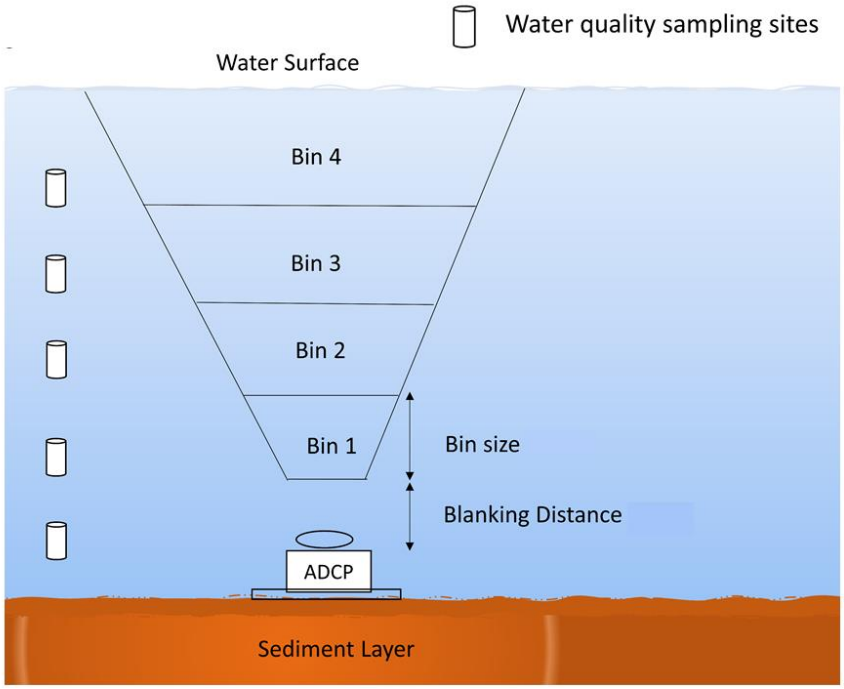

Figure 4.2 An illustration of a deployment of an acoustic Doppler current profiler (ADCP) used to collect high temporal resolution (minutes) data in the L-29 Canal.

A detailed description of the methods used to convert echo intensity (EI) from the ADCP to TPP can be found in Onwuka et al. 2023. In brief, calibrations were done between EI and measured total suspended solids (TSS) at each site, and the calibration coefficients were used to convert the EI to TSS estimates for the ADCP deployment period at each site. Then the measured TSS used in the initial calibrations were analyzed for TPP (μg mg^{-1}) - using the ascorbic acid method after digestion, (USEPA, 1983) and multiplied to the corresponding TSS estimates (mg L^{-1}) to get TPP (μg L^{-1}) estimates in the water column.

4.2.2.2 Sediment collection and analysis

Triplicate intact sediment cores were collected from the four sites using a piston corer with PVC pipe screw-ins. The corer was extended into the water column (using PVC pipe add-ons) till resistance was felt, which denoted the canal bottom was reached. Cores

at UP, DS and INT (25°45'39.1"N 80°32'03.5"W) were collected in April 2021, and at EA (25°45'40.6"N 80°30'13.4"W) in September 2021. The cores were sectioned with depth according to physically observable differences. High-aspect ratio traps (HARTs), with a 10:1 (length to diameter) ratio, were deployed in the canal in triplicates (trap tree) and singly (bottom traps) to collect suspended particulates in the water column and near the bed, respectively, in 2021 (Figure 4.3). The trap tree (Figure 4.3a) was constructed of PVC with a center mast of about 4 meters in length to which three arms, one meter apart, were attached to hold HARTs at varying depth in the water column. HARTs were positioned so the openings were nominally 1 meter apart (vertically) and were offset from each other by 120° to collect suspended solids at the surface, middle and deep layers of the canal water column. The trap tree was deployed once at UP (in November, UP_Nov) and at INT (in August, INT_Aug) and twice at DS (July, DS_ July and December DS_Dec) for two to three-week periods. The single bottom traps (Figure 4.3b) were deployed on the bottom of the canal to collect settling suspended particulates. These were deployed twice between UP and DS for two-week periods between October and November 2021.

Trapped sediments and sectioned sediment cores were analyzed for bulk density (BD), organic matter content (OM), and total phosphorus (TP). The cores were processed for the dry weight (80°C till constant weight: for about 3 days), and the bulk density was estimated by dividing the dry weight by the sediment core volume (core depth X core surface area). Afterwards, portions of the dried sample were set aside for TP analysis. Organic matter content was determined using the loss-on-ignition method, where oven-dried sediment subsamples were heated at 550°C for 4 h in a muffle furnace (Andersen, 1976).

Figure 4.3 a) A photo of a trap tree about 4 m long with 1 m between each trap to collect suspended particulates in the surface mid and low layers in the canal water column. b) a bottom trap deployed near the canal bed with settling particulates. The traps are high aspect ratio (10:1) traps.

4.2.3 Concentration-discharge (C-Q) relationships

Concentration–discharge (C–Q) relationship, which is a power law function, can be linearly expressed as:

$$log_{10}\, C = log_{10} a + b\, log_{10} Q \qquad (4.1)$$

where a and b are the coefficients that represent the intercept (same unit as concentration) and slope (unitless), respectively (Moatar et al. 2017). For each canal, discharge and P concentration data were paired by date and time. Since discharges are regulated in the canals, the discharge data used were limited to periods when the canals were flowing. The

data pairs were log-transformed and regressed to yield slopes (*b*) (Moatar et al,.2017), which were then used to quantify the influence of discharge on P concentrations. More details on the methodology and statistical analysis for C-Q relationships are available in Onwuka et al. 2021.

4.2.4 Statistical analyses

All statistical analyses were performed in excel and R (R Institute for Statistical Computing, Vienna, Austria) using RStudio (RStudio Inc., Boston, MA, USA). Assumptions of normality and homogeneity of variance were verified, and ANOVA was conducted on variables. If ANOVA assumptions were not met, the data were log-transformed. Post Hoc Tukey test was then done to determine the statistically different between variables. Since discharge is not usually normally distributed, the non-parametric equivalent of ANOVA, the Kruskal Wallis test was conducted and the Dunne's post-hoc test was applied to determine the statistical difference between the discharges at the sites. Where possible, linear regressions and Pearson product-moment correlations were conducted to measure the relationship, and the strength and direction of association between variables respectively.

4.3. Results

4.3.1 Concentration–Discharge C-Q relationship for Phosphorus in the lower Everglades canals

4.3.1.1 Lower resolution data (Data from South Florida Water Management District)

There was a range in TP concentrations from the northern canals to the southern canals (Figure 4.4). At G316 and S5a, TP concentrations ranged from 10 to 1000 μg L^{-1}

while at S9 and S333, they ranged from 10 to 100 μg L^{-1}. From the C-Q relationship models, the discharges in the canals had quantifiable effects on TP concentrations in three of the four canal sites (Table 4.1). At G136, S5a and S9, enrichment patterns were observed with higher discharges (positive *b*) but at S333, the slight dilution pattern (*b* = -0.02) observed was taken as a chemostatic pattern because the slope was not statistically different from zero ($p > 0.05$). Piecewise regression analysis further revealed the presence of statistically significant slope inflections in the linear log (C)-log (Q) regressions for TP at G136, S5a, and S9 (Table 4.1). At G136, there was a slight enrichment pattern at low discharge (*b* = 0.06) and a stronger enrichment pattern at higher discharge (*b* = 0.45). At S5a, there was a chemostatic pattern at low discharge (*b* = -0.05) and an enrichment pattern at higher discharge (*b* = 0.25). Similarly, at S9, there was a chemostatic pattern at low discharge (*b* = -0.02) and an enrichment behavior at high discharge (*b* = 0.41). At S333, although the *p-value* for the Davies' test was significant at 0.003, ANOVA showed that these slopes were not statistically different from zero. Furthermore, visual inspection of the *C–Q* plot showed that there was not a definite pattern, and a few extreme data pairs skewed the low discharge slope. Therefore, chemostasis was taken as the pattern at both low and high discharge. The discharge thresholds ranged from 0.57 $m^3 s^{-1}$ at G136 in the northern part of the lower Everglades to 7.67 $m^3 s^{-1}$ at S9 further downstream.

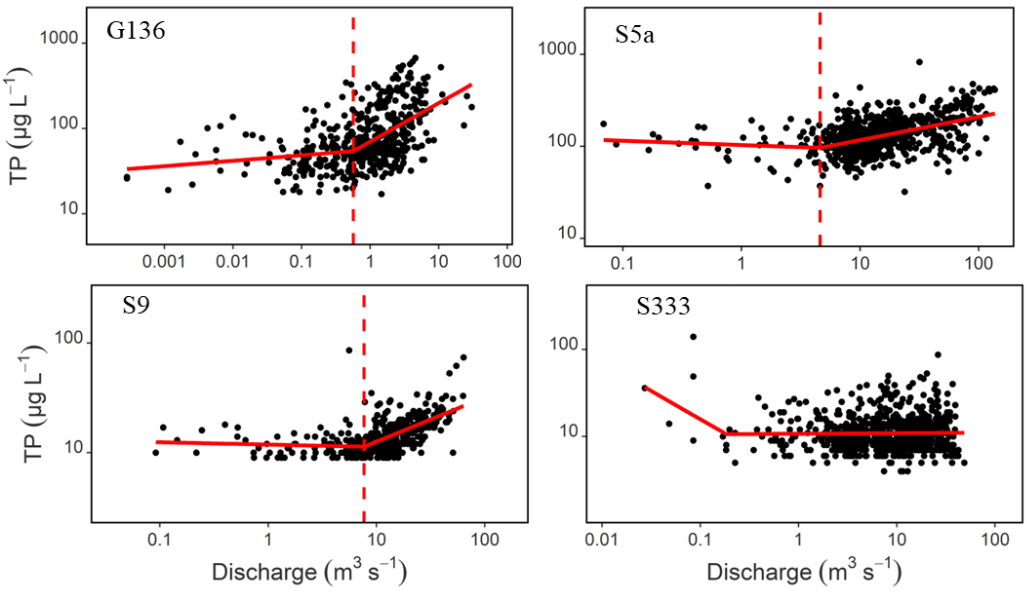

Figure 4.4 C-Q relationship models with piecewise (solid red line) regression for total phosphorus (TP) in canal G136 and S5a, which borders the Everglades Agricultural Area, S9 that borders the urbanized East Coast and S333, in the Everglades Protection Area. There is a change in TP from north to south within the lower Everglades as shown by differentially scaled axes.

4.3.1.2 Higher resolution data

From the higher resolution data estimates, conducted in the L-29 Canal, the total particulate phosphorus (TPP) concentration was approximately three times higher at DS than at UP (Figure 4.5). In the L-29 Canal, the discharge had a statistically significant relationship with TPP at UP and DS (Figure 4.5, Table 4.1). At UP, TPP was enriched at higher discharge (positive linear *b*) while at DS there was a dilution pattern with increasing discharge (negative linear *b*). Piecewise regression analysis also revealed the presence of statistically significant slope inflections (discharge thresholds) in the linear log (*C*)-log (*Q*) regressions at both sites. At UP, there was a chemostatic pattern at low discharge (*b* = -0.04) and a steep positive slope (*b* =1.92) at high discharge that indicated a strong enrichment pattern where higher discharges increased the concentration of TPP. The point

where the slope inflection (discharge threshold) occurred was 52.54 $m^3 s^{-1}$ (Figure 4.5, Table 4.1). At DS, there was a chemostatic pattern at low discharge (*b*= 0.03) and dilution at high discharge (*b* =-0.24), with the discharge threshold at 16.12 $m^3 s^{-1}$.

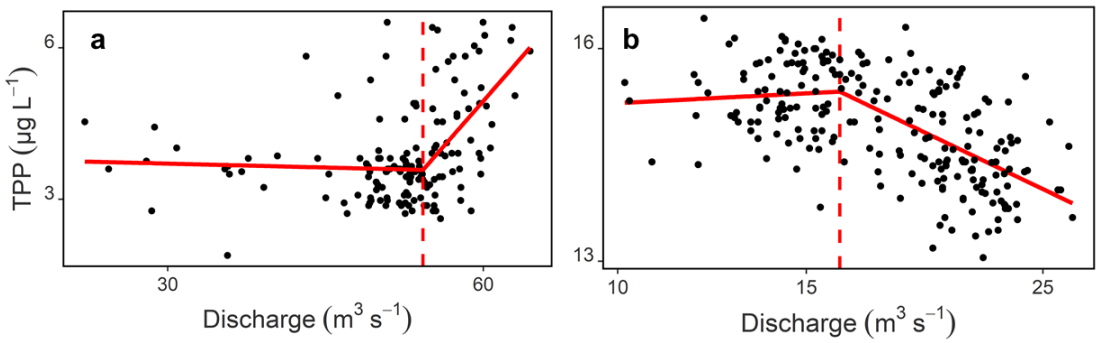

Figure 4.5 C-Q relationship with slope inflections (discharge thresholds) for total particulate phosphorus (TPP) in the water column (a) at the Upstream (UP) and (b) Downstream (DS) sites in the L-29 Canal.

Table 4.1 C-Q (log-log) relationship linear and piecewise (segmented) regression slopes for total phosphorus (TP) and total particulate phosphorus (TPP) in lower Everglades canals using low temporal resolution and high temporal resolution data. Statistically significant inflections in *b* (discharge thresholds) according to Davies' test are also listed.

Phosphorus	Data resolution	Canal	Data pairs (n)	Linear regression slopes (*b*)	Davies' Test	Discharge threshold (m^3s^{-1}) [CI]	Piecewise regression slopes (*b*)	
							low	high
Total Phosphorus (TP)	Lower	G136	878	0.22*	p <0.0001	0.57 [0.34, 0.95]	0.06*	0.45*
		S5a	1252	0.17*	p <0.0001	4.60 [2.68, 7.87]	-0.05	0.25*
		S9	1025	0.16*	p <0.0001	7.67 [6.23, 9.45]	-0.02	0.41*
		S333	1022	-0.02	p = 0.003	0.18 [0.08, 0.43]	-0.65	0.01
Total Particulate Phosphorus (TPP)	Higher	L-29 Upstream (UP)	148	0.29*	p <0.0001	52.54 [50.30, 54.88]	-0.04	1.92*
		L-29 Downstream (DS)	225	-0.15*	p <0.001	16.12 [14.76, 17.60]	0.03	-0.24*

Significant p values at 0.05 (*) according to Student's t test (linear slopes) and ANOVA test of independence (piecewise slopes) indicating slopes are significantly different from zero. * indicates a significant difference.

4.3.2 Physicochemical properties of suspended particulates

4.3.2.1 Trap tree

Across the sites, there were increases in volumes and mass accumulation rates (MAR) of the suspended particulates from the top traps to the low traps, except at DS_Dec and INT_Aug, where the mid traps had the lowest values (Table 4.2, Figure 4.6b). The low traps had consistently higher MAR compared to the top and mid traps. Although the deployments were at different times of the year, UP_Nov, which was the closest to the inflow drainage structure, had high MAR vertically, with the low trap having the highest MAR (0.0516 g cm^{-2} d^{-1}). Conversely, the most interior site (INT_Aug), had the least MAR from top to bottom (vertically) in the water column. There was little variation in bulk density, OM, and TP content vertically within sites. INT_Aug had the least bulk density compared to the other sites, while UP-Nov and DS-Dec had the highest values. Across sites, the TP did not vary much vertically except at INT_Aug, where the top trap had a much higher TP compared to the mid and low traps.

The discharges during the trap tree deployments were between 0 to 40 m^3s^{-1} (Figure 4.6a). The discharges at UP_Nov and DS_Dec were statistically similar, while DS_July and IN were different from these and each other ($p < 0.05$, Kruskal Wallis Test). Thus, the discharges can broadly be differentiated into high flow (UP_Nov and DS_Dec), mid flow (DS_July), and low flow (INT_Aug). The highest discharge correlated with the highest MAR which was at the mid and low traps of the UP_Nov site (Figure 4.6b).

For the combined trap analysis across depths and locations, there is a good, statistically significant, positive relationship between MAR and discharge ($r^2 = 0.50$, $p = 0.006$, Figure 4.7a) with the highest discharges leading to the most accumulation of

suspended particulates. Similarly, there is an even stronger statistically significant positive relationship between bulk density (BD) and discharge (r^2= 0.90, p<0.0001, Figure 4.7b).

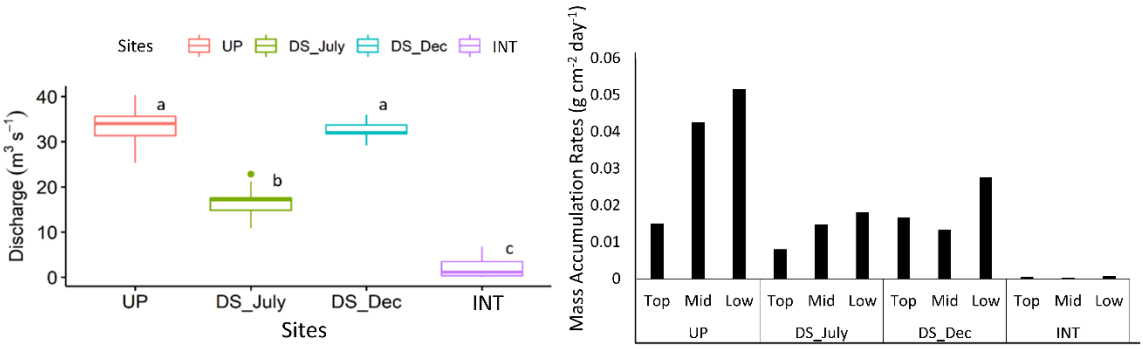

Figure 4.6 a) Box and whisker plot of discharge during the deployment of trap trees. Trap trees were deployed at the DS location during low (DS_July) and high (DS_Dec.) flows. b) Mass accumulation rates (MAR) of sediments during trap tree deployments

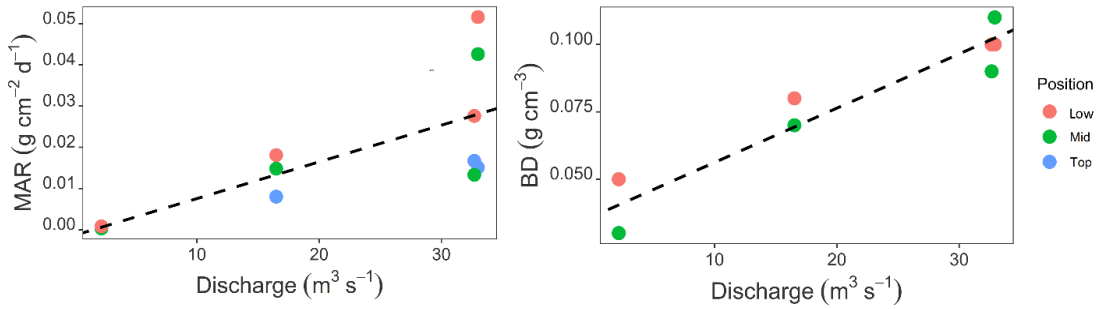

Figure 4.7 Plots of a) mass accumulation rate (MAR) vs discharge (r^2= 0.50, p<0.01, n= 12, and b) Bulk density (BD) vs discharge (r^2= 0.90, p<0.0001, n= 11) of the trap trees. Included in these plots are the trap positions (depths): top, mid and low. (For BD, the top values are masked by the mid).

Table 4.2 Trap tree suspended particulate characteristics at upstream (UP_Nov), downstream (DS_July, DS_Dec), and interior (INT_Aug) stations in the L-29 Canal and at three different depths within the canal water column.

Trap Name	Trap position	Volume (cm^3)	Mass Accumulation Rate ($g\ cm^{-2}\ d^{-1}$)	Bulk Density ($g\ cm^{-3}$)	Organic Matter (%)	Total Phosphorus ($mg\ g^{-1}$)
UP_Nov	Top	97.75	0.0151		35.06	0.91
	Mid	140.36	0.0426	0.11	38.54	0.94
	Low	192.17	0.0516	0.10	36.61	0.94
DS_July	Top	36.50	0.0080	0.08	38.44	0.95
	Mid	75.00	0.0148	0.07	38.47	0.96
	Low	85.00	0.0181	0.08	37.71	1.01
DS _Dec	Top	82.94	0.0167	0.10	38.14	0.99
	mid	72.73	0.0133	0.09	40.00	1.03
	Low	140.36	0.0276	0.10	39.01	0.99
INT_Aug	Top	6.00	0.0005	0.03		1.24
	Mid	3.50	0.0003	0.03		1.10
	Low	5.50	0.0008	0.05	34.74	0.89

Blank cells are either lost samples or insufficient samples for analysis.

4.3.2.2 Single bottom traps

The bottom traps (BT 1-8) during deployment 1 (high discharge) had the highest MAR in the most downstream location (0.0659 g cm^{-2} day^{-1}) at BT8. (Table 4.3, Figure 4.8). The bulk densities decreased with distance from BT1 (closest to the inflow structure) to BT8 and the opposite was true for OM. During deployment 2 (low discharge) and with

the addition of more bottom traps, there is a gradual increase in MAR from upstream (BT2) to downstream with a peak value of 0.1201 g cm^{-2} day^{-1} at BT5 (Table 4.3, Figure 4.8). A similar pattern was observed for OM while the reverse was the case for BD. There was not much variation in TP within deployments, except at BT4 where it was the highest (2.909 mg g^{-1}) during deployment 2. From a discharge perspective, the discharges during the deployment events were statically different from one another according to the Kruskall-Wallis test (Figure 4.9).

Table 4.3 Sediment characteristics and accumulation in bottom traps (BT) during a) high discharge and b) low discharge deployment events. Deployment 1 occurred between 28 Oct and Nov 11, 2021, and deployment 2 occurred between 11 Nov and 24 Nov, 2021.

Deployment	Bottom Traps	Approx. distance from S333 station (m)	Volume (cm^3)	Mass Accum. Rates (g cm^{-2} day^{-1})	Bulk Density (g cm^{-3})	Organic matter (%)	Total Phosphorus (mg g^{-1})
Deployment 1[a]	BT1	312	100.81	0.0484	0.170	19.72	0.723
	BT6	1279	54.87	0.0098	0.060	48.20	0.965
	BT8	2392	441.51	0.0659	0.053	65.02	0.655
Deployment 2[b]	BT2	425	108.46	0.0371	0.113	36.26	0.877
	BT3	547	198.30	0.0572	0.096	44.69	0.879
	BT4	717	354.74	0.0928	0.087	51.07	2.909
	BT5	916	586.98	0.1201	0.066	56.10	0.801
	BT6	1279	172.78	0.0366	0.071	46.09	0.906
	BT8	2392	118.67	0.0329	0.095	38.14	0.987

[a] Only three traps were available to be deployed at that time. [b] More traps were created and deployed, but BT1 and BT7 were not recovered during retrieval.

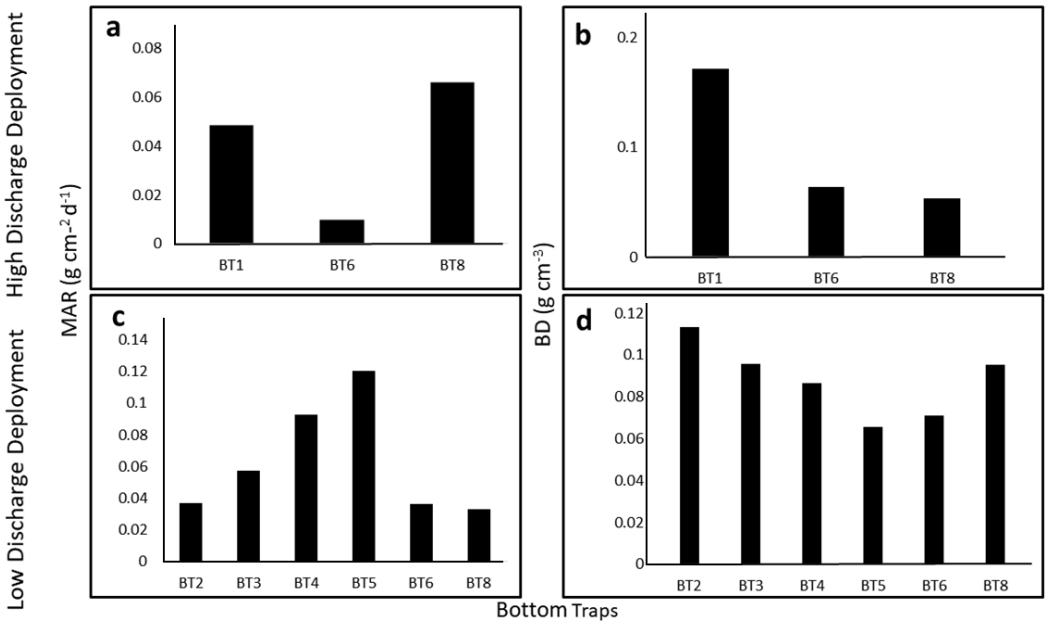

Figure 4.8 Plots of the mass accumulation rates (MAR) and bulk density (BD) during high discharge deployment (a and b) and low discharge deployment (c and d) from settling suspended particulates collected in bottom traps on the canal bed between upstream (UP) and DS in the L-29 Canal.

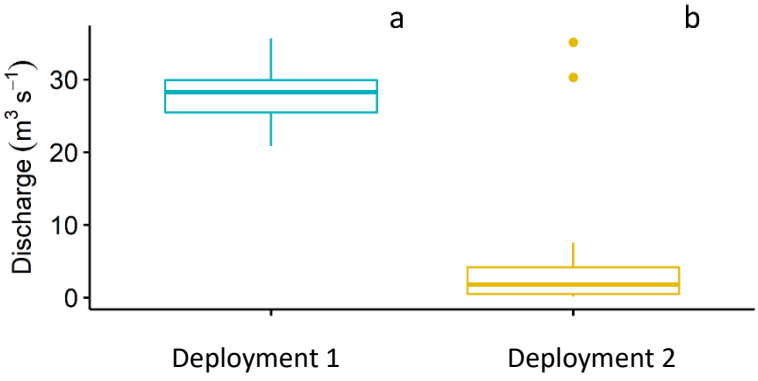

Figure 4.9 Discharge during two deployments of bottom traps using the USGS station located proximal to trap sites. Discharges during the bottom trap deployments were significantly different (Kruskal–Wallis test). These events were two-week deployments in succession. Deployment 1 (high discharge) occurred between 28 Oct and Nov 11, 2021, and deployment 2 (low discharge) occurred between 11 and 24 Nov, 2021.

In deployment 2, there was a strong correlation ($p<0.001$) between MAR and volume which is expected (Table 4.4), as MAR is calculated from the volume. Also, there was a strong significant positive correlation ($p<0.01$) between OM and volume and a significant positive correlation ($p<0.05$) between OM and MAR. There was also a significant inverse relationship ($p <0.05$) between OM and BD, which is expected because higher organic matter indicates a low bulk density.

Table 4.4 Pearson product moment correlations (2-tailed) for suspended particulate characteristics collected in bottom traps during deployment 2 (low flow). Volume (Vol), mass accumulation rate (MAR), bulk density (BD), organic matter (OM) and total phosphorus (TP) (n= 6).

	Vol (cm^3)	MAR ($g\ cm^{-2}\ day^{-1}$)	BD ($g\ cm^{-3}$)	OM (%)	TP ($mg\ g^{-1}$)
Vol (cm^3)	1				
MAR ($g\ cm^{-2}\ day^{-1}$)	0.98***	1			
BD ($g\ cm^{-3}$)	-0.70	-0.57	1		
OM (%)	0.93**	0.90*	-0.83*	1	
TP ($mg\ g^{-1}$)	0.21	0.35	-0.01	0.32	1

$p<0.05$ *, $p<0.001$**, $p<0.0001$***

4.3.3 Physicochemical characteristics of bed sediments

Across the sites, the top sediment layer at UP was consistently, statistically different from the surface sediments at the other sites (Table 4.5). For TP, UP (71.58 mg kg^{-1}) and DS (1042.10 mg kg^{-1}) were statistically different from each other and from the other two sites, while INT (703.11 mg kg^{-1}) and EA (558.93 mg kg^{-1}) were not statistically different. Organic matter content (OM) was the least at UP (0.71%) and highest at INT (31.30%). Bulk density (BD) values ranged from 0.15 g cm^{-3} at INT to 1.30 g cm^{-3}, at UP in the

surface layer. For both OM and BD, UP values were significantly different from the other sites.

At the depth profile, TP and OM generally decreased with depth across all sites except at UP, where the reverse was the case (Table 4.5). BD generally increased with depth at all sites except at UP, which had the highest BD at the surface layers. Across depths, average TP was least at UP (257.45 mg kg^{-1}) and highest at DS (590.36 mg kg^{-1}). Similarly, the least average OM was at UP (8.05 %) and the highest was at DS (20.24 %). There was a strong positive relationship between TP and OM across all sites combined (r^2 = 0.52, p <0.0001, Figure 4.10). Across depth, DS had the least average BD (0.35 g cm^{-3}) of all the sites while UP had the highest average (0.85 g cm^{-3}). The greatest bulk density value was observed in the top layers at UP which were characterized by lower organic matter content and were sandier in texture (Figure 4.11). At DS, INT, and EA, there was a general decrease in TP concentration and OM with depth, and an increase in BD with depth, while the reverse was observed at UP.

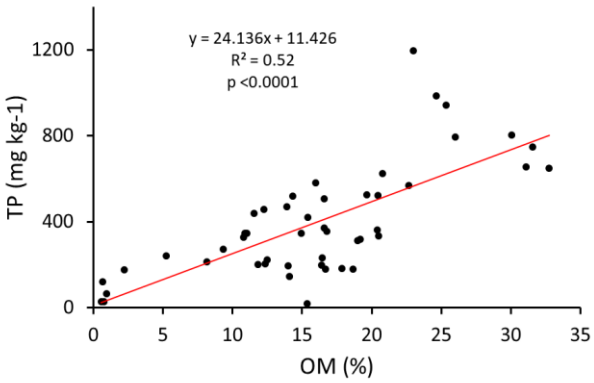

Figure 4.10 Relationship between total phosphorus (TP) and organic matter (OM) using sediments from four cored sites in the L-29 canal (n = 48).

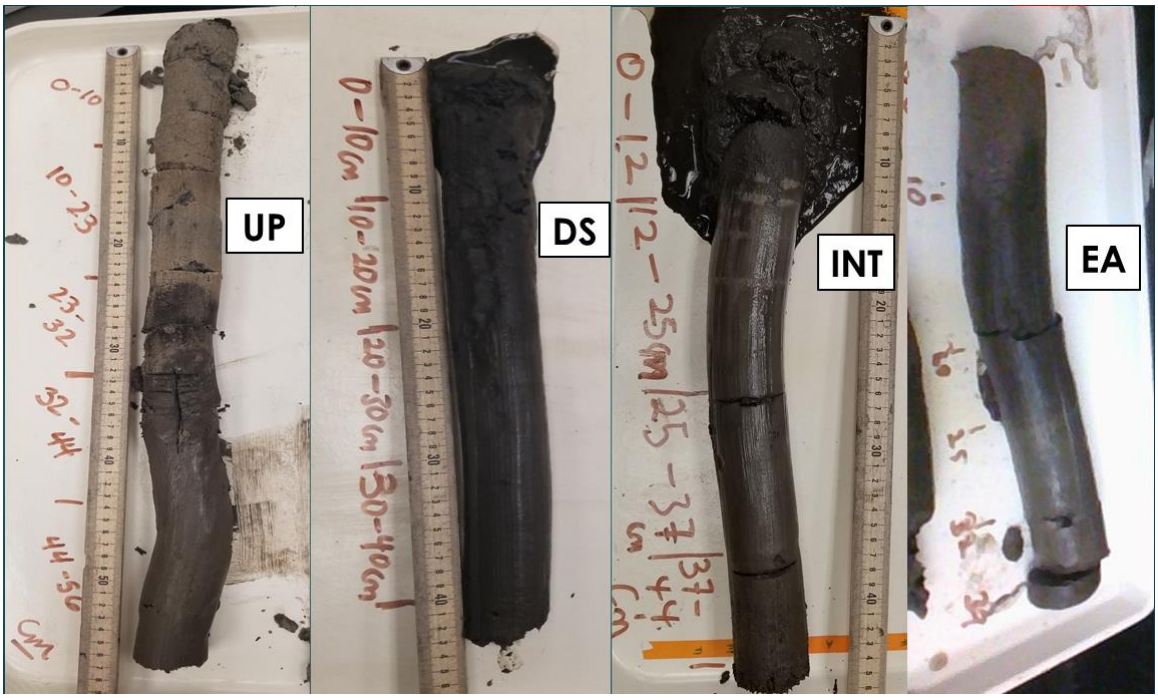

Figure 4.11. Sediment profiles across the 4 sites in the L-29 Canal

Table 4.5 Mean (± st dev) sediment characteristics with depth in collected cores. Total phosphorus (TP), organic matter (OM) and bulk density (BD) values of UP, DS, INT, and EA sediments were observed in the sediment profiles (n=3).

Site	Site+ Depth	Average depth from surface (cm)	TP (mg kg^{-1})	OM (%)	BD (g cm^{-3})
UP	UP D1	15	71.58 ± 45.71a	0.71 ±0.20a	1.30 ±0.06a
UP	UP D2	24	214.13 ±208.39	4.89± 5.87	1.01 ± 0.41
UP	UP D3	35	319.78 ±69.62	10.96± 5.67	0.72 ± 0.27
UP	UP D4**	44	336.34 ± 13.68	12.85±2.92	0.55±0.16
UP	UP D5*	56	345.43	10.88	0.67
DS	DS D1	11	1042.10± 134.03b	24.32 ± 1.19b	0.18 ± 0.01b
DS	DS D2	21	631.63 ± 144.38	18.77 ± 6.31	0.36± 0.15
DS	DS D3	33	372.1 ± 43.94	18.76± 2.92	0.41± 0.06
DS	DS D4**	40	315.62± 5.64	19.09 ± 0.13	0.45± 0.09
INT	IN D1	11	703.11± 87.41c	31.30± 1.37b	0.15± 0.01b
INT	IN D2	19	260.53± 83.2	13.87± 2.53	0.66± 0.2
INT	IN D3	30	137.5± 102.95	15.26± 1.22	0.52± 0.04
INT	IN D4	38	168.99± 19.97	16.47± 2.3	0.55± 0.06
EA	EA D1	8	558.93 ± 164.66c	19.24± 10.7b	0.35± 0.19b
EA	EA D2	16	539.05 ±27.13	20.91± 1.58	0.3± 0.04
EA	EA D3	23	467.54 ± 179.96	15.56± 5.78	0.66± 0.29
EA	EA D4**	32	207.58 ± 8.13	9.98± 2.58	0.88± 0.18
EA	EA D5**	40	206.91 ± 35.42	17.14± 1.02	0.53± 0.08

*n=1, ** n=2 ANOVA and Tukey's test were performed on the surface cores to determine significant differences between the sites.

4.4. Discussion

4.4.1 Particulate and phosphorus dynamics in the water column of the lower Everglades canals

From the results, the fate and transport of particulates and phosphorus in the lower Everglades canals depend on the amount of incoming discharge (Figure 4.12) as discharge is a big driver of suspended particulates export (Rose et al. 2018). During high discharge periods, particulates from upstream of the inflow structure, together with resuspended bed sediments can be transported downstream, while during low discharge events, particulates are more likely to settle out into the canal bed where they can be biogeochemically processed. From the literature, the behavior of TP with discharge is either chemostasis, enrichment or dilution at low discharge, but usually enrichment at high discharge (Diamond and Cohen, 2018, Moatar et al. 2017, Underwood et al. 2017, Onwuka et al. 2021). This high discharge enrichment was also observed in the canals in this study, except at S333 -where no definite behavior was observed.

The chemostasis and slight enrichment behavior at low discharge in the canals in this study, suggest TP concentrations depended more on biogeochemical regulations (e.g., adsorption-desorption, biologic uptake and decomposition of OM), and non-advective (lateral and vertical) exchanges of sediments and P between the water column and canal bed (Withers and Jarvie, 2008; Underwood et al. 2017). During high discharge, there can be advection-driven transport of P which includes the entrainment of soluble and particulate P from bed sediments, and the desorption of P from suspended particulates (Diamond and Cohen 2018; Reddy et al. 1999; Withers and Jarvie, 2008).

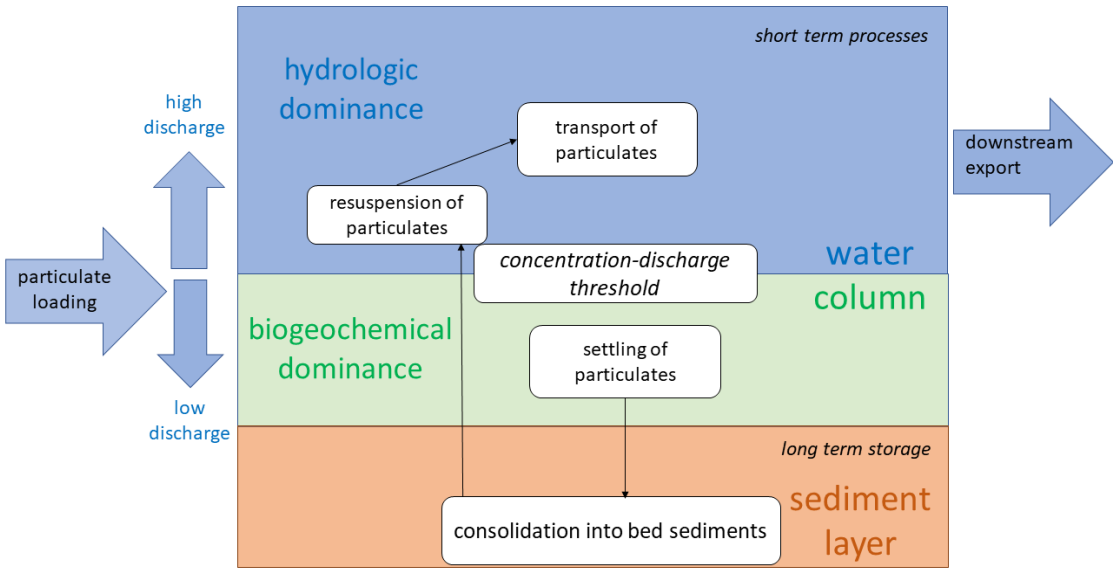

Figure 4.12 An illustration of particulate dynamics in the water column and sediment layer in a canal

In the L-29 Canal, the availability of higher temporal resolution data allowed an assessment and quantification of the effect of discharge on particulate phosphorus (PP). The proximity of UP to the inflow structure (S333 spillway) made the impact of discharge more substantial on P export as shown by the very strong enrichment behavior of PP at higher discharges. The PP export behavior of high discharge dilution at DS was different from the other sites. From riverine studies, the reason for a dilution behavior at high discharge for particulate constituents like phosphorus is the exhaustion of such particles at high discharge, for example, from deposition in floodplains (Rose et al. 2018, Zhang et al. 2018, Onwuka et al. 2021). In the L-29 Canal, at DS, the exhaustion of particles occurred because most of the incoming particulates possibly settled before reaching the site - the highest discharge did not reach 30 $m^3 s^{-1}$, which is low compared to the discharges at the other canal sites. Also, the L-29 Canal is a relatively low particulate canal, with the average

TSS at DS approximately 10 mg L^{-1} (Onwuka et al. 2023). Low TSS values like these are found in less than 5% of lotic systems worldwide (Trefry et al. 2021), even though the TSS in the L-29 has higher P content than global averages for rivers (Onwuka et al. 2023). Furthermore, the TP in the water column in the L-29 Canal can be greater than 80 μg L^{-1}, with the particulate fraction ranging from 9 to 46 % (Appendix I). Also, the discharge during the estimation of TPP at DS, came from a newer secondary structure (S333N), while the primary structure S333 was inactive (did not release discharge into the canal). Therefore, it is possible that given the right volume of discharge, there could be an enrichment behavior at DS at higher discharges. A C-Q pattern was not observed at S333, located at the start of the L-29 Canal, because the weekly sampling at the site could not capture the variability in TP in relations to the discharge releases. The presence of higher resolution (~hourly) TPP estimates provided an alternative solution to this problem.

A good separation between low discharge chemostasis (biogeochemical driven) and high discharge mobilization (hydrologic driven) behavior is the C-Q discharge threshold. Across the lower Everglades, the upstream canals had lower discharge thresholds while the downstream canals had higher thresholds for TP. The lower discharge thresholds at G136 and S5a reflect the nature of the incoming loads and canal sediments. Historically, these canals received P loads from the EAA farms, with 54 % in particulate form (Daroub et al. 2002 a). For example, S5a is on the West Palm Beach Canal, a major drainage canal on the of the eastern part of the EAA upstream and G1356 is on the L-1 Canal that directly borders the western portion of the EAA. Long-term loadings of P from EAA and urban areas to canals have increased P in the sediments and in the water column (Diaz et al. 2006). In the EAA, canal sediments have had OM as high as 54% (Das et al.

2012), and suspended particulates have had OM up to 77%, BD as low as 0.08 g cm^{-3} and TP concentrations greater than 2500 mg kg^{-1} (Bhadha et al. 2017). Furthermore, farm canals in the EAA have some organic matter made up of biological living and dead matter that grow in the canals during inter-pumping events. These high P organic materials can easily be exported downstream even at low discharges (Bhadha et al. 2017). This explains why the EAA canals had much higher TP concentrations and why their discharge thresholds were at much lower discharges compared to the downstream canals.

However, the implementation of agricultural best management practices (BMPs) in the EAA and the creation of the stormwater treatment areas (STAs) south of the EAA, have been largely successful in P export prevention and retention, leading to lower P concentrations in the lower Everglades. Some BMPs include sediment control initiatives that minimize the transport of sediments from farms, and sediment removal from canals. This is done through the construction of canal sumps to trap sediments, the reduction of drainage velocities near pumps, and the establishment of canal cleanup endeavors (Daroub et al. 2011). Likewise, the STAs are constructed wetlands that remove P through biological assimilation (emergent aquatic vegetation, submerged aquatic vegetation, periphyton), chemical adsorption, and settling and accretion of P in sediments (Chimney and Goforth, 2001; Das, 2010). Although studies have shown that PP is a dominant form of total phosphorus exported from STAs (Dierberg and Debusk, 2008).

Thus, suspended particulates can still be a major source of P downstream in the EPA. In the L-29 Canal, in addition to discharge, proximity to the S333 inflow structure was important in determining the fate and transport of suspended particulates and P. Discharge releases and proximity to S333 dictated the quantity and characteristics of the

suspended particulates accumulated in the water column (trap tree) and near the canal bed (bottom traps). Results in the water column indicated that suspended particulates accumulated highest in the deeper layers of the water column across the deployments, with the highest accumulation at the low trap at UP (closest to S333). The high accumulation in deeper water is because materials tend to settle out at greater depths (Wang et al. 2011), and resuspension from the canal bed can occur due to the advection of water near the bed (Dwinovantyo et al. 2017). Furthermore, the S333 spillway opens from the bottom up, therefore the introduction of new material is concentrated in the deeper waters relative to the surface layers. Even though the deployments were at different periods, the highest accumulation of suspended particulates closest to the S333 implies that higher canal discharges can introduce new materials originating from upstream of S333,while also enabling velocities that can erode and resuspend bed sediments (Stuck et al. 2002). In a study in the L-40 Canal, north of the L-29 Canal, during discharge (flowing) periods, a higher concentration of TSS (often used as a measure of particulate matter in the water) was generally found closest to the inflow structures (Daroub et al. 2007; 2009). High discharges are crucial for particulate transport (Stuck et al. 2002) as they mobilize both incoming materials and produce shear velocities necessary to resuspend in-channel materials (Rose et al, 2018). This explains why at DS, the higher discharge in December resulted in a higher volume of collected suspended particulates from the surface to the deeper layer of the water column (except at the mid) compared to June. Conversely, the canal interior (INT), which had the least discharge and was the farthest from the S333 had the least accumulation of suspended particulates. The suspended particulates at INT also had the least bulk density compared to the other sites. Furthermore, the collected

particulates at the top trap at INT were green and had the highest TP content, indicating that they were perhaps rich in chlorophyll (floating algal cells). These observations show that the decreasing effect of discharge in the interior parts of the canal can give rise to the domination of biogeochemical processes (such as organic matter production and decomposition) in determining the type of particulates generated. The light (low bulk density) and P-rich suspended particulates generated during low discharges or stagnant conditions in some lower Everglades canals have been attributed to biological growth (Daroub et al. 2002b).

Overall, the strong positive correlation between bulk density and discharge across all deployments and sites suggests that lighter particulates are easily transported at lower discharges while higher discharges are required to mobilize and transport heavier materials. In a study by Trefry et al. 2008 in the Lake Worth Lagoon, a preceding low discharge had less TSS with a higher percent of OM, while the succeeding higher discharge, had higher TSS that contained less OM. Thus, low discharges can easily mobilize high OM and low bulk density particulates, while higher discharges can additionally mobilize the heavier particles.

Near the canal bed (bottom traps), the high-discharge deployment preceded the low-discharge deployment. During the high discharge deployment, the highest accumulation of suspended particulates occurred at the most downstream site (BT8) while during the succeeding low discharge deployment, the highest accumulation of settling particulates was at BT5 -almost 1 km from the S333 inflow structure- which was midway between UP (BT1) and DS (BT8). During low discharge periods, suspended particulates settle rather than get transported (Fugate et al. 2021). Therefore the force of the water

during the high discharge deployment mobilized and transported suspended particulates farther (before they were deposited) compared to the low discharge deployment. This is further confirmed by the increase in organic matter (and decrease in bulk density) of the settling particulates with distance from the inflow structure that suggested that the more organic (lighter) materials were transported the furthest, during the high discharge period. Conversely, during the low discharge deployment, beyond 1km, the lower accumulation of particulates and the decrease in OM and TP, and increase in BD suggest the following: 1) all the incoming particulates settled out at BT5 (which had a lot of leafy detritus) and 2), the particulates that settled and accumulated further downstream (BT6 and BT8) may have been sourced elsewhere (e.g. from the preceding high discharge deployment that had begun to decompose). Low discharge events can be periods of active biogeochemical processing of organic materials (O'Donnell and Hotchkiss, 2019). From this study, higher discharges from S333 can transport materials all the way to DS, which is by the first bridge on the L-29 Canal. This means that higher discharges can export suspended particulates and P into the ENP, which is not good for Everglades restoration.

4.4.2 Benthic sediment characteristics and their relationship to discharge

Bulk density (BD) values from 0.12 to 0.54 g cm-^{3} have been observed in the agricultural canals of the EAA (Das et al. 2012) which is a lower range than in the L-29 Canal. The presence of detritus from aquatic plants can cause low bulk density values in surface sediments (Diaz et al. 2006). Bulk density values less than 0.60 g cm-^{3} have been observed in WCA canals' sediments which are low for mineral soils (Diaz et al. 2006). The bulk densities of wetland organic soils range from 0.1 to 0.4 g cm^{-3} while for wetland mineral soils it is between 1 – 1.5 g cm^{-3} (DeLaune et al. 2008) while non-wetland mineral

soils can have bulk densities between 1.0 and 2.0 g cm^{-3} (Brady and Weil, 2002). The bulk density values in the sediments of the L-29 Canal are lower than mineral soils, except at the surface layers at UP. Thus, these sediments are more likely to be transported with canal discharges as resuspended solids (along with P) (Das et al. 2012). The high correlation between organic matter and TP concentration shows that TP is bound in organic matter and thus a significant portion of the TP may be organically derived (Das et al. 2012). This correlation was also found in the EAA farm canals (Das et al. 2012). Just like in our study, Diaz et al. 2006, also recorded a decrease in organic matter and TP and an increase in BD with depth in their sediment inventory study of the EPA (WCA) canals.

The sediment TP content in our study was lower than in other EPA canal studies. For example, the TP in EPA canals ranged from 258 to 1700 mg kg^{-1} for the sediment profile and 320 – 1700 mg kg^{-1} at the surface layer between 0 and 12 cm (Diaz et al. 2006). These TP values are higher possibly due to the upstream location of these canals, relative to the L-29, and are thus closer in proximity to the EAA (agriculture). TP content of over 2000 mg kg^{-1} has been observed in EAA canal sediments between 0-10 cm depth (Das et al. 2012; Bhadha et al. 2017). The increase in TP with depth at UP (our study) was observed in another EPA (WCAs) canal study (Wang et al. 2011), in which deeper sediment layers (25cm-35cm) had TP concentrations greater than 4000 mg kg^{-1}. A reason for the lower P in the surface sediment layer in WCA canals is the effect of the implementation of the BMPS and STAs that reduced P load (Wang et al. 2011). Furthermore, the historic discharge data at S333 inflow, which started in 1978, showed an increase in discharge to date (DBHYDRO). Therefore, it is possible that earlier on, the lower discharges only imported high organic P-rich materials that settled out closer to the S333 structure in the

L-29 Canal. But as more discharges were released subsequently, heavier materials were also mobilized and transported into the L-29 Canal, and eventually settled near the S333 structure, while the lighter materials were transported and deposited further downstream in the canal.

The top layer of the UP sediments, closest to the S333 inflow structure, appeared to be made of light-colored grains compared to the dark organic features of the more downstream locations, while at the EA, close to the S356 pump, the top sediment layer appeared to be a mixture of light-colored grains and dark colored sediments (Figure 4.11). The higher bulk density, lower organic matter, and lower TP content in the topmost layer at UP demonstrate the effects of canal discharges on the type of sediments that accumulates. Das et al. 2012, found that the transects closer to the pump in EAA farm canals had lower OM due to the greater velocities associated with pumping, that could efficiently mobilize light flocculent sediment from the top layer. In Everglades canals, water flow is discrete and regulated through the inflow structures resulting in quiescent (no-flow) periods between discharge events (Bhadha et al. 2017). This can result in the accumulation of new suspended and detrital materials in the canals, during the quiescent periods, that can be easily mobilized during discharge release events. At the S333 inflow structure, instantaneous releases from zero to 60 $m^3 s^{-1}$ have been observed (Onwuka et al. 2023). Such rapid increases in water releases can mobilize the new (organic) material that accumulated in the water column, resuspend the lighter bed sediments, and export both sediment types downstream, leaving behind the heavier more mineral sediments.

Canal studies in the lower Everglades have characterized new accumulated materials as being highly organic and P-rich (for example, from biological growth of

aquatic plants) while the heavier more mineral sediments are older and P-poor (Daroub et al. 2002b). The inflow structure S356, located at the eastern end of the L-29 was continuously discharging into the canal to prevent flooding in the eastern adjacent areas (Crawford, Daniel, USACE, 2021), and thus it did not have the same instantaneous and rapid changes in discharge like at S333. This resulted in the sediments at EA, the site closest to S356, having characteristics intermediate between UP (closest to S333) and the downstream sites – DS and INT. The P-rich organic sediments at DS and INT possibly resulted from the deposition of lighter organic matter from upstream as well as the breakdown of organic material that released P.

Fractionation studies in the lower Everglades canals have shown calcium-bound P, a relatively unavailable form, as the major P storage in sediments (Diaz et al. 2006; Wang et al. 2011; Das et al. 2012). However, these canal sediments can be transported through disturbances like high canal discharges and can become a source of P to downstream environments (Das et al. 2012). TP concentrations in the water column of WCA canals are higher than in the adjacent wetland sediments (Wang et al. 2011). In the study by Wang et al. 2011, the canals had TP concentrations that ranged from 19 to 210 $\mu g\ L^{-1}$, while in the surrounding wetlands, TP ranged from 4.2-18 $\mu g\ L^{-1}$. In the L-29 Canal, where concentrations can exceed 80 $\mu g\ L^{-1}$, there is a risk of exporting excess P downstream into ENP through the export of P-containing suspended particulates from upstream regions of the canal during high discharges, as well as the movement of dissolved P in canal water. This is especially crucial because there is a target mandate of 10 $\mu g\ L^{-1}$ for phosphorus in EPA wetlands. Therefore, canal discharges need to be regulated to prevent the unwanted downstream export of P-rich sediments into sensitive ecosystems, including ENP. Potential

management strategies include operating canal discharge releases below the discharge thresholds from C-Q curves and switching from high-volume rapid releases to longer low-volume discharge releases.

4.5. Conclusion

Results from this study showed that incoming discharges export phosphorus (P) to both the water column and bed sediment layer in canals across the lower Everglades. Higher discharges can increase the concentrations and potential downstream export of particulates and P by importing more particulate masses and facilitating resuspension from the canal bed. During low canal discharges, suspended particulates can accumulate closer to the inflow structure, while high canal discharges can transport particulates further downstream and away from the inflow structure. Furthermore, high canal discharges can resuspend lighter organic and P-rich sediments and transport them further downstream, potentially impacting sensitive Everglades wetlands.

Knowledge from this study has management implications. The discharge thresholds from C-Q relationship models can be used to create canal management practices to determine the optimal range of discharges (sweet spot) where freshwater delivery is maximized, and exports of particles and P are minimized. Bottom sediment traps can also be utilized to determine the range of discharges that will allow settling of most of the incoming suspended particulates to the canal bed, rather than being transported to sensitive downstream ecosystems.

A canal management practice from using the C-Q discharge thresholds and sediment traps can include breaking up a large canal discharge release into smaller ones. The adoption of this practice, and many others, will aid in obtaining the multibillion-dollar

Everglades restoration goal which includes increasing cleaner freshwater delivery to the downstream wetlands and attaining low TP concentration in Everglades wetlands as mandated by the Everglades Forever Act.

This study also highlights the weakness of using lower temporal resolution data (weekly) and demonstrates the usefulness of higher resolution (minutes- hours) data, in quantifying the impact of discharge on particulate and P export dynamics. Using surrogate estimates for suspended particulates and P developed from the backscatter of acoustic devices is a solution for providing higher temporal resolution data. As acoustic devices are deployed to measure velocity in flowing waters by agencies, such as the USGS, their use for estimating suspended particulates and phosphorus should be adopted broadly.

4.6. References

Abtew, W. and Ciuca, V., 2019. South Florida Hydrology and Water Management. *2019 South Florida Environmental Report*, pp.2-1.

Abtew, W. and Obeysekera, J., 1996. Drainage Generation and Water Use in the Everglades Agricultural Area Basin 1. *JAWRA Journal of the American Water Resources Association*, *32*(6), pp.1147-1158.

Andersen, J.M., 1976. An ignition method for determination of total phosphorus in lake sediments. *Water research*, *10*(4), pp.329-331.

Beusen, A.H.W., Dekkers, A.L.M., Bouwman, A.F. and Ludwig, W., és Harrison, J.(2005): Estimation of global river transport of sediments and associated particulate C, N, and P. *Global Biogeochemical Cycles*, *19*(4).

Bhadha, J.H., Lang, T.A. and Daroub, S.H., 2017. Influence of suspended particulates on phosphorus loading exported from farm drainage during a storm event in the Everglades Agricultural Area. *Journal of Soils and Sediments*, *17*, pp.240-252.

Brady, N.C. and Weil, R.R., 2002. Soil and the hydrologic cycle. *The Nature and Properties of Soils*, *2*.

Carter, K., Redfield, G., Ansar, M., Glenn, L., Huebner, R., Maxted, J., Pettit, C. and VanArman, J., 2010. Canals in South Florida: A technical support document.

Childers, D.L., Doren, R.F., Jones, R., Noe, G.B., Rugge, M. and Scinto, L.J., 2003. Decadal change in vegetation and soil phosphorus pattern across the Everglades landscape. *Journal of Environmental Quality*, *32*(1), pp.344-362.

Chimney, M.J. and Goforth, G., 2001. Environmental impacts to the Everglades ecosystem: a historical perspective and restoration strategies. *Water Science and Technology*, *44*(11-12), pp.93-100.

Daroub, S.H., Stuck, J.D., Lang, T.A. and Diaz, O.A., 2002. Particulate phosphorus in the everglades agricultural area: I–Introduction and sources. *Soil Water Department of University of Florida IFAS Extension Publication SL*, *197*.

Daroub, S.H., Stuck, J.D., Lang, T.A. and Diaz, O.A., 2002. Particulate phosphorus in the Everglades Agricultural Area: II–Transport mechanisms. *Inst. of Food and Agric. Sci., Ext. Office. Univ. of Florida, Gainesville*.

Daroub, S.H., Van Horn, S., Lang, T.A. and Diaz, O.A., 2011. Best management practices and long-term water quality trends in the Everglades Agricultural Area. *Critical Reviews in Environmental Science and Technology*, *41*(S1), pp.608-632.

Das, J., Daroub, S.H., Bhadha, J.H., Lang, T.A. and Josan, M., 2012. Phosphorus release and equilibrium dynamics of canal sediments within the Everglades Agricultural Area, Florida. *Water, Air, & Soil Pollution*, *223*, pp.2865-2879.

DeLaune, R. D., Reddy, K. R., Richardson, C. J., and Megonigal, J. P. (Eds.). 2008. *Methods in biogeochemistry of wetlands* (Vol. 28). John Wiley & Sons.

Diamond, J.S. and Cohen, M.J., 2018. Complex patterns of catchment solute–discharge relationships for coastal plain rivers. *Hydrological Processes*, *32*(3), pp.388-401.

Diaz, O.A., Daroub, S.H., Stuck, J.D., Clark, M.W., Lang, T.A. and Reddy, K.R., 2006. Sediment inventory and phosphorus fractions for water conservation area canals in the Everglades. *Soil Science Society of America Journal*, *70*(3), pp.863-871.

Dierberg, F.E. and DeBusk, T.A., 2008. Particulate phosphorus transformations in south Florida stormwater treatment areas used for Everglades protection. *Ecological Engineering*, *34*(2), pp.100-115.

Dorioz, J.M., Cassell, E.A., Orand, A. and Eisenman, K.G., 1998. Phosphorus storage, transport and export dynamics in the Foron River watershed. *Hydrological processes*, *12*(2), pp.285-309.

Dwinovantyo, A., Manik, H.M., Prartono, T. and Susilohadi, S., 2017. Quantification and analysis of suspended sediments concentration using mobile and static acoustic Doppler current profiler instruments. *Advances in Acoustics and Vibration, 2017*.

Faridmarandi, S. and Naja, G.M., 2014. Phosphorus and water budgets in an agricultural basin. *Environmental science & technology*, *48*(15), pp.8481-8490.

Fugate, D.C., Thomas, S. and Scinto, L.J., 2021. Particle dynamics in stormwater treatment areas. *Ecological Engineering*, *160*, p.106131.

Godsey, S.E., Kirchner, J.W. and Clow, D.W., 2009. Concentration–discharge relationships reflect chemostatic characteristics of US catchments. *Hydrological Processes: An International Journal*, *23*(13), pp.1844-1864.

Labry, C., Youenou, A., Delmas, D. and Michelon, P., 2013. Addressing the measurement of particulate organic and inorganic phosphorus in estuarine and coastal waters. *Continental Shelf Research*, *60*, pp.28-37.

Lopez-Roque Christian D - ScienceBase-Directory (Internet). (cited 2022 April 7]. Available from: https://www.sciencebase.gov/directory/person/6250

McLean A., 2015. Modified Water Deliveries: Improving Hydrologic Condition in Northeast Shark River Slough. https://www.nps.gov/ever/learn/nature/modwater.htm (accessed 10 May, 2020).

Meybeck, M. 1982. Carbon, nitrogen, and phosphorus transport by world rivers. *Am. J. Sci*, *282*(4), 401-450. https://doi.org/10.2475/ajs.282.4.401

Moatar, F., Abbott, B.W., Minaudo, C., Curie, F. and Pinay, G., 2017. Elemental properties, hydrology, and biology interact to shape concentration-discharge curves

for carbon, nutrients, sediment, and major ions. *Water Resources Research*, *53*(2), pp.1270-1287.

O'Donnell, B. and Hotchkiss, E.R., 2019. Coupling concentration-and process-discharge relationships integrates water chemistry and metabolism in streams. *Water Resources Research*, *55*(12), pp.10179-10190.

Onwuka, I.S., Scinto, L.J. and Fugate, D.C., 2023. High-Resolution Estimation of Suspended Solids and Particulate Phosphorus Using Acoustic Devices in a Hydrologically Managed Canal in South Florida, USA. *Sensors*, *23*(4), p.2281.

Onwuka, I.S., Scinto, L.J. and Mahdavi Mazdeh, A., 2021. Comparative Use of Hydrologic Indicators to Determine the Effects of Flow Regimes on Water Quality in Three Channels across Southern Florida, USA. *Water*, *13*(16), p.2184.

Rahul, A.K., Shivhare, N., Dwivedi, S.B. and Dikshit, P.K.S., 2020. Estimation of behavioral change of SSC of bed profile in the river using ADCP. *Arabian Journal of Geosciences*, *13*, pp.1-9.

Reddy, K.R., Kadlec, R.H., Flaig, E. and Gale, P.M., 1999. Phosphorus retention in streams and wetlands: a review. *Critical reviews in environmental science and technology*, *29*(1), pp.83-146.

Rose, L.A., Karwan, D.L. and Godsey, S.E., 2018. Concentration–discharge relationships describe solute and sediment mobilization, reaction, and transport at event and longer timescales. *Hydrological processes*, *32*(18), pp.2829-2844.

Stuck, J.D., Lang, T.A., Diaz, O.A., Daroub, S. and Aziz, T., 2002, May. Studies of particulate phosphorus sources and potential management practices for control in the Everglades Agricultural Area. In *Proceedings of the seventh biennial stormwater research & watershed management conference, Tampa, Florida. Southwest Florida Water Management District* (pp. 164-174).

Svendsen, L.M. and Kronvang, B., 1993. Retention of nitrogen and phosphorus in a Danish lowland river system: implications for the export from the watershed. *Nutrient Dynamics and Retention in Land/Water Ecotones of Lowland, Temperate Lakes and Rivers*, pp.123-135.

Trefry, J.H. and Fox, A.L., 2021. Extreme runoff of chemical species of nitrogen and phosphorus threatens a Florida barrier island lagoon. *Frontiers in Marine Science*, *8*, p.752945.

Underwood, K.L., Rizzo, D.M., Schroth, A.W. and Dewoolkar, M.M., 2017. Evaluating spatial variability in sediment and phosphorus concentration-discharge relationships using Bayesian inference and self-organizing maps. *Water Resources Research*, *53*(12), pp.10293-10316.

United States Army Corps of Engineers (2020). Environmental Impact Statement (EIS) for the Combined Operational Plan (COP). https://www.saj.usace.army.mil/Missions/Environmental/Ecosystem-Restoration/G-3273-and-S-356-Pump-Station-Field-Test/ (Accessed April, 2020)

United States Environmental Protection Agency. (1983). Methods for chemical analysis of water and wastes. *Environmental Monitoring and Support Laboratory*. Cincinnati, Ohio (pp. 475–490).

Wang, Q. and Li, Y., 2010. Phosphorus adsorption and desorption behavior on sediments of different origins. *Journal of Soils and Sediments*, *10*, pp.1159-1173.

Wang, Q., Li, Y. and Ouyang, Y., 2011. Phosphorus fractionation and distribution in sediments from wetlands and canals of a water conservation area in the Florida Everglades. *Water Resources Research*, *47*(5).

Whalen, P.J., VanArman, J., Milliken, J., Swift, D., Bellmund, S., Worth, D., Fontaine, T.D., Golick, L. and Formati, S., 1992. Surface water improvement and management plan for the Everglades. *South Florida Water Management District, West Palm Beach, FL*.

Withers, P.J.A. and Jarvie, H.P., 2008. Delivery and cycling of phosphorus in rivers: a review. *Science of the total environment*, *400*(1-3), pp.379-395.

Yoshimura, T., Nishioka, J., Saito, H., Takeda, S., Tsuda, A. and Wells, M.L., 2007. Distributions of particulate and dissolved organic and inorganic phosphorus in North Pacific surface waters. *Marine chemistry*, *103*(1-2), pp.112-121.

Zhang, Q., 2018. Synthesis of nutrient and sediment export patterns in the Chesapeake Bay watershed: Complex and non-stationary concentration-discharge relationships. *Science of the Total Environment, 618*, pp.1268-1283.

CHAPTER 5: CONCLUSION

South Florida is globally recognized as a unique region. It has a subtropical climate and low topography and possesses human-made manipulated canals, as opposed to free-flowing natural rivers. Additionally, South Florida is home to the once oligotrophic Everglades, whose hydrology and land use have been changed and has suffered consequences of nutrient and phosphorus pollution via canal discharges. The overarching objective of this dissertation was to characterize the discharges, water quality, and sediment attributes of South Florida Everglades' canals, and evaluate how short- and long-term discharge changes affect the export behavior of water quality constituents with a focus on sediments and phosphorus.

In the first study (Chapter 2), a comparison between the Hillsboro Canal, a major South Florida human-made and discharge-managed canal, the Peace River, a slightly channelized river in South-west Florida, that still maintains riverine attributes like floodplain and sinuosity, and the Shark River Slough, a shallow wetland slough in Everglades National Park. Characterization of the flow regimes and the determination of the water quality constituent behaviors from these three channels were done using long-term low-resolution data. The results revealed that the operationally managed Hillsboro Canal had the greatest flow variability, characterized by flashy and voluminous discharges, and lacked eco-morphological features such as riparian zones, that resulted in increases in the concentrations of water quality constituents with high discharge. The sinuous Peace River had a natural flow regime, with intermediate flow variability and the longest high pulse duration. These flow regime characteristics combined with the

connection to riparian zones and gentler channel slopes enabled the deposition of water quality constituents outside the channel and a reduction in concentrations at high discharge. The flow regime of Shark River Slough had the least variability and the longest low pulse duration, which when combined with the shallow depth, resulted in decreased concentrations at high discharge. This study further highlights the usefulness of long-term water quality and discharge data in delineating the export behavior of constituents in channels.

The second study (Chapter 3), conducted at three sites in the Tamiami (L-29) Canal - a crucial canal involved in delivering freshwater to Everglades National Park - developed high temporal and spatial estimates of total suspended solids and total particulate phosphorus from the backscatter from acoustic devices, to assess the effects of flashy canal discharges on the potential export of these constituents. Results showed that flashy and voluminous discharges led to an increase in the concentration of the constituents in the water column and near the canal bed. This was most observable in the site closest to the inflow structure S333. Also, analyses of field-collected suspended solids revealed an increase in phosphorus (P) fraction with increasing distance from S333. This indicates that canal discharges likely transported P-rich light (organic) particles to the downstream sites, while P-poor heavier (mineral) particles remained closest to S333. This study shows how flashy canal discharges impact the short-term dynamics of suspended solids and P behavior and highlights the importance of high spatiotemporal resolution water quality constituent data.

The final study (Chapter 4) built on the preceding two studies by: 1) combining long term -lower temporal resolution data and short term higher temporal resolution data across different spatial gradients and 2) incorporating canal suspended particulates and bed sediments analyses to paint a holistic picture about P and particulate export dynamics in South Florida' Everglades Canals. It can be inferred from this study, and several similar studies across the region, that canals bear, in their sediments, the physico-chemical characteristics and P content of the land uses they drain. And these characteristics, as well as canal discharge releases, determine the magnitude of particulates and phosphorus exported downstream. These inferences were made from the results of 1) discharge thresholds from concentration-discharge (C-Q) relationship models for P in the lower Everglades canals and 2) the mass accumulation rates, physicochemical characteristics (organic matter, bulk density), and P content of suspended particulates collected in traps, and cored bed sediments in the L-29 Canal. Results showed a predominant enrichment P behavior at higher discharges in the canals because of the mobilization of P and resuspension of sediments. Results also showed that the volume of discharges and the proximity to the inflow structure (S333) determined the type of suspended particulates that were exported through the L-29 Canal, and the kind of sediments that accrued in the bed. Furthermore, during the high discharge deployment, suspended particles were able to settle all along the canal reach between the S333 and the first bridge on the L-29 Canal, while during the low discharge deployment, suspended particles only settled out about halfway through the canal reach, marking a "threshold".

Since one of the goals of Everglades restoration is to increase the delivery of clean freshwater from upstream sources, the usefulness of this dissertation research is in the determination of suitable discharges across South Florida's Everglades canals that will maximize freshwater delivery to hydrate the Southern Everglades while minimizing the export of suspended sediments and phosphorus. I propose that the discharge thresholds from the concentration-discharge (C-Q) relationship models and the threshold from sediment traps that collect settling particulates be used as diagnostic and management tools for this goal. I also support their inclusion in best management practices for canal discharge regulations in South Florida. Based on the research in the Lower Everglades, the upstream canals (around the EAA) should have the least discharge releases ($< 5\ m^3\ s^{-1}$), since these canals are the most enriched with P, while the more downstream canals can have higher discharge releases since they have less P concentrations.

5.1. Future Work

From this work, the development of surrogate estimates from acoustic devices provided high spatial and temporal resolution water quality estimates, that enabled the relationship between discharge and water quality to be assessed and quantified in the short term. Therefore, these acoustic devices, which already measure velocity, can complement the existing water monitoring protocols in South Florida by providing suspended sediments and particulate phosphorus estimates. Furthermore, since there is a positive relationship between acoustic backscatter and TSS, backscatter from a deployed acoustic device can be compared with the corresponding discharge record to determine

the effects of discharge on particulate dynamics. This can help determine canals that should be prioritized for canal discharge management and sediment retention.

For future work, the surrogate method should be tested in other canals across South Florida to provide near-time estimates of the behaviors of water quality constituents in response to changing canal discharge release operations. Furthermore, the deployment of sediment traps in a spatial gradient in such canals will be useful in establishing suitable discharge operations. Implementation of these methods will facilitate a more targeted approach to sediment and P management.

APPENDICES

I) Water quality parameters in the water column in the L-29 Canal at the upstream (UP) site, closest to the S333 structure in April 2021.

Date	Depth from surface (m)	TP in SS (mg g^{-1})	TSS (mg L^{-1})	TPP (μg L^{-1})	TP in water (μg L^{-1})	percent of TPP (μg L^{-1}) in TP (μg L^{-1}) (%)
April 1, 2021	0.5	1.66	3.64	6.04	64.79	9.32
	1.0	2.13	3.27	6.96	70.43	9.89
	1.5	1.83	4.24	7.77	68.94	11.27
	2.0	1.39	6.35	8.82	71.30	12.37
	2.5	1.46	5.95	8.67	62.74	13.81
	3.0	1.52	5.40	8.19	70.37	11.64
	3.5	1.68	4.75	7.97	76.38	10.44
	4.0	1.41	6.10	8.62	71.98	11.97
	4.35	1.42	5.60	7.95	76.32	10.41
April 16, 2021	0.5	1.82	4.89	8.91	71.05	12.54
	1.0	1.60	5.70	9.11	83.64	10.89
	1.5	1.80	4.50	8.11	83.89	9.67
	2.0	1.75	4.80	8.38	81.84	10.24
	2.5	1.66	5.30	8.79	81.90	10.73
	3.0	1.68	4.90	8.24	59.68	13.80
	3.5	1.66	5.50	9.12	68.82	13.25
	4	1.67	5.40	9.00	74.77	12.03
	4.5	1.55	6.90	10.72	36.86	29.08

II) Water quality parameters in the water column in the L-29 Canal at the Downstream (DS) and Interior (INT) sites.

Site	Date	Depth from surface (m)	TPP (μg L^{-1})	TP in water (μg L^{-1})	percent of TPP (μg L^{-1}) in TP (μg L^{-1}) (%)
Downstream	June 22, 2021	1.2	11.25	46.53	24.18
		2.2	12.02	46.22	26.00
		3.2	10.64	47.21	22.53
		4.2	14.60	54.13	26.98
Interior	August 19, 2021	0.5	3.99	34.40	11.61
		1	4.03	33.80	11.92
		1.5	4.20	45.80	9.18
		2	4.64	41.90	11.09
		2.5	5.54	28.40	19.50
		3	5.19	35.50	14.63
		3.5	5.07	34.30	14.78
		4.0	7.39	35.40	20.89

VITA

IKECHUKWU SAMUEL ONWUKA

Born in Ibadan, Nigeria

2013 B.Sc. Oceanography and Fisheries, University of Ghana, Legon

2020 M.S., Environmental Studies, Florida International University, Miami, Florida

2023 Ph.D., Earth Systems Science, Florida International University, Miami, Florida

PUBLICATIONS

Onwuka, I. S., Scinto, L. J., & Mahdavi Mazdeh, A. (2021). Comparative Use of Hydrologic Indicators to Determine the Effects of Flow Regimes on Water Quality in Three Channels across Southern Florida, USA. *Water*, *13*(16), 2184. https://doi.org/10.3390/w13162184

Onwuka, I.S. ; Scinto, L.J. ; Fugate, D.C. (2023). High-Resolution Estimation of Suspended Solids and Particulate Phosphorus Using Acoustic Devices in a Hydrologically Managed Canal in South Florida, USA. *Sensors*, 23, 2281. https://doi.org/10.3390/s23042281